ALMA MATER STUDIORUM
UNIVERSITÀ DI BOLOGNA

DOTTORATO DI RICERCA IN

SCIENZE BIOMEDICHE E NEUROMOTORIE

Ciclo 37

Settore Concorsuale: 05/D1 - FISIOLOGIA

Settore Scientifico Disciplinare: BIO/09 - FISIOLOGIA

SENSORIMOTOR INTEGRATION IN VISUOMOTOR TASKS: TRAJECTORY ANALYSIS IN OCCIPITOPARIETAL LESIONS AND ACTION-DEPENDENT EFFECTS ON PERCEPTION IN VIRTUAL REALITY

Presentata da: Caterina Foglino

Coordinatore Dottorato

Matilde Yung Follo

Supervisore

Patrizia Fattori

Co-supervisore

Annalisa Bosco

Esame finale anno 2025

Table of Contents

1. ABSTRACT

Sensorimotor integration is a fundamental process that underlies our ability to interact with and perceive the world around us. The integration of sensory information with motor actions enables precise movement execution and plays a crucial role in shaping our perception.
Neurological conditions caused by parietal lesions can disrupt this intricate process, leading to impairments in movement execution and control (Perenin & Vighetto, 1988). In the first study of this thesis, we evaluated how visuomotor disruption caused by an occipitoparietal lesion in a patient with optic ataxia symptoms impairs motor trajectories during visually guided reaching movements. To this end, we compared the trajectories performed by the patient with those performed by a healthy control group by using a novel decoding approach. We found that the trajectories of the two groups were highly distinguishable already before the midpoint of the movement, suggesting the potential of this decoding method to characterize pathological motor behaviours.

In the second study of this thesis, we investigated sensorimotor integration using another novel approach: virtual reality. In fact, previous research indicates that the perception of space and objects in virtual environments is usually inaccurate (Waller & Richardson, 2008; Stefanucci et al., 2015; Kelly et al., 2018) but can be improved by interacting with the environment through walking, though not by reaching (Kelly et al., 2013). To evaluate this, we used a size-judgment task to assess how different interactions, such as simulated walking, reaching and grasping, affect object perception in virtual reality. Contrary to our expectations, which were based on real-world studies showing that grasping enhances size perception (Wykowska et al., 2009; Gutteling et al., 2011), we found that mere observation was the most beneficial interaction for performing the task.

The exploration of the effects of neurological impairments on movement trajectories and the influence of various actions on perception in virtual reality offers significant implications for clinical rehabilitation and our understanding of sensorimotor processing.

2. GENERAL INTRODUCTION

2.1 Sensory information and motor responses

The synchronization of sensory information and motor responses allows for precise and adaptive behaviours that define our interaction with the world. This synchronized process starts with perceiving the environment around us, with our visual system gathering information about the characteristics of the elements that surround us.

When we decide to perform an action in the environment, such as picking up an object, our brain then predicts the necessary trajectory of movement required to reach out and grasp the object. This involves planning the movement of the arm, hand, and fingers to successfully lift the object. Throughout the action, our visual and proprioceptive systems provide continuous feedback, allowing us to correct our movement if needed.

Various regions of the brain work in concert to coordinate visual sensory information and motor responses, each contributing distinct functions to ensure smooth and accurate performance during visually guided actions.

Historically, Ungerleider and Mishkin (1982) posited the existence of two distinct cortical pathways specialized for visual processing originating from the primary visual cortex: one dorsal pathway projecting to the parietal cortex, and another ventral projecting to the temporal lobe. In their view, the dorsal stream was responsible for encoding “where” an object is, while the ventral stream was involved in the process of “what” the object is.

Later, Milner and Goodale (1992) highlighted how both pathways process information about object characteristic and their spatial locations, and how the difference between the two streams lies in the way they use visual information coming from the primary visual cortex. In fact, the authors proposed that ventral stream uses visual inputs to form long-term perceptual representations, while the dorsal one uses the same information but to mediate the visual control of skilled actions, such as reaching and grasping, in real-time.

In support of this, brain lesions located along the dorsal stream can cause impairments in the performance of visually guided actions, independent of misperception of the visual space, and vice versa. As matter of fact, the model developed by Milner and Goodale was inspired by a series of partial or complete double dissociations observed between patients with ventral-stream damage and patients who had damage to the dorsal stream (see Figure 1 and 2). Specifically, patients with lesions in the ventral visual areas experience agnosia, a disorder that causes difficulty in recognizing objects, whereas patients with lesion in the dorsal visual areas experience optic ataxia, which induces difficulty in correctly reaching and grasping objects (Milner and Goodale, 2008).

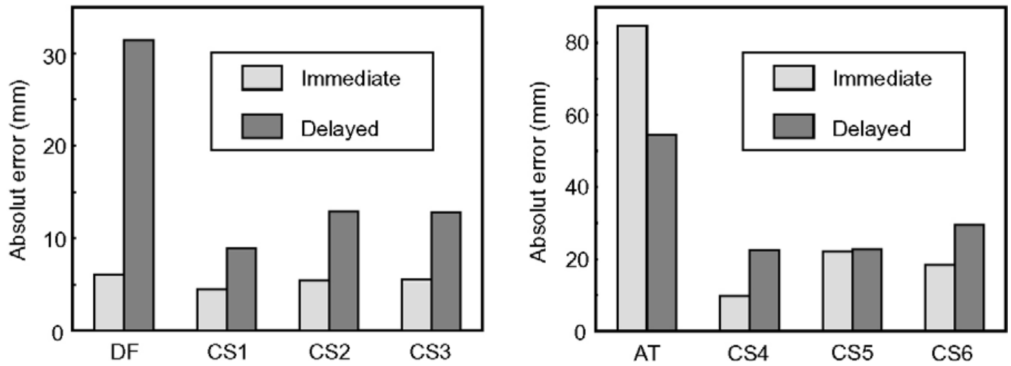

Figure 1. Double dissociation of pointing ability following damage to the ventral and dorsal streams. The image illustrates pointing performance to a peripheral visual target in a patient with visual form agnosia (D.F.), as contrasted with the performance of a patient with optic ataxia (patient A.T.). Data are presented in both an immediate pointing condition (light grey bars) and a delayed testing condition, in which the patient had to wait several seconds before responding (dark grey bars). The two graphs are taken from two separate experiments, each of which included three age-matched healthy controls (who were therefore rather younger in the D.F. experiment). The y-axis shows the resultant absolute errors in millimetres in both studies. The data are re-plotted from Milner, Dijkerman, and Carey (1999) and Milner, Paulignan, et al. (1999), respectively, with permission (from Milner and Goodale, 2008).

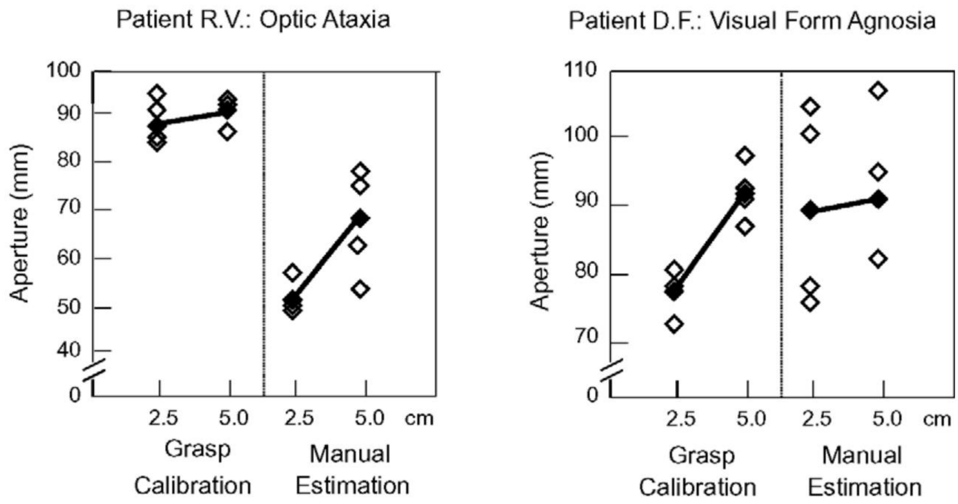

Figure 2. Double dissociation of grasping ability following damage to the ventral and dorsal streams. The image illustrates grip calibration performance in a patient with visual form agnosia (D.F.) as contrasted with the performance of a patient with optic ataxia (patient R.V.). For both experiments, the stimuli were presented centrally, and the patient was asked either to reach out and pick up the object using a finger-thumb precision grip (left panel in each case), or to mime its width using finger and thumb (right panel in each case). The y-axis shows the maximum separation of markers attached to the tips of forefinger and thumb during reaching to grasp, or at asymptote when the patient had arrived at her judgement, respectively. Data are plotted in each graph for rectangular blocks of 2.5 and 5.0 cm width, respectively. Open shapes show data points from individual trials, and closed shapes the mean of these individual scores.

The data for D.F. are re-plotted from Goodale et al. (1991), with permission (from Milner and Goodale, 2008).

2.2 Clinical evidence: Optic Ataxia

The typical example of damage to the dorsal stream of visual inputs is optic ataxia (see lesion sites in Figure 3) , a visuomotor disorder caused by unilateral or bilateral lesions located in the posterior parietal cortex (Perenin & Vighetto, 1988; Karnath & Perenin, 2005). The disorder compromises the ability to reach targets in peripheral vision and to make online movement corrections based on visual feedback (Pisella et al., 2000).

Specifically, patients with unilateral lesions present two main effects caused by the dorsal damage. A hand effect, characterized by reaching errors with their contralesional hand in both visual fields, as well as a field effect when these errors occur towards an object presented in the contralesional hemifield (Perenin & Vighetto, 1988; Prado et al., 2005).

Moreover, patients suffering from these deficits can also experience problems in orienting and shaping the hand during grasping (Jakobson et al., 1991; Jeannerod et al., 1994; Milner et al., 2001; Perenin & Vighetto, 1988), and can exhibit a deficit in proprioceptively guided reaching, such as when the contralesional hand is reaching to the other hand in the dark (Blangero et al., 2007; Jackson et al., 2009; Pisella et al., 2000).

Nevertheless, the disorder does not occur when reaching for auditory or tactile stimuli (Rossetti et al., 2003), suggesting that optic ataxia results from a specific impairment in linking vision with action. In fact, the Greek term “ataxia” was chosen to highlight a lack of coordination between visual inputs and motor outputs (Balint, 1909). Therefore, one of the primary frameworks proposed to explain optic ataxia is the disruption of visuomotor processing, which suggests a deficit in sensorimotor integration (Rondot et al., 1977; Perenin & Vighetto, 1988).

The linkage between vision and action is crucial for movements that need precise eye-hand coordination. This process involves converting the location of visual stimuli coded in eye coordinates, into the appropriate motor actions represented in motor coordinates. As a result, it has also been suggested that optic ataxia involves, at least in part, a difficulty in making transformations between different coordinate frames (Dijkerman et al., 2006; Blangero et al., 2010).

Furthermore, the difficulty of reaching targets located in the visual periphery has also been observed to manifest along with a strong bias of the movement towards the gaze’s direction

(Jackson et al., 2005). This symptom, called “magnetic misreaching” (Carey et al., 1997; Buxbaum and Coslett, 1997), has been suggested to result from a breakdown in the ability to decouple eye and hand movements for spatially independent actions.

The analysis of the dynamics of limb and eye movements in patients with posterior parietal lesions has led to an alternative hypothesis to further explain optic ataxia. As previously mentioned, patients affected by this deficit also show an inability to make real-time adjustments based on visual feedback. To test the capacity of patients with this disorder to make rapid movement corrections, a target jump paradigm has been used (Pisella et al., 2000; Rossetti et al., 2005; Gaveau et al., 2008). It has been observed that patients with optic ataxia are unable to adjust their reaching movement in response to a change in the target’s location. Therefore, the alternative framework explains the disorder as a product of a disruption in the online visuomotor control.

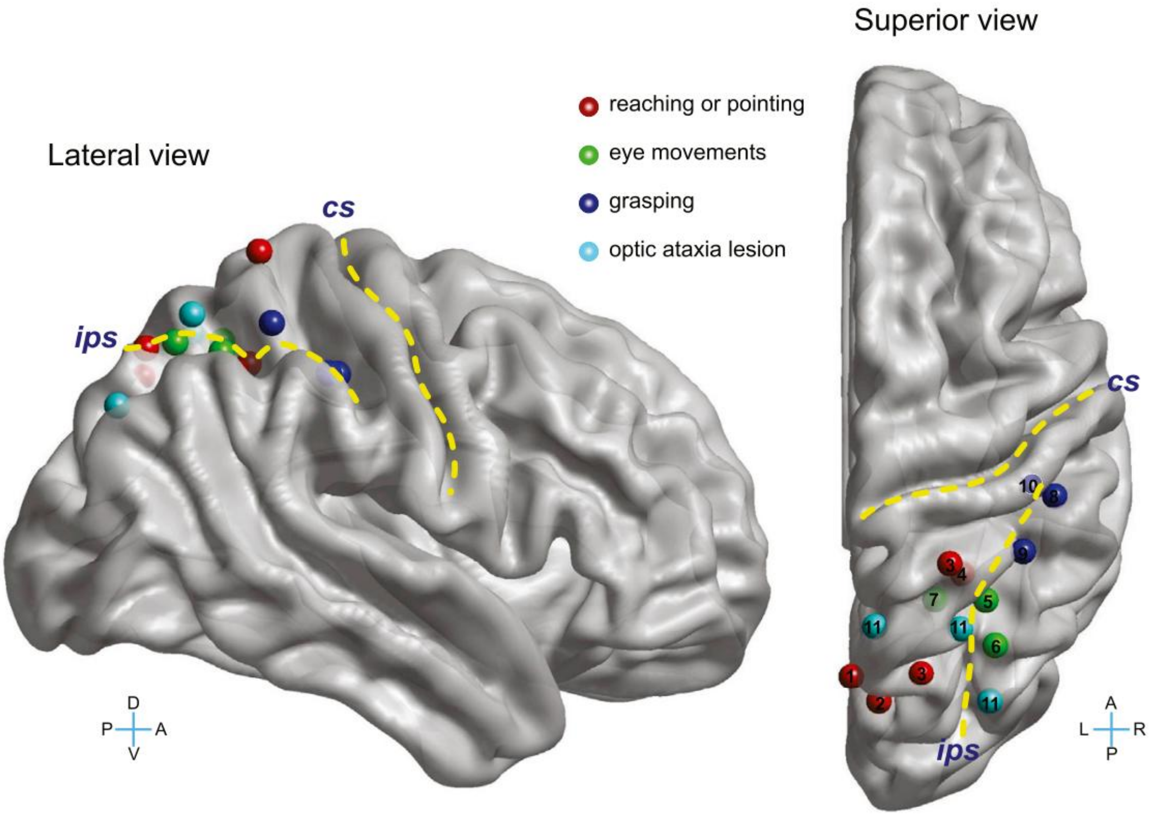

Figure 3. Lesion sites in optic ataxia and action-specific regions for reaching, pointing, eye movements, and grasping are mapped in the human posterior parietal cortex (PPC). The yellow lines indicate the central (CS) and intraparietal (IPS) sulci. L stands for left, R for right, D for dorsal, and V for ventral. The Talairach coordinates of these sites, reported by Culham et al. (2006), have been translated to the Montreal Neurological Institute template and visualized using BrainNet Viewer (Xia et al., 2013). Due to brain convolutions, not all sites are visible in the lateral view. The numbers in the superior view correspond to the original studies that identified these sites: (1) Connolly et al., 2003, (2) Astafiev et al., 2003, (3) Prado et al., 2005, (4) Grefkes et al., 2004, (5) Petit and Haxby, 1999, (6) Sereno et al., 2001, (7) Medendorp et al., 2003, (8) Binkofski et al., 1998, (9) Culham et al., 2003, (10) Frey et al., 2005, and (11) Karnath and Perenin, 2005. (from Andersen et al., 2014)

Finally, monkey studies have demonstrated a link between the posterior parietal cortex, and the deficits observed in optic ataxia through direct causal evidence (Hwang, Hauschild, Wilke, & Andersen, 2012). Battaglini et al. (2002) has demonstrated that V6A lesions in monkeys produce misreaching and misgrasping with the arm contralateral to the lesion in visually guided movements (see Figure 4). In fact, V6A is a bimodal visual/somatosensory area that processes visual information such as shape, motion, and spatial details essential for guiding both reaching and grasping movements.

Therefore, it has been suggested that selective lesions of area V6A in monkeys produce deficits similar to those observed in humans with optic ataxia, indicating that lesions in the "human" area V6A, i.e. the superior parieto-occipital cortex, are responsible for these deficits (Cavina-Pratesi et al., 2010).

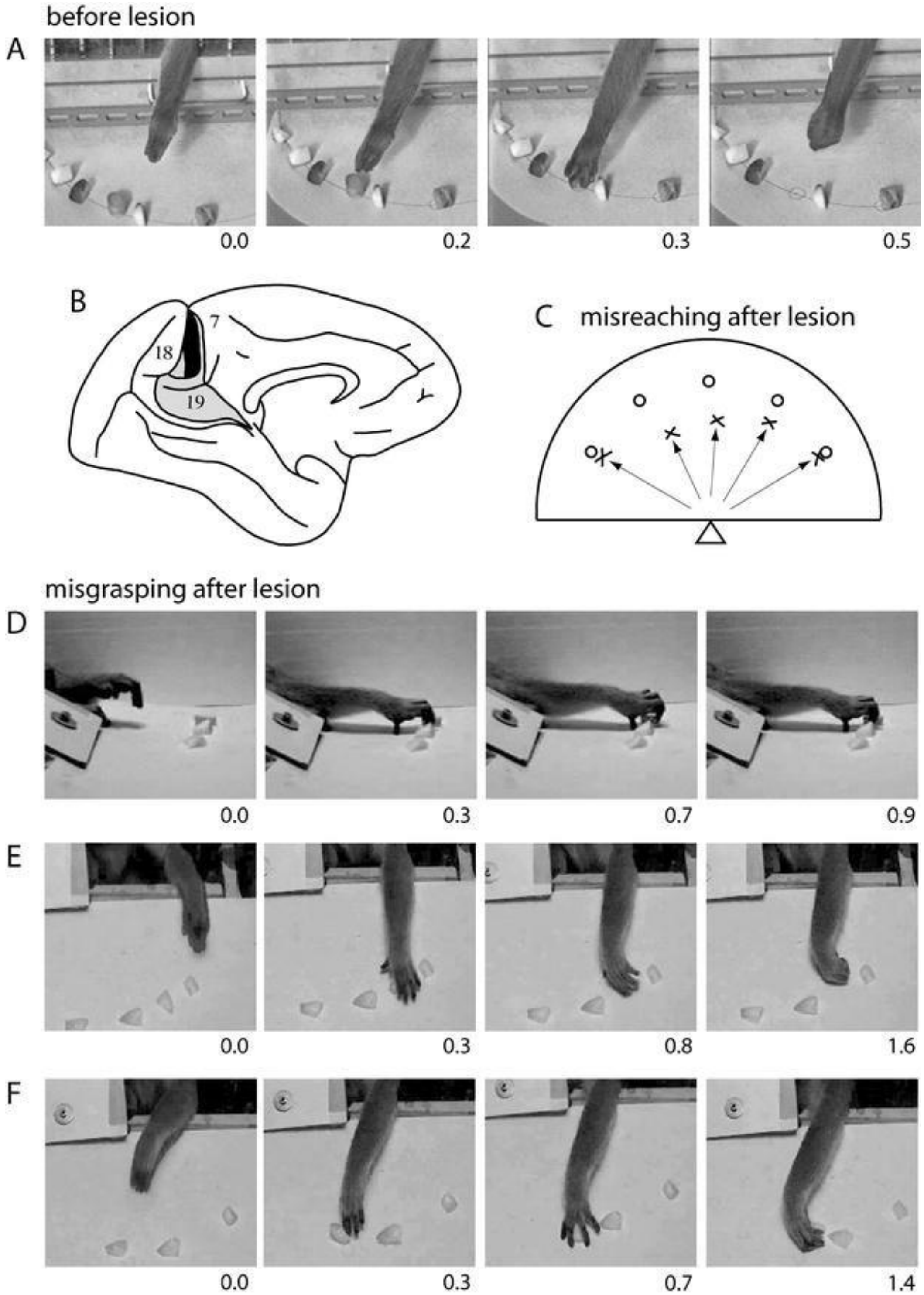

Figure 4. Misreaching and misgrasping after lesion of monkey area V6A. A) Frames from a digital TV camera illustrating the behaviour of a normal animal in reaching and grasping food. Time below frames is in seconds. B) Reconstruction of location and extent of the brain damage in case V6M2 of Battaglini et al. (2002). The lesion is indicated on the silhouette of monkey brain reported by Brodmann (1909), adapted in size to match the brain of the monkey reported by Battaglini et al. (2002). The lesion was bilateral, but here is reported (in black) only the lesion in

the left hemisphere; that in the right hemisphere was very similar in location and extent (see Battaglini et al. 2002). Dorsal area 19 is shown in grey; its location and extent, as well as locations of areas 18 and 7, are according to Brodmann (1909). C) Misreaching after bilateral V6A lesion. Food (raisins) was distributed on a semicircular plate placed horizontally in front of the animal, as shown in the frames at the top of the figure. The plate is seen here from above, and the position of the monkey is indicated by the triangle. Open circles indicate food locations. Crosses indicate the locations where the hand landed in the first attempt to reach the food. D–F) Frames from a video camera illustrating the excessive widening of grip aperture, the delayed grip of the object (see times below frames), and the anomalous rotation of the wrist that led the fingers to close laterally rather than downward. Time below frames is in seconds (from Galletti et al., 2003).

2.3 Reaching and grasping actions

The ability to perform actions is a crucial human skill learned throughout life. This distinctive interaction with the environment encompasses the exposure and learning of specific set of routines to master the appropriate gestures for effective object use. The two main functional components to perform object-related actions are reaching and grasping (Vingerhoets, 2014). Reaching can be described as the transportation component performed by the upper limb as it moves the hand toward an external object location. Therefore, this movement component requires an integration of the hand and object positions into a single reference frame, combining proprioceptive and visual information.

Instead, grasping is considered the grip component of object-related actions and involves extracting specific characteristics from objects, such as size, shape, orientation, texture and estimated weight. This allows for proper hand preshaping, regulation of movement speed, and finally, closing the fingers around the object with the appropriate grip force.

Although a case of dissociated compromission of the reaching and grasping components after a unilateral left lesion of the posterior parietal cortex has been reported (Cavina-Pratesi et al, 2010; 2013), grasping impairments have been associated with optic ataxia since the earliest reports of misreaching following parietal damage in both monkeys and humans (La Motte and Acuna, 1978; Damasio and Benton, 1979; Faugier-Grimaud et al., 1985; Ferrier, 1886, 1890; Jeannerod, 1986b; Perenin and Vighetto, 1988). This is also demonstrated by the kinematics of a reach-and-grasp movement, which shows adaptation of the grip aperture during the reaching phase of the gesture (Jeannerod et al., 1995; Castiello, 2005).

Finally, it seems that several areas are activated during both reaching and grasping, although a preference for responsiveness to either action can often be observed (Vingerhoets, 2014).

2.4 The interplay of reaching and grasping actions with perception in the real world

In everyday life, the transport and grip components of object-related movements merge into a seamless action, forming a continuum. However, different actions can induce different effects on our perception of the object we interact with.

As aforementioned, the reaching phase, which involves moving the arm to direct the hand towards an object, is primarily guided by visual cues indicating the precise object's location. In contrast, the simultaneous preparation of the hand and fingers for grasping the object, i.e. the grip component, is mainly influenced by the geometric characteristics of the object, such as its shape and size.

Therefore, the preparation and execution of reaching and grasping are greatly influenced by the perception of the object's location and its physical characteristics, respectively, during interaction. In fact, visual information significantly contributes to the planning phase of movements, providing the relevant information that facilitates the success of an action.

For example, when preparing a reaching action towards an object, the eyes perform a saccade, a rapid ballistic eye movement to direct the fovea to an area of interest, and then fixate it constantly until it is reached by the hand (Johansson et al., 2001). Moreover, it has been observed how the pattern of fixations varies depending on the nature of the task to perform with an object (Brouwer et al., 2009). During a viewing task, fixations fall on the object's center of gravity, whereas during a grasping task, fixations first focus on the point of contact for the index finger and then move the object's center of mass.

Interestingly, action and perception mutually influence each other, so that the spatial perception of an object is also influenced by the action we want to perform. In the context of eye movements, it has been found that the perception of the area of interest of an object is enhanced shortly before execution (Hoffman & Subramaniam, 1995; Deubel & Schneider, 1996; Neggers et al., 2007; Bosco et al., 2023).

Other studies have tested whether action planning affects perceptual processing, by testing the combination of different types of actions with specific object features. These studies have demonstrated that the type of action being planned biases visual search toward important action-related features, facilitating their perception (Fagioli et al., 2007; Wykowska, Schubö, & Hommel, 2009; Wykowska, Hommel, & Schubö, 2011).

Specifically, it was found that the preparation of a grasping movement towards 2-dimensional targets on a frontal screen facilitated the detection of a size-related parameters, while the preparation of a pointing movement facilitated the detection of a location-related parameters. In fact, size-related parameters are fundamental for preparing the grip aperture in a grasping movement (Wykowska et al., 2009), and location-related parameters, such as luminance, are crucial for preparing a pointing movement (Anderson & Yamagishi, 2000; Graves, 1996).

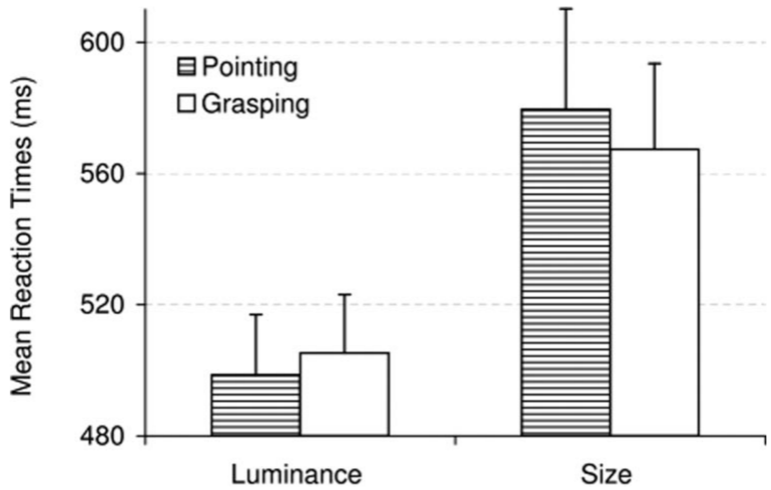

Figure 5. Significant interaction between task-relevant dimension and movement type. The image illustrates faster mean reaction times to luminance as task-relevant dimension and size as task-relevant dimension while participants prepared a pointing movement (filled bars) or a grasping movement (empty bars) respectively (from Wykowska et al., 2009).

Likewise, Gutteling et al. (2011) found that preparing for a grasping action increases the detection of object orientation changes, relative to the preparation of a pointing action for which orientation is an irrelevant parameter. These studies suggest that the perception of object's features, such as size, is facilitated when the planned action requires the elaboration of those properties.

A significant number of studies on the action modulation effect focused on the preparation phase of the movement (Deubel & Schneider, 1996; Gutteling et al., 2011; Hoffman & Subramaniam, 1995; Neggers et al., 2007), while other studies found that also after the execution of a grasping movement the perception of two-dimensional object size was modulated, revealing a tendency for the perceived sizes of objects to be scaled by the type of action (Bosco et al., 2017; Sans Diez et al., 2022). In particular, it has been found that grasping influences the perception of size more than reaching, supporting the idea that different body-based movements affect the perception of different object characteristics.

Finally, the impact of action planning and execution on perception can extend to the leg effector domain. As a matter of fact, it has been observed how the effort required to walk a certain distance influence the perception of the distance itself (Witt et al., 2004; Proffitt, 2006), and how the walking action can improve the perception of distance in virtual environments, where a compression of space is usually perceived (Waller & Richardson, 2008).

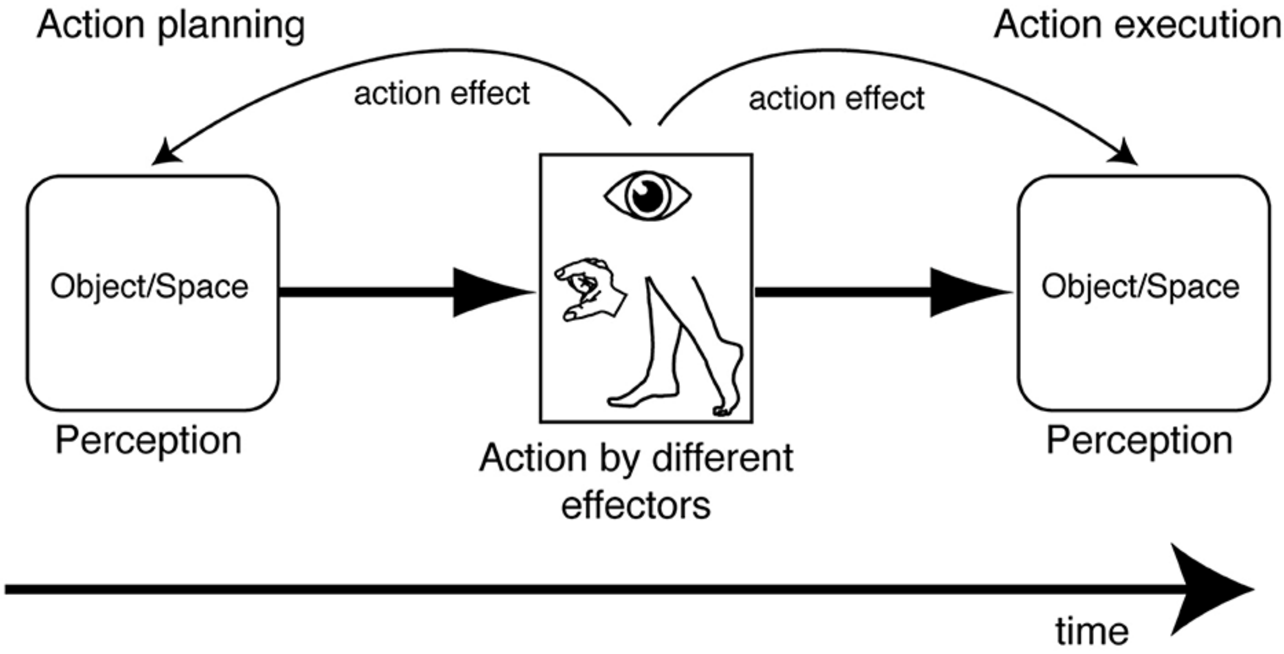

Figure 6. Summary of object/space perception modulation by action planning and action execution evoked by movement of different effectors. (from Bosco et al., 2023)

2.5 The interplay of reaching and grasping actions with perception in virtual reality

The connection between physical actions and perceptual adjustments provides valuable insights into how our bodies interact with and interpret not only the physical world but also the virtual one.

Virtual reality is a multisensory experience that allows users to interact with objects or events in computer-generated three-dimensional environments (Shultheis, 2002).

However, perception in these environments has been found to differ from physical reality, particularly in terms of spatial perception. Both size and distance are perceived less accurately in virtual reality with systematic underestimations of size and distance typically observed (Waller & Richardson, 2008; Stefanucci et al., 2015; Kelly et al., 2018). The cause of these distortions is unclear and cannot be entirely attributed to factors such as a reduced field of view, quality of the graphics, or the physical weight of the head-mounted display (Repka et al., 2022).

One common approach to improve distance perception in virtual reality allows participants to interact with the virtual environment while receiving visual feedback of their movements (Kelly, Donaldson, Sjolund & Freiberg, 2013; Kelly, Hammel, Siegel, & Sjolund, 2014; Mohler, Creem-Regehr & Thompson, 2006; Richardson & Waller, 2005, 2007; Waller & Richardson, 2008). A study of Waller & Richardson (2008) showed that distance judgments in a virtual environment were unaffected by interactions in which participants viewed only a simulation of visual walking. Thereby, physical walking was found to be necessary to elicit an increase in post-interaction distance judgments and simulated visual walking without concomitant physical walking was found to be insufficient.

Moreover, because of the size-distance variance hypothesis (Sedgwick, 1986), which postulates that perceived size and perceived distance are tightly coupled, Kelly et al. (2013) used size-based distance judgments to evaluate the effect of different actions on the perception of the distance of an object in a virtual environment. They found that distance judgments increased after a walking action, while they did not improve after participants interacted with the virtual environment by performing a reaching movement (see Figure 7 and 8). This suggests that not all body-based interactions are sufficient to cause an improvement in distance judgments in virtual reality.

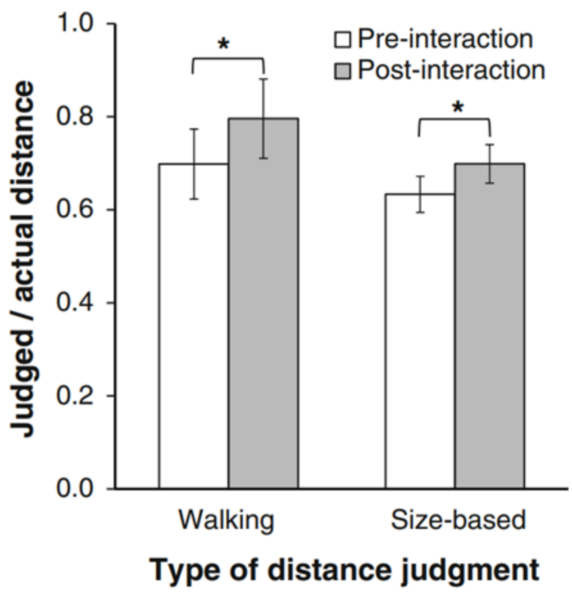

Figure 7. Mean ratios of judged distance to actual distance in a virtual environment. Participants made walking distance judgments and size judgments (which were later converted to size-based distance judgments) before and after interacting in the environment by walking. The asterisks indicate significant differences between the conditions at $p < .05$ (from Kelly et al., 2013).

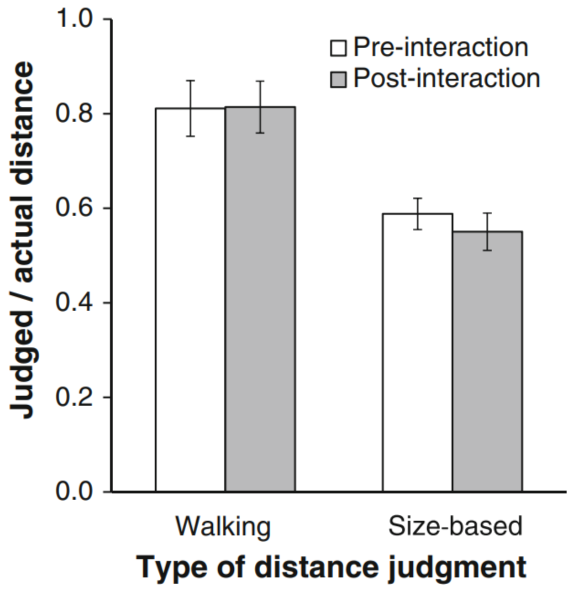

Figure 8. Mean ratios of judged distance to actual distance in a virtual environment. Participants made walking distance judgments and size judgments (which were later converted to size-based distance judgments) before and after interacting with a virtual environment by reaching. No significant differences were found (from Kelly et al., 2013).

Virtual spaces are increasingly being used as a delivery system for rehabilitating upper and lower limb impairments and activities of daily living post-stroke (Adamovich et al., 2009). However, given that the viewing environment's quality can affect how movement is executed (Ustinova et al., 2010), it is crucial to ascertain whether movements performed in a virtual environment resemble those executed in an equivalent physical setting (Subramanian et al, 2011) and this includes exploring the reciprocal impact between movements and perception.

3. AIM OF THE THESIS

The aim of the present thesis is to investigate the intricate processes of sensorimotor integration and its impact on movement execution and perception. Specifically, the research focuses on two main objectives. The first objective is to evaluate the impact of visuomotor disruption caused by occipitoparietal lesions on motor trajectories. In fact, a kinematic characterization of the entire reaching action in depth and direction in patients with a posterior parietal cortex damage and optic ataxia syndrome is still lacking. To this end, the first study presented compares the reaching movements of a patient with optic ataxia symptoms to those of a healthy group, employing a novel decoding method to identify and characterize pathological motor behaviours. This first part of the thesis highlights the possibility to discriminate the performance of a patient by observing kinematic components of arm movement well in advance with respect to the conclusion of the action. In the long term, this result could provide a methodology for exploring to which extent the available kinematic information could reliably predict an impaired versus a healthy reaching behaviour.

The second objective of the thesis is to explore the effects of different interactions on object perception in virtual reality. Perception in virtual environments is usually less accurate than in physical environments and no studies were performed to systematically evaluate the influence of multiple actions on the possible facilitation of object perception in the virtual space. To bridge this gap in the literature, the second study presented here compares the effect of different interaction conditions on the perception of objects in the virtual space.

Finally, by integrating findings from these studies on neurological impairments and healthy populations using advanced experimental paradigms, this thesis aims to contribute to our understanding of sensorimotor integration in real and virtual environments.

4. FIRST STUDY

"Machine learning methods detect arm movement impairments in a patient with parieto-occipital lesion using only early kinematic information"

4.1 INTRODUCTION

In our daily life, successful reaching movements in the peripersonal space rely on our ability to correctly plan and execute arm trajectories to targets located in the three-dimensional (3D) space. This capacity depends on the coordinated activity of different areas, some of them located in the posterior parietal cortex (PPC). Indeed, unilateral (Karnath & Perenin, 2005; Perenin & Vighetto, 1988) or bilateral (Karnath & Perenin, 2005; Khan et al., 2005; Pisella et al., 2000, 2004) PPC lesions often cause optic ataxia (OA), typically described as a high-order motor disorder with impaired visually guided reaching (Perenin & Vighetto, 1988). The sites of the lesion in patients with OA typically involve the parietal occipital junction, the superior parietal lobule (SPL), and areas around the posterior end of the intraparietal sulcus (Karnath & Perenin, 2005; Martin, Karnath, & Himmelbach, 2015). These parietal regions have been shown to contain reach-selective neurons in the monkey (Battaglia-Mayer et al., 2001; Bosco, Breveglieri, Chinellato, Galletti, & Fattori, 2010; Bosco, Breveglieri, Hadjidimitrakis, Galletti, & Fattori, 2016; Bosco, Breveglieri, Reser, Galletti, & Fattori, 2015; Fattori, Gamberini, Kutz, & Galletti, 2001; Fattori, Kutz, Breveglieri, Marzocchi, & Galletti, 2005; Ferraina et al., 1997; Grafton, 2010; Hwang, Hauschild, Wilke, & Andersen, 2014; McGuire & Sabes, 2011; Snyder, Batista, & Andersen, 1997) and in the human (Aflalo et al., 2015; Zhang et al., 2017) brain.

OA is characterized by misreaching toward peripheral (Rossetti, Pisella, & Vighetto, 2003) and central (Buiatti, Skrap, & Shallice, 2013; Buxbaum & Coslett, 1997; Ferrari-Toniolo et al., 2014; Goodale et al., 1994; Jeannerod, Decety, & Michel, 1994; Perenin & Vighetto, 1988) visual targets. This deficit does not appear with reaches to auditory or tactile stimuli (Rossetti et al., 2003), thus suggesting that OA is caused from a specific deficit in coupling vision with action. Most OA studies focused on examining reaching end points and on the trajectory of the transport phase of arm movement. In particular, the literature reported a systematic deviation of both end points and movement trajectories for reaching to peripheral targets (Blangero et al., 2010; Dijkerman et al., 2006; Jackson, Newport, Mort, & Husain, 2005; Khan et al., 2007;

Milner, Dijkerman, McIntosh, Rossetti, & Pisella, 2003). In addition, patients with OA show a lack of the ability to change the movement trajectory to avoid possible collision with no-target stimuli (Schindler et al., 2004) as well as a lack of the correction of reaching movements in relation to rapid changes of target location (Blangero et al., 2008; Pisella et al., 2000). Monkey studies have demonstrated the link between PPC to the deficits observed in OA by direct causal evidence (Hwang, Hauschild, Wilke, & Andersen, 2012). Furthermore, in monkeys, the existence of a combined encoding of depth and direction signals was found in some PPC sectors during reaching movement (Bosco et al., 2016; Hadjidimitrakis, Bertozzi, Breveglieri, Bosco, et al., 2014; Hadjidimitrakis, Dal Bo', Breveglieri, Galletti, & Fattori, 2015), whereas other sectors showed segregated processing of these signals (De Vitis et al., 2019; Lacquaniti, Guigon, Bianchi, Ferraina, & Caminiti, 1995). In patients with OA, few studies have investigated encoding of depth and direction in reaching movements (Brain, 1941; Cavina-Pratesi, Ietswaart, Humphreys, Lestou, & Milner, 2010; Danckert, Goldberg, & Broderick, 2009; Holmes & Horrax, 1919). In the work by Danckert et al. (2009) in particular, the authors found that the movements executed by patients with OA along the sagittal axis were more impaired than the movements executed along the horizontal axis, thus corroborating the evidence that reach depth and direction might have a distinct neural control.

However, a kinematic characterization of the entire reaching action in 3D space in patients with PPC damage and OA syndrome is still lacking. Here, we reconstructed the movement trajectory and measured the end point errors in one patient with occipitoparietal lesion that reached toward targets located at different depths and directions in 3D space, and we compared them with those measured in healthy participants. Using a novel decoding approach for these studies, we assessed how well kinematic predictors were able to discriminate whether the movement was performed by the patient or by healthy participants and at which stage during movement unfolding. In the long term, our results could provide a methodology for exploring to which extent the available kinematic information could reliably predict an impaired versus a healthy reaching behavior.

4.2 METHODS

The study was approved by the Ethical Committee of the University of Bologna and carried out in accordance with the recommendations of the Bioethical Committee of the University of Bologna and with the Declaration of Helsinki. All participants gave written informed consent to participate and were naïve to the purpose of the experiment.

4.2.1 Participants

Ten right-handed, healthy control participants took part in this study (mean age, 21.5 ± 2.0; 9 females and 1 male). They all had normal, or corrected to normal, vision. All participants had no history of musculoskeletal or neurological disorders.

In addition to control participants, patient S.T. was also tested. S.T. is a 19-year-old, right-handed man. At the time of testing session, he was a student with 12 years of education. Six years before testing session, at the age of 13, he suffered from a cardiocirculatory arrest, with a resulting vegetative state owing to severe cerebral anoxia. The most recent magnetic resonance image (MRI; 3 years before testing session) documented the presence of altered signal, plausibly owing to ischemic damage in the occipitoparietal cortex in both hemispheres. The lesion was traced manually on the most recent MRI obtained using T1-weighted template MRI scan from the Montreal Neurological Institute provided with the MRIcro software (Rorden & Brett, 2000). Localization of the damaged brain regions was obtained by superimposing the traced lesion reconstruction on the automated anatomical labelling template. Damage in the left hemisphere was located in the superior and inferior parietal lobule, in the angular gyrus and the precuneus, whereas damage in the right hemisphere mainly involved the precuneus (Figure 9).

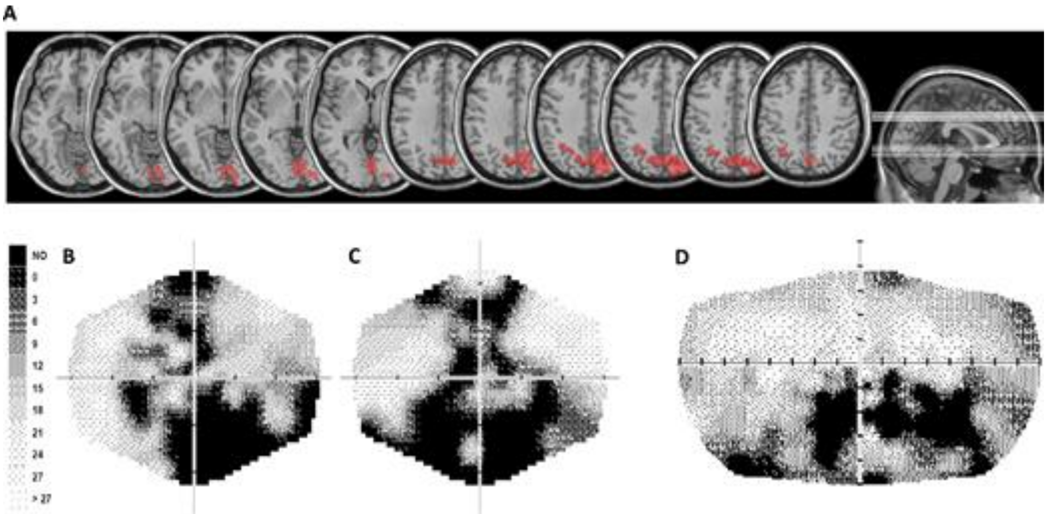

Figure 9. Patient S.T. lesion reconstruction. The image shows patient S.T. lesion projected onto axial slices of the standard MNI brain. In each slice the left hemisphere is on the left side. The levels of the axial slices are marked by white lines on the sagittal view of the brain (right). (B-D) Computerized automated visual perimetry of S.T. Greyscale images for the left (B) and the right (C) eye and for the binocular visual field (D). Axial hash marks denote 10 visual degree increments. Color map reports decibel values corresponding with each point in the gray scale.

4.2.2 Apparatus and stimuli

Participants sat in a dimly illuminated room in front of a 19-inch touchscreen (ELO IntelliTouch 1939L) laid horizontally on a desk located at waist level. The head of participants was supported on a chin rest to minimize movements. Participants sat with the dominant right hand on a board placed adjacent to the screen within a square marked with a tape and detectable by touch (size 12 × 12 cm) placed in front of the participant's chest, as sketched in Figures 10A and 10B.

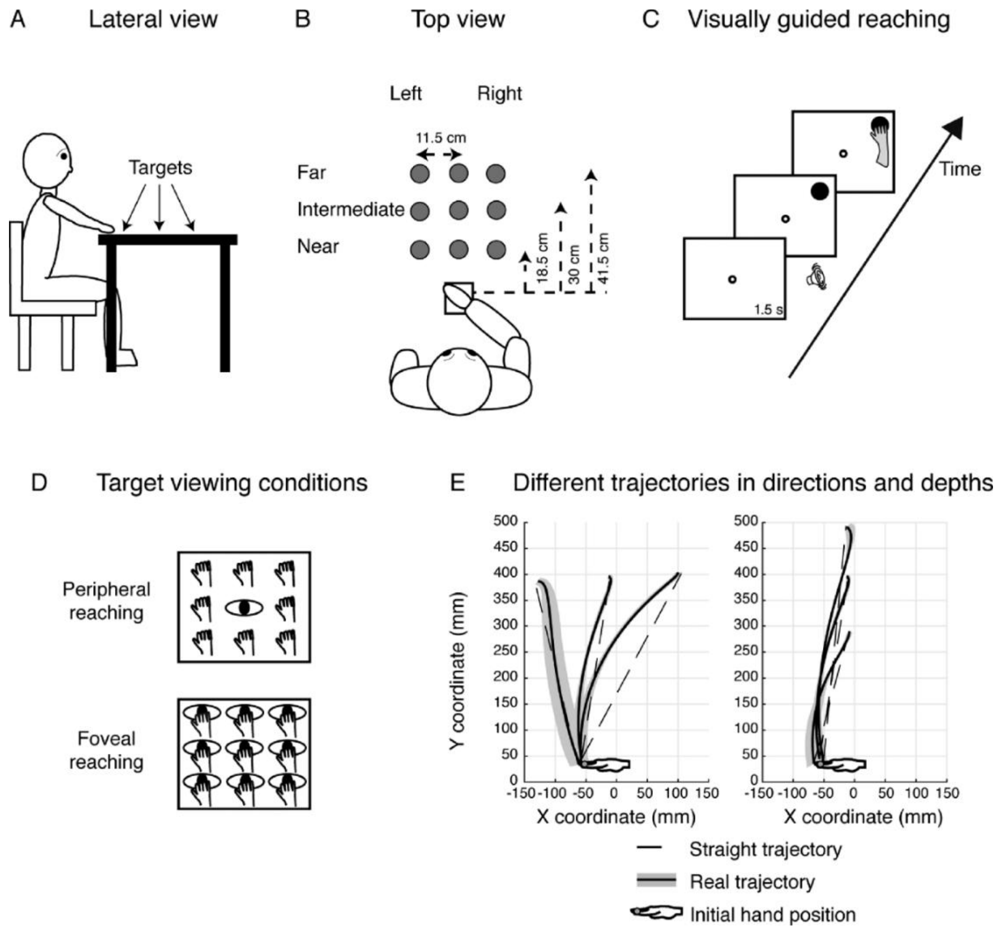

Figure 10. Experimental setup. (A) Lateral view of the target arrangement with respect to the participant's body. (B) Top view of the target arrangement in the peripersonal space. The participants performed reaching movements with their right hand toward one of the nine dots projected on the screen at different depths (near, intermediate, and far) and in different directions (left and right positions). Reaching movements were performed in a dimly lighted room, starting from the initial hand position located next to the body and marked by a squared surface (white square). (C) Time sequence of the visually guided reaching in the peripheral reaching configuration. The small white dot represents the fixation target; the filled black dot represents the reaching target. The fixation target stayed on for 1.5 s and then the reaching target was turned on in one of the nine locations. As soon as the reaching target appeared on the screen, a sound indicated to the participant to reach with his or her right hand the position of the target while maintaining fixation on the fixation target. The fixation target lasted until the participant completed the movement. (D) Top view of the two task configurations. (Top)

Peripheral reaching: reaching movements were performed toward one of the nine targets (hands). The spatial position of the target changed trial to trial, but gaze was kept constant at the central position (eye). (Bottom) Foveal reaching: reaching movements were performed toward one of the nine targets. During the task, the participant had to fixate and reach the same target (eye and hand on the panel). (E) Representation of real and straight trajectories in a control participant. (Left) Distribution of the real (shaded traces) and straight (dotted lines) two-dimensional trajectories toward left and right targets (direction dimension). (Right) Distribution of the real (shaded traces) and straight (dotted line) two-dimensional trajectories toward the near, intermediate, and far targets (depth dimension).

Green (diameter 0.3 cm) and red (diameter 1.2 cm) dots were presented at different depths and directions with respect to participant's midline. The screen on which stimuli were presented had a visible display size of 37.5 × 30 cm and 15,500 touch points/cm2 with a resolution of 1152 × 864 pixels and a frame rate of 60 Hz.

Reaching movements were recorded using a motion tracking system (VICON motion capture system) by sampling the position of two markers at a frequency of 100 Hz; markers were attached to the wrist (on the scaphoid bone) and on the nail of the index finger (reaching finger). The marker on the wrist was used to detect the onset and offset of reaching movements. The marker on the tip of the index finger was used for kinematic analysis, because it was the hand portion that made contact with the target (Carey, Hargreaves, & Goodale, 1996).

4.2.3 Behavioural paradigm

Participants performed reaching movements toward the touchscreen using their right hand. As depicted in Figure 10B, there were nine possible locations in which targets could appear: three placed at near distance (18.5 cm from the initial hand position), three at intermediate distance (30 cm from the initial hand position), and three at far distance (41.5 cm from the initial hand position) (as in Bosco, Piserchia, & Fattori, 2017). The targets were arranged in a square of 23 × 23 cm, and were located 11.5 cm one from each other, either on the left or the right side, the central targets were placed along the sagittal midline. All targets were located within a comfortable reaching distance. Although patient S.T. reported visual field defects to the lower parts of the peripheral visual field, he could effortlessly detect all the targets presented in our task. Indeed, stimuli were located in the central part of the visual field, in which S.T. reported no detection impairment. However, he was instructed not to perform any arm movement unless he had a good view of the target.

We tested participants in a visually guided reaching task as shown in Figure 10C. The sequence of visually guided reaching consisted in the presentation of a fixation target (green dot) that stayed on for 1.5 s. Then, the appearance of reaching target (red dot) and an acoustic signal indicated to participants that they could reach the position of the target maintaining the fixation on the green fixation dot. Both fixation and reaching targets remained illuminated until participants completed the arm movement. Participants were asked to move at a fast but comfortable speed and to be as accurate as possible. We tested two different viewing conditions (see Figure 10D): the peripheral reaching, where the gaze was fixed on the central and intermediate target position and the hand reached toward one of the remaining positions, and the foveal reaching, in which fixation and reaching targets were coincident. Note that the spatial location of the targets to be reached was identical in the two tasks. During the arm movement, fixation was controlled online by the experimenter. We are aware that this was not a reliable method for controlling eye movements and represents a limit of the study, but it allowed us to qualitative detect on average 1.2% for each participant and 1.8% for patient S.T. trials where participants did not maintain fixation. Based on this online inspection, all trials without correct fixation were discarded from the analyses.

The task was composed of five blocks with 17 trials each. Within each block, trials of the two viewing conditions were randomized. We used MATLAB (MathWorks, Natick, MA) with the Psychophysics toolbox extension (Brainard, 1997) for stimuli presentation and data analysis.

4.2.4 Data analysis

For data processing and analysis, the velocity profiles of all markers were computed with custom software written in MATLAB. The onset of movement was defined as the time point when wrist velocity was higher than 5 mm/s; the following offset was detected when wrist velocity dropped decreased to less than 5 mm/s. In addition, the experimenter carefully checked for the movement onset that after the threshold of 5 mm/s the wrist velocity increased without interruptions until the peak of velocity. For the movement offset, the first point of wrist velocity remaining below the threshold of 5 mm/s was considered to exclude any adjustment of reaching on the screen.

To study the trajectories of reaching movements and to quantify how participants' motor responses were stereotyped, we calculated the horizontal, sagittal and vertical deviations of each single trajectory with respect to a straight (virtual) trajectory. In reaching movements, deviations from a straight-line path are likely influenced by a combination of biomechanics, due to joint rotations and muscular coordination, and cognitive representations of space. The straight trajectory used was defined as the line connecting the starting position of the hand to the reaching-target position. This approach has been used by Kasuga, Telgen, Ushiba, Nozaki, and Diedrichsen (2015). Along the horizontal axis we calculated the horizontal trajectory deviation as the difference between the X component of the real trajectory and the X component of the straight trajectory (Figure 10E, left), whereas along the sagittal axis, we calculated the sagittal trajectory deviation considering the difference between the Y component of the real trajectory and the Y component of the straight trajectory (Figure 10E, right). For vertical deviation, we took into account the Z component of the real trajectory, as the straight trajectory had no elevation component. To minimize the interindividual variability observed in movement time and to normalize across participants, horizontal, sagittal, and vertical deviations were separately calculated on 10 time intervals across the entire duration of movement in each participant. The 10 time intervals were calculated for each trial and then averaged across each participant. Then, we plotted the x, y, and z trajectory deviations as a function of the percentage of movement time, resulting in curved lines with negative and positive inflections. Negative values of trajectory deviations correspond with real trajectory on the left, behind, or down with respect to the straight one considering the x, y, or z components, respectively. Positive values of trajectory deviations correspond with real trajectory on the right, in front or up with respect to the straight one according to the x, y, and z trajectory components, respectively. We calculated the time when minimum deviation toward negative values occurred and compared them by a modified version of the independent sample two-tailed t test (Crawford & Garthwaite, 2002; Crawford & Howell, 1998; Danckert, Goldberg, & Broderick, 2009). This analysis allows to test whether an individual's score is significantly different from a control or normative sample and provide a point estimate of the abnormality of the scores (i.e., it estimates the percentage of the population that would obtain a lower score) according to the formula:

$$t = \frac{X_1 - X_2}{S_2\sqrt{(N_2 + 1)/N_2}}$$

where X_1 is the individual's score, X_2 the mean score in the control sample, S2 the standard deviation of scores in the control sample, and N_2 the number of participants in the control sample. The statistical test follows a t distribution on $N_2 - 1$ d.f. Multiplying the one-tailed probability of t by 100 gives the point estimate of the abnormality of the individual's score in percent.

Decoding from reaching trajectories

To evaluate whether a movement was performed by the patient or a control participant, we adopted a machine learning approach and applied a linear discriminant analysis (LDA). This classification analysis was executed to compare the power of the LDA in recognizing the patient's performance from that of control participants in all targets tested and for both peripheral and foveal conditions. A LDA is a standard classification technique used to allocate a new observation to one of N_G of two or more groups (usually referred to as classes) based on its measured parameters, that in our case are the horizontal, sagittal, and vertical deviations in each temporal division considered (features). The prediction of LDA consists in finding discriminant functions that divide the features space in N_G regions, so that each region spans the range of feature values that most likely characterize a given class. This is done on the basis of a set of previous observations for which the group assignment is known (training dataset), by maximizing the ratio of the between-groups to within-group variabilities (Marcia, Kent, & Bibby, 1995; Maselli et al., 2017). We divided the whole time interval into 10 equal parts, for each time interval an independent classifier was trained. Features were extracted as follows: deviations were calculated as detailed in the previous section, when the classifier was trained to separate left center and right target positions or near, intermediate and far positions, features always included x, y and z components of the movement. Each time interval comprising 10% of the movement (and corresponding with a single classifier) was further subdivided into three time bins, so each classifier was trained with n consecutive values each corresponding with 3.3% of the movement time. In this way, a temporal information has been provided to the model. The samples thus corresponded to vectors of n elements × 3 (x, y, and z components), each sample being computed on a possible repetition of the movement (trial). Because the left, middle, right, or three depth levels were considered over six different classifiers, trials corresponding with the same group were considered together, for example, the classifier that considered left deviations was fed with the three positions, namely, near, center, and far from left targets. Also taking together multiple positions, the available trials were few (15 trials), so we used a leave-one-out cross-validation technique to validate our model. Final accuracy results were reported averaging recognition rates over the 15 test set (error bars were 95% bootstrapped confidence intervals). The analysis was proposed to train separate classifiers to resolve a binary classification between patient and single controls (10 combinations), and to compare the power of the LDA in recognizing the patient's performance from that of control participants and in recognizing the performance between healthy participants in all targets tested and for both peripheral and foveal conditions (Figures 19 and 20).

Reaching end point analysis

Movement accuracy and precision were extracted by end points recorded as the x and y coordinates of index finger when it touched the screen and the x and y coordinates of the target locations. The spatial coordinates of the target locations were obtained by recording the X and Y positions of reflective markers placed on the corresponding position of the targets projected on the screen at the end of each experimental session. The two measures were extracted for each control participant and the patient in the peripheral and foveal reaching task. The accuracy was calculated as follows:

$$Accuracy = \sqrt{(x_M - x_{loc})^2 + (y_M - y_{loc})^2}$$

where x_M and y_M are the average end point coordinates and x_{loc} and y_{loc} are the target location coordinates. The precision was calculated as it follows:

$$Precision = \ mean\left(\sqrt{(x_i - x_M)^2 + (y_i - y_M)^2}\right)$$

where xi and yi are the end point coordinates for each trial and x_M and y_M are the average end point coordinates. We statistically compared the accuracy and precision of control participants with those of the patient S.T. using a one-tailed t-test analysis and Bonferroni post hoc tests. The significant level for all analyses was set to 0.05.

4.3 RESULTS

Patient S.T. is a young man with bilateral occipitoparietal lesions. MRI reconstructed lesion extent of S.T. revealed damage in the left hemisphere encompassing the superior and inferior parietal lobule, in the angular gyrus and the precuneus, and damage in the right hemisphere, mainly involving the precuneus (Figure 9A). He performed clinical tests reported below in this article and the experimental task described in the Method section.

4.3.1 Clinical tests

A complete neuropsychological examination at the time of testing session showed: attentional deficits (in the subtests “acoustical vigilance,” “alertness,” “divided attention,” and “response flexibility” of the Italian version of the Test of Attentional Performance (Zimmermann & Fimm, 1992; Zoccolotti, Pizzamiglio, Pittau, & Galati, 1994); impairments in executive functions (Tower of London (Culbertson & ZIllmer, 2000), working memory (subtest "Working Memory" of the Italian version of the Test of Attentional Performance; Zimmermann & Fimm, 1992), long-term and short-term spatial memory (Caffarra, Vezzadini, Dieci, Zonato, & Venneri, 2002; Osterrieth, 1944); Corsi-Block tapping test (Spinnler & Tognoni, 1987), and constructive apraxia (Osterrieth, 1944) (Rey-Osterrieth Complex Figure Test (Caffarra et al., 2002). S.T. also showed defective visual exploration abilities (subtest "visual exploration" of the Italian version of the Test of Attentional Performance (Zimmermann & Fimm, 1992; Zoccolotti et al., 1994). S.T.'s performance was within the normal range in verbal memory (short story recall (Novelli et al., 1986); digit span (Orsini et al., 1987), and logical and reasoning abilities (verbal judgments; Spinnler & Tognoni, 1987). The results of neuropsychological assessment are reported in Table 1. A neurological examination did not show any hemiparesis or motor deficit and did not reveal somatosensory deficit. S.T. reported visual field defects that were mainly confined to the lower peripheral parts of his left and right visual fields, as documented by static perimetry (Medmont M700 automated perimetry apparatus, Melbourne, Australia) (Figures 9B–9D).

Table 1. Neuropsychological assessment. Notes. *A ‘Pathological performance. Patient's scores are reported in the left column, while cut-off scores are reported in the right column. CS, correct score; ES, equivalent score; SCS, screening score; SS, standard score; T, T-value. The ES ranges from 0 to 4, with 0 = pathological performance, 1 = borderline performance, and 2–4 normal performance.

	SS/CS/T/ ScS	Cut-off/ES
Attention		
Test of Attentional Performance		
Subtest acoustical vigilance		
Reaction times, minutes		
0–5	T = 43	T = 40
5–10	T = 45	T = 40
False reactions, minutes		
0–5	T = 48	T = 40
5–10	T = 36*	T = 40
Subtest alertness (reaction times)		
Without warning	T = 25*	T = 40
With warning	T = 20*	T = 40
Subtest divided attention		
Reaction times	T = 57	T = 40
Omissions	T = 20*	T = 40
Subtest response flexibility		
reaction times	T < 20*	T = 40
False reactions	T = 29*	T = 40
Executive functions		
Tower of London		
Total move score	SS = 64*	SS = 70
Total correct score	SS = 86	SS = 70
Total rule violation	SS < 60*	SS = 70
Total time violation	SS < 60	SS = 70
Total initiation time	SS = 122	SS = 70
Total execution time	SS < 60*	SS = 70
Total problem solving time	SS < 60*	SS = 70
Working memory		
Test of Attentional Performance		
Subtest working memory		
Reaction times	T = 54	T = 40
Omissions	T = 20*	T = 40
Memory		
Verbal memory		
Digit span	CS = 3.75	ES = 1
Short story	CS = 8	ES = 1
Visuospatial memory		
Corsi-Block tapping test	CS = 1.75*	ES = 0
Rey-Osterrieth Complex Figure Test (memory)	CS = 0*	ES = 0
Logical and reasoning abilities		
Verbal judgments	CS = 42.5	ES = 2
Constructive apraxia		
Rey-Osterrieth Complex Figure Test (copy)	CS = 3*	ES = 0
Visual exploration		
Test of Attentional Performance		
Subtest visual exploration test		
Target present		
Reaction times	T < 20*	T = 40
Omissions	T = 24*	T = 40

At the time of testing, S.T. showed OA as documented by clinical observation. Indeed, while looking at the examiner's nose, S.T. could correctly identify objects located in the periphery, but he could not accurately point to these objects. He also performed a pointing task (Frassinetti, Bonifazi, & Làdavas, 2007), in which he sat at a distance of 57 cm in front of a semicircular apparatus consisting of a vertical transparent plastic support. The transparent plastic support was graduated (in visual degree) and the experimenter, sitting behind the support, could record the final landing position of each pointing movement. The patient's spatial accuracy in pointing was quantified as the difference between the landing position in pointing and the actual target position.

Visual targets (i.e., a pen) were presented randomly in one of three possible positions: in a central position (0°) or to the left or the right of patient's body midline (21°). The patient was instructed to keep his head in a midline position and to fixate on a central point and the fixation was controlled online by the experimenter; he was asked to reach the targets through a pointing movement with the extended index finger, both with the right and the left hand, both in the absence (open loop condition) and in the presence (closed loop condition) of visual feedback of ongoing movement. Specifically, in the open loop condition, a cardboard covered the semicircular apparatus and prevented vision of the arm performing the movement. Ten stimuli per position, in each condition, were presented. In this clinical task, the patient's performance in each condition was compared with the performance of 10 controls (mean age, 43.8 ± 11.4; 6 females) using a modified version of the independent sample two-tailed t-test (Crawford & Garthwaite, 2002; Crawford & Howell, 1998; Danckert et al., 2009). The 10 control participants involved in this clinical task were different from those involved in the experimental task described in the next paragraph of this article.

The patient's performance was defective with both hands, both in the open loop and closed loop conditions and irrespective of target position (all Ps < 0.011) with the exception of pointing movements performed with the right hand toward the right target in the closed loop condition ($P = 0.37$) and movements performed with the left hand toward right targets in the closed loop condition ($P = 0.017$) and toward the left and central targets in the open loop condition (all $P > 0.033$). Overall, pointing errors were more pronounced when pointing was performed with the right hand, in the open loop condition and toward targets located in the left visual space. These results are shown in Table 2.

Table 2. Pointing performance of patient S.T. and mean pointing performance of controls. Notes. Localization errors are expressed in visual degree. Positive and negative values indicate errors toward the right and the left, respectively. Asterisks denote a neuroatypical performance.

	Left Target	Central Target	Right Target
Right hand			
Closed-loop			
Patient S.T.	−6.3*	1.4*	0.5
Controls	0.44	0.05	−0.01
Open loop			
Patient S.T.	8.5*	2*	5.6*
Controls	1.02	−0.02	−0.47
Left hand			
Closed loop			
Patient S.T.	3.8*	1.1*	−1.6
Controls	−0.32	0	−0.59
Open loop			
Patient S.T.	−2.4	1.3	−5.7*
Controls	0.01	0.07	−1.17

4.3.2 Reaching end points

Patient S.T. and 10 healthy participants performed the visually guided reaching task in 3D space sketched in Figures 10A–10C. They reached visual targets (presented on a horizontal touch screen) at different depths and directions with respect to participant's midline. We tested two viewing conditions: peripheral reaching, where gaze was kept central, uncoupled from the position of reaching target, and foveal reaching, where gaze and reaching target positions were the same (Figure 10D). No gender effect was found on movement time of both peripheral and foveal reaching (one-way analysis of variance; $P = 0.481$ and $P = 0.3728$, respectively).

A typical analysis of reaching end points is shown in Figure 11, where a comparison of the accuracy and precision parameters between the patient and controls was performed by a *t*-test analysis. Figures 11A and 11C show the distribution of average reaching end points corresponding to control participants and patient S.T. in peripheral and foveal reaching, respectively. It is qualitatively evident a higher accuracy and precision of control participants with respect to patient S.T. The statistical results of accuracy and precision analysis are shown in Figures 11B and 11D as color maps. In peripheral reaching, the accuracy was statistically lower when the patient reached the farthest targets (Bonferroni post hoc test, $P < 0.001$), the left-intermediate target (Bonferroni post hoc test, $P < 0.001$), and the nearest central and right targets (Bonferroni post hoc test, $P < 0.05$ and $P < 0.001$, respectively). The precision was significantly lower for all targets tested (Bonferroni post hoc test, $P < 0.001$). In foveal reaching, the accuracy was significantly lower when the patient reached the right targets (Bonferroni post hoc test, $P < 0.001$), the left and right farthest targets (Bonferroni post hoc test, $P < 0.001$) and the nearest central target (Bonferroni post hoc test, $P < 0.001$). The precision was significantly lower for all targets tested except for the nearest central target (Bonferroni post hoc test, $P < 0.001$). In summary, patient S.T. showed a lower accuracy with respect to control participants, giving origin to hypometric and hypermetric misreaches when the targets were located farthest and nearest, respectively. He showed also a decreased precision for all the targets tested.

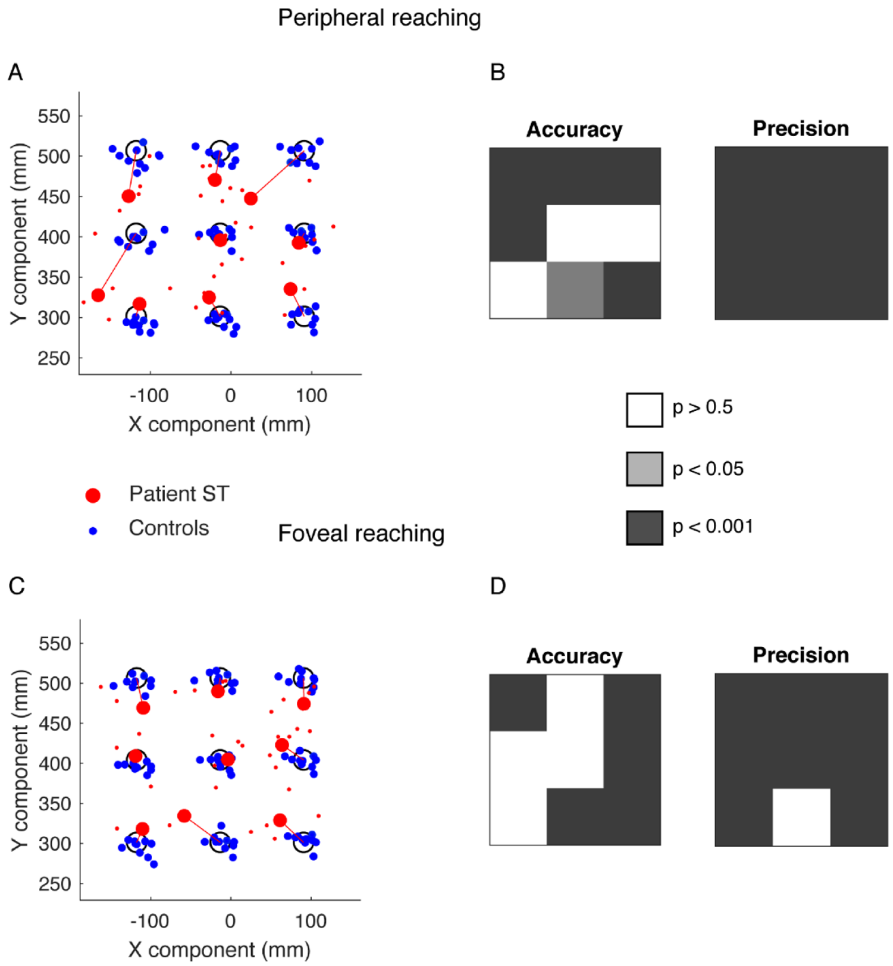

Figure 11. Reaching end points of patient S.T. and control participants. (A) Averaged reaching end points calculated in the peripheral reaching for control participants (blue dots) and patient S.T. (red dots). Red lines represent the patient's end point accuracy (B) P values of patient's accuracy (left) and precision (right) in peripheral reaching. (C) Averaged reaching end points calculated in the foveal reaching for control participants (blue dots) and patient S.T. (red). (D) P values of patient's accuracy (left) and precision (right) in foveal reaching.

In addition to abnormalities of reaching end points, we observed differences in performing the trajectory necessary to reach the targets located along the horizontal and sagittal axes. This difference is shown in Figure 12 where the average trajectory of the patient is graphically compared with that of control participants. For all targets tested, abnormal deviations of the patient's trajectory (in red) are visible compared with the controls' ones (in black). From this qualitative observation, we performed a detailed characterization of the trajectory performance, as described below in this article.

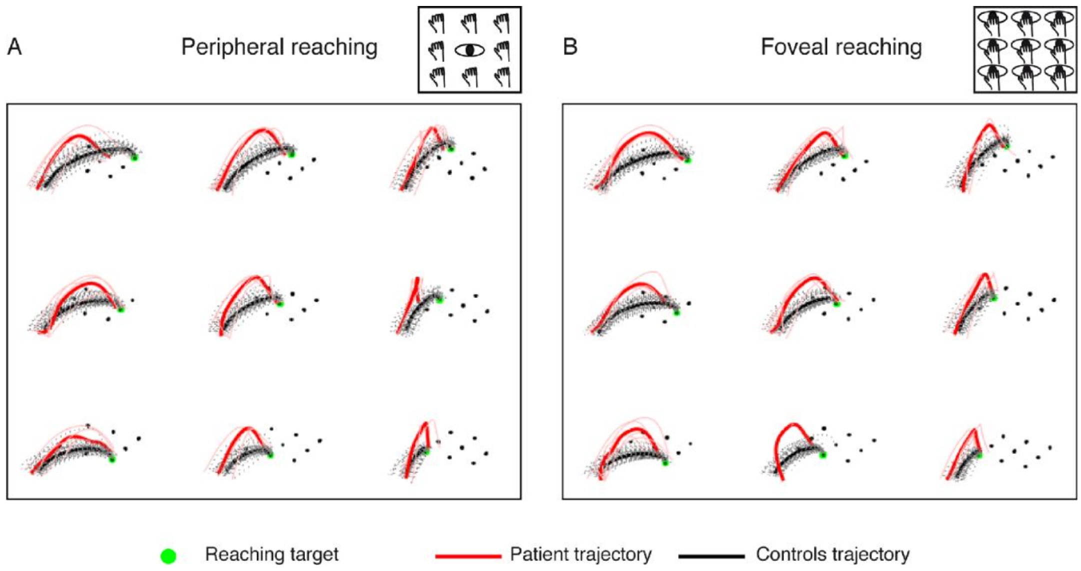

Figure 12. Reaching trajectories of patient S.T. and control participants. (A) Averaged reaching trajectories calculated in the peripheral reaching for control participants (black lines) and patient S.T. (red lines). (B) Averaged reaching trajectories calculated in the foveal reaching for control participants (black lines) and patient S.T. (red lines). Black dots represent the nine target positions in both (A) and (B).

4.3.3 Decoding from reaching trajectories – horizontal axis

Figure 13 shows an analysis of the trajectory deviations, with respect to the straight trajectory, for reaching targets distributed along the horizontal axis in peripheral and foveal conditions (Figures 13, left, and Figure 13, right, respectively). Kinematic data are reported separately for targets located in the left (Figure 13A), middle (Figure 13B), and right (Figure 13C) spaces.

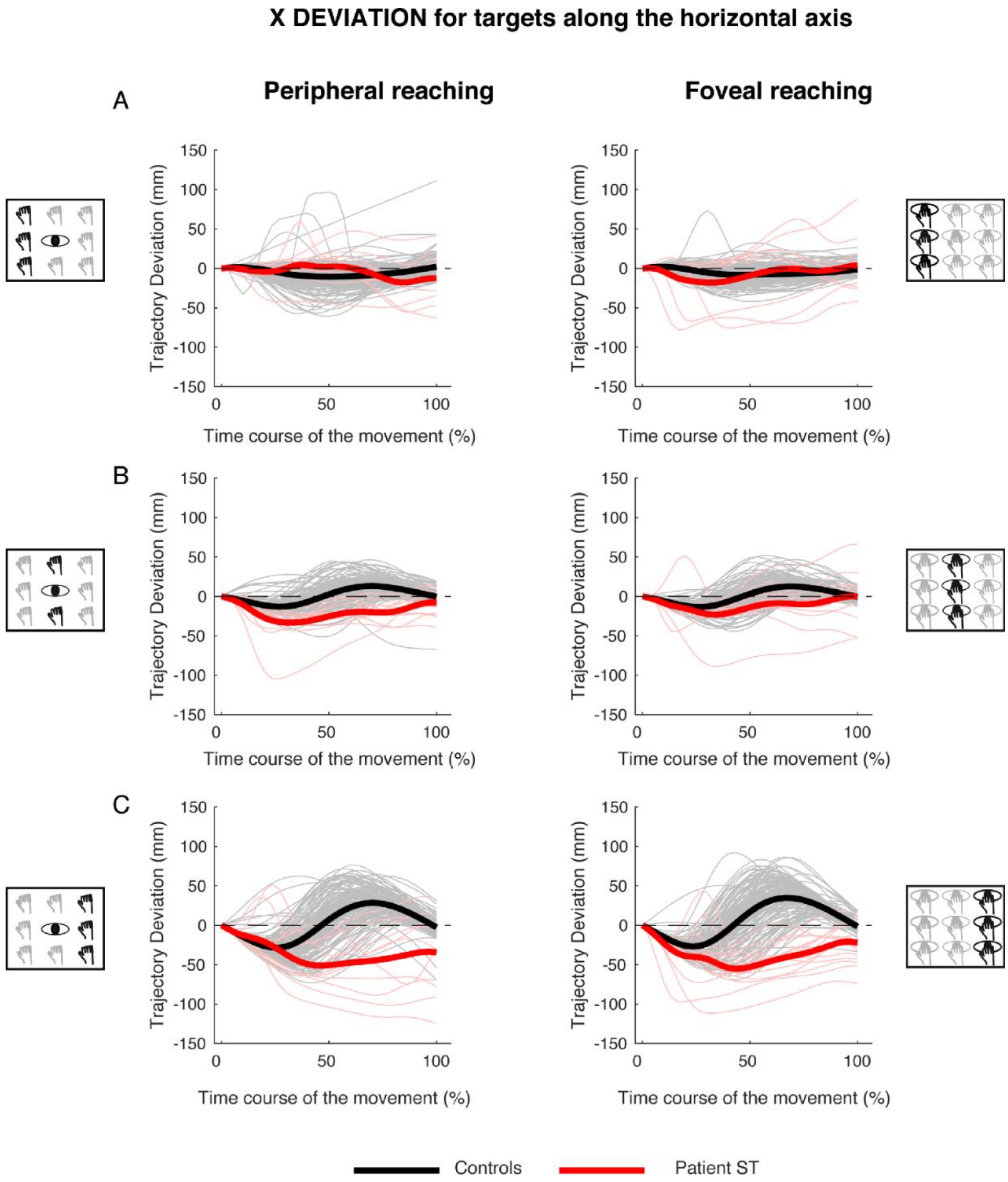

Figure 13. X deviations of reaching trajectory toward targets along the horizontal axis. (A, left) Temporal evolution of the horizontal deviations from the straight trajectory for reaching to left targets in peripheral reaching in patient S.T. (red line) and control participants (black line). Negative values correspond with left deviations, positive values correspond with right deviations. Thin lines represent individual trajectories. (Right) Temporal evolution of the horizontal trajectory deviations for reaching to left targets in foveal reaching. (B, left) Temporal evolution of the horizontal trajectory deviations for reaching to middle targets in peripheral reaching. (Right) Temporal evolution of the horizontal trajectory deviations for reaching to middle targets in foveal reaching. (C, left) Temporal evolution of the horizontal trajectory deviations for reaching to right targets in peripheral reaching. (Right) Temporal evolution of the horizontal trajectory deviations for reaching to right targets in foveal reaching.

In control participants, the movements toward left targets started with a trajectory that was close to the straight one and then deviated to the left (see Figure 13A, left, black line). At the half of the movement, the trajectory displayed the maximum deviation and then deviation progressively decreased until the end of the movement. The same trajectory evolution was observed in both peripheral and foveal reaching of left targets (compare the black lines in Figures 13A, left, and 13A, right). In the patient, the pattern of trajectory was totally different. For targets located to the left in peripheral condition, S.T. reached the targets following a trajectory that was close to the straight one (Figure 13A, left, red line) and significant deviations toward the left (negative values) were observed only in the last 30% of movement execution. In the last 20% of movement, the trajectory was outside the confidence range of the trajectory deviation of the control participants.

In the foveal condition, the trajectory of S.T. toward the left targets was completely different. He showed the maximum leftward (negative) deviation during the first half of movement, with the trajectory being outside the range of control participants deviations from the onset of movement (Figure 13A, right, red line). In the second part of the movement, the trajectory was within the range of control participants and progressively approached the straight line. We calculated the time at which maximum deviation from the straight trajectory occurred. Because the reaching movements toward targets located in the horizontal axis were principally executed along the x component of the trajectory, for left targets, we analyzed the occurrence of maximum negative deviation with respect to the straight trajectory. A significant difference was found in the time where maximum negative deviation occurred in patient and controls in peripheral reaching (controls, 0.31 ± 0.19 s; patient S.T., 0.78 ± 0.1 s; t = 3,076; P = 0.013)., where the deviation occurred later in patient with respect to controls. However, this did not affect the total movement time (controls, 0.73 ± 0.08 s; patient S.T., 0.62 ± 0.07 s; t = −1.360; P = 0.104). In foveal reaching, no significant difference was found either in the time of maximum negative deviation (controls, 0.27 ± 0.19 s; patient S.T., 0.46 ± 0.36 s; t = 0.920; P = 0.382) and in the total movement time (controls, 0.72 ± 0.10 s; patient S.T., 0.56 ± 0.09 s; t = −1.480; P = 0.086).

For targets located in the middle row, in both peripheral and foveal conditions, control participants presented a negative and a positive peak in trajectory deviations. The first negative peak representing the deviation to the left of the straight trajectory occurred around the 30% of the total movement time (Figures 13B, left, and 13B, right, black lines). The positive peak represented the deviation to the right of the straight trajectory and occurred around the 70% of the movement in both peripheral and foveal condition (Figures 13B, left, and 13B, right, black lines). Patient S.T. started the movement following the same path as control participants, by deviating the arm to the left. However, S.T. was then not able to correct this initial leftward deviation (contrary to the controls) and remained abnormally deviated to the left of straight trajectory for the entire duration of arm movement (Figure 13B, left, red line). This behavior was observed also in the foveal condition (Figure 13B, right). The time where maximum negative deviation that occurred in peripheral (controls, 0.32 ± 0.16 s; patient S.T., 0.40 ± 0.14 s) and foveal conditions (controls, 0.29 ± 0.13 s; patient S.T., 0.52 ± 0.38 s) did not show significant differences (peripheral, $t = 0.446$; $P = 0.666$, foveal, $t = 0.588$; $P = 0.571$). No significant differences were found in the total movement time in both peripheral (controls, 0.67 ± 0.16 s; patient S.T., 0.53 ± 0.08 s; $t = -0.867$; $P = 0.409$) and foveal reaching (controls, 0.67 ± 0.15 s; patient S.T., 0.58 ± 0.19 s; $t = -0.551$; $P = 0.595$).

For targets located at the right side, in both peripheral and foveal conditions, control participants displayed a pattern of trajectory deviations similar to those observed for reaching toward the middle targets. The first peak, to the left of the straight trajectory, occurred at about the first 30% of movement's duration. The second peak, to the right, occurred at approximately 70% of movement time (Figures 13C, left, and 13C, right, black lines). However, the two negative and positive peaks of trajectory deviations displayed larger amplitudes with respect to those observed in the middle targets. Significant differences between the patient and controls were found in the time where maximum negative deviation occurred in both peripheral (controls, 0.21 ± 0.07 s; patient S.T., 0.55 ± 0.22 s; $t = 4.698$; $P = 0.001$) and foveal reaching (controls, 0.19 ± 0.07 s; patient S.T., 0.37 ± 0.1 s; $t = 2.482$; $P = 0.035$). Patient S.T. showed more delayed maximum negative deviations with respect to controls in both reaching conditions. However, no significant differences were found in the total movement time in both peripheral (controls, 0.71 ± 0.11 s; patient S.T., 0.55 ± 0.26 s; $t = -1.309$; $P = 0.112$) and foveal reaching (controls, 0.71 ± 0.12 s; patient S.T., 0.53 ± 0.08 s; $t = -1.388$; $P = 0.099$).

These results show that mild, but significant, trajectory deviations were detected also during reaching to left targets in peripheral reaching. However, the worst performance of patient S.T. compared with controls was observed during reaching to right targets, where greater horizontal deviations, distributed across movement execution and delayed maximum negative deviations, were found.

Figure 14 shows the time course of the trajectory deviations for the y component for left (Figure 14A), middle (Figure 14B) and right (Figure 14C) targets in peripheral and foveal reaching. In all target positions, the y deviation of the patient showed less pronounced negative and positive deviations with respect to the controls. In fact, control participants showed first a negative deviation and, during the second stage of the movement, a larger positive one. The averaged positive deviation was 83.2 ± 11.14 mm for peripheral reaching and 91.78 ± 4.99 mm for foveal reaching (see Figures 14A, 14B, and 14C, black lines). In the patient, the averaged positive deviation was 4.77.2 ± 20.6 mm for peripheral reaching and 25.37 ± 2.15 mm for foveal reaching (see Figures 14A, 14B, and 14C, red lines).

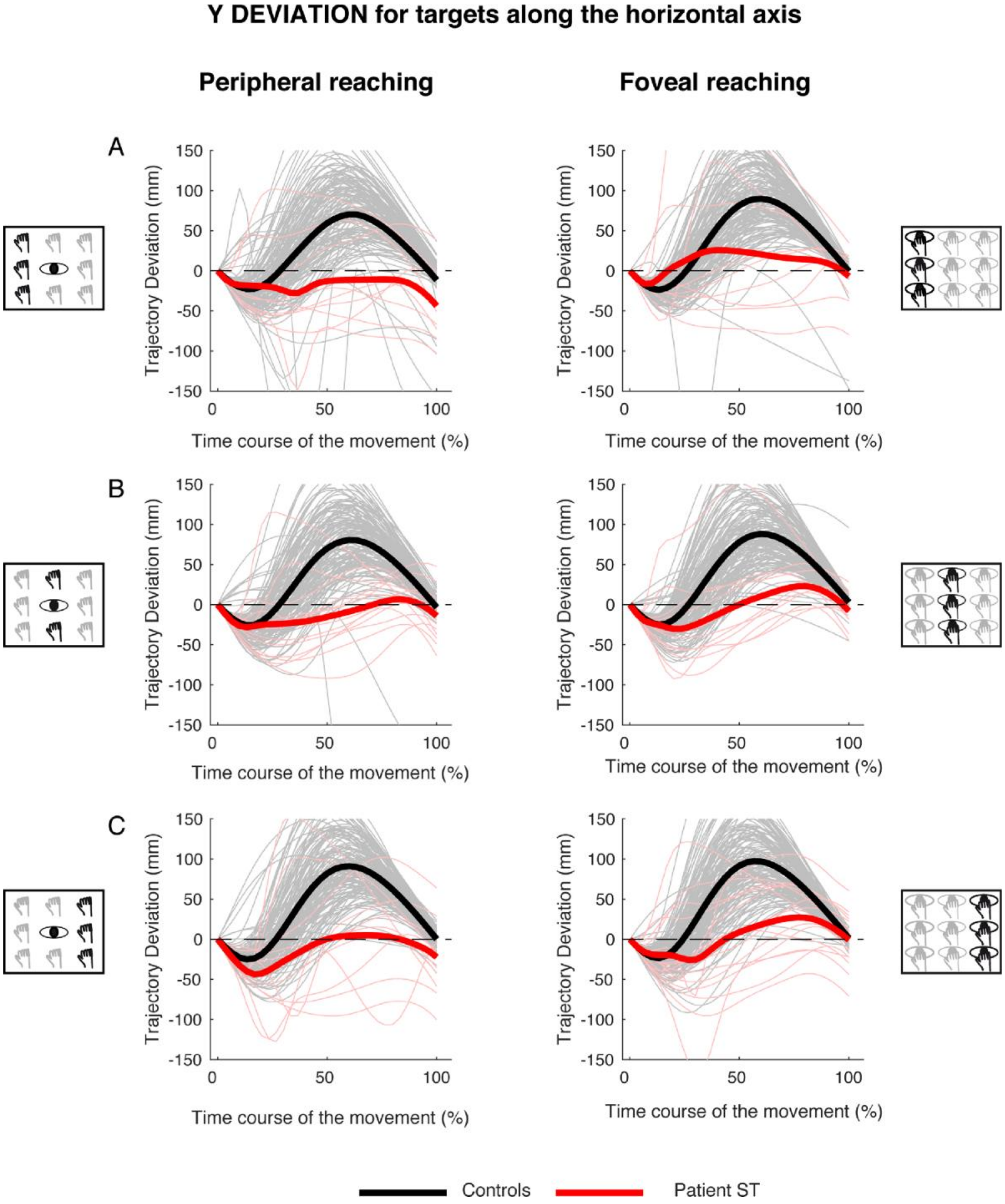

Figure 14. Y deviations of reaching trajectory toward targets along the horizontal axis. (A, left) Temporal evolution of the horizontal deviations from the straight trajectory for reaching to left targets in peripheral reaching in patient S.T. (red line) and control participants (black line). (Right) Temporal evolution of the horizontal trajectory deviations for reaching to left targets in foveal reaching. (B, left) Temporal evolution of the horizontal trajectory deviations for reaching to middle targets in peripheral reaching. (Right) Temporal evolution of the horizontal trajectory

deviations for reaching to middle targets in foveal reaching. (C, left) Temporal evolution of the horizontal trajectory deviations for reaching to right targets in peripheral reaching. (Right) Temporal evolution of the horizontal trajectory deviations for reaching to right targets in foveal reaching.

Figure 15 shows the time course of the trajectory deviations for the z component for reaching targets distributed along the horizontal axis in peripheral and foveal conditions (Figures 15, left, and Figure 15, right). The kinematic data are reported separately for targets located in the left (Figure 15A), middle (Figure 15B), and right (Figure 15C) spaces. In all target positions tested in the peripheral condition, the control participants showed a single positive peak at the 50% of the movement execution and the averaged deviation was 29.83 ± 17.25 mm. Patient S.T. presented a positive peak more tardive with respect to control participants at the 70% of the movement execution with a larger average deviation equal to 124.84 mm ± 7.51 mm (see Figure 15, left). In foveal condition, the results show similar temporal profiles of positive peaks of deviation between control participants and the patient (50% and 70%, respectively). The average maximum deviation was 30.63 ± 15.91 mm in control participants and 127.97 ± 5.46 mm in the patient (see Figure 15, right).

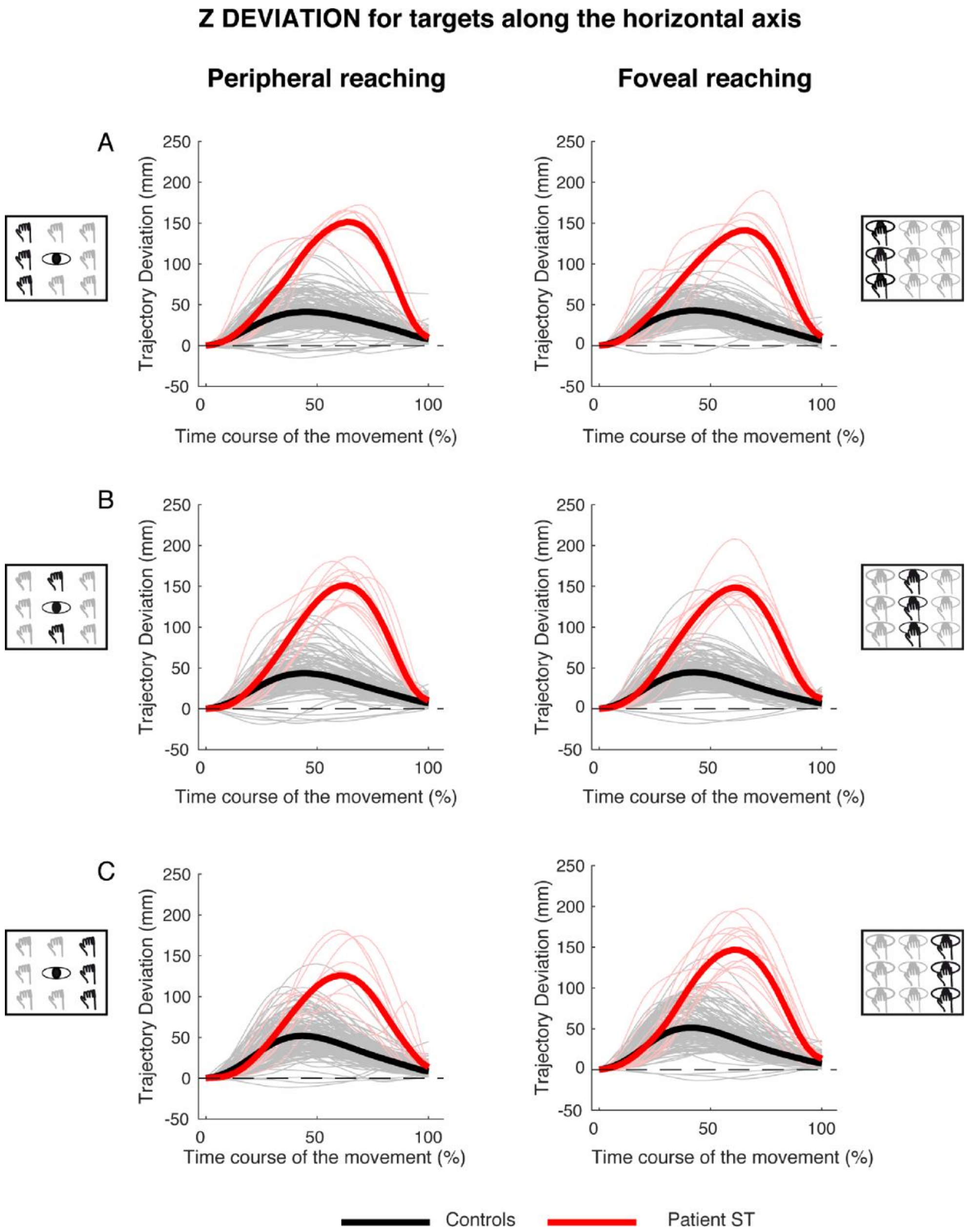

Figure 15. Z deviations of reaching trajectory toward targets along the horizontal axis. (A, left) Temporal evolution of the horizontal deviations from the straight trajectory for reaching to left targets in peripheral reaching in patient S.T. (red line) and control participants (black line). (Right) Temporal evolution of the horizontal trajectory deviations for reaching to left targets in foveal reaching. (B, left) Temporal evolution of the horizontal trajectory deviations for reaching to middle targets in peripheral reaching. (Right) Temporal evolution of the horizontal trajectory deviations for reaching to middle targets in foveal reaching. (C, left) Temporal evolution of the horizontal trajectory deviations for reaching to right targets in peripheral reaching. (Right) Temporal evolution of the horizontal trajectory deviations for reaching to right targets in foveal reaching.

4.3.4 Decoding from reaching trajectories – sagittal axis

Along the sagittal axis, control participants showed quite consistent trajectory deviations on the x component of the trajectory during reaching movements toward near, intermediate and far targets in both peripheral and foveal conditions. As shown in Figure 16, the control participants showed a negative deviation in the first stage of the movement and a positive deviation in the second stage of the movement for peripheral and foveal reaching (Figures 16A, 16B, and 16C, see black lines). On the contrary, patient S.T. showed only a negative deviation suggesting an inability in correcting the trajectory to appropriately direct the hand toward the final target (Figures 16A, 16B, and 16C, see red lines).

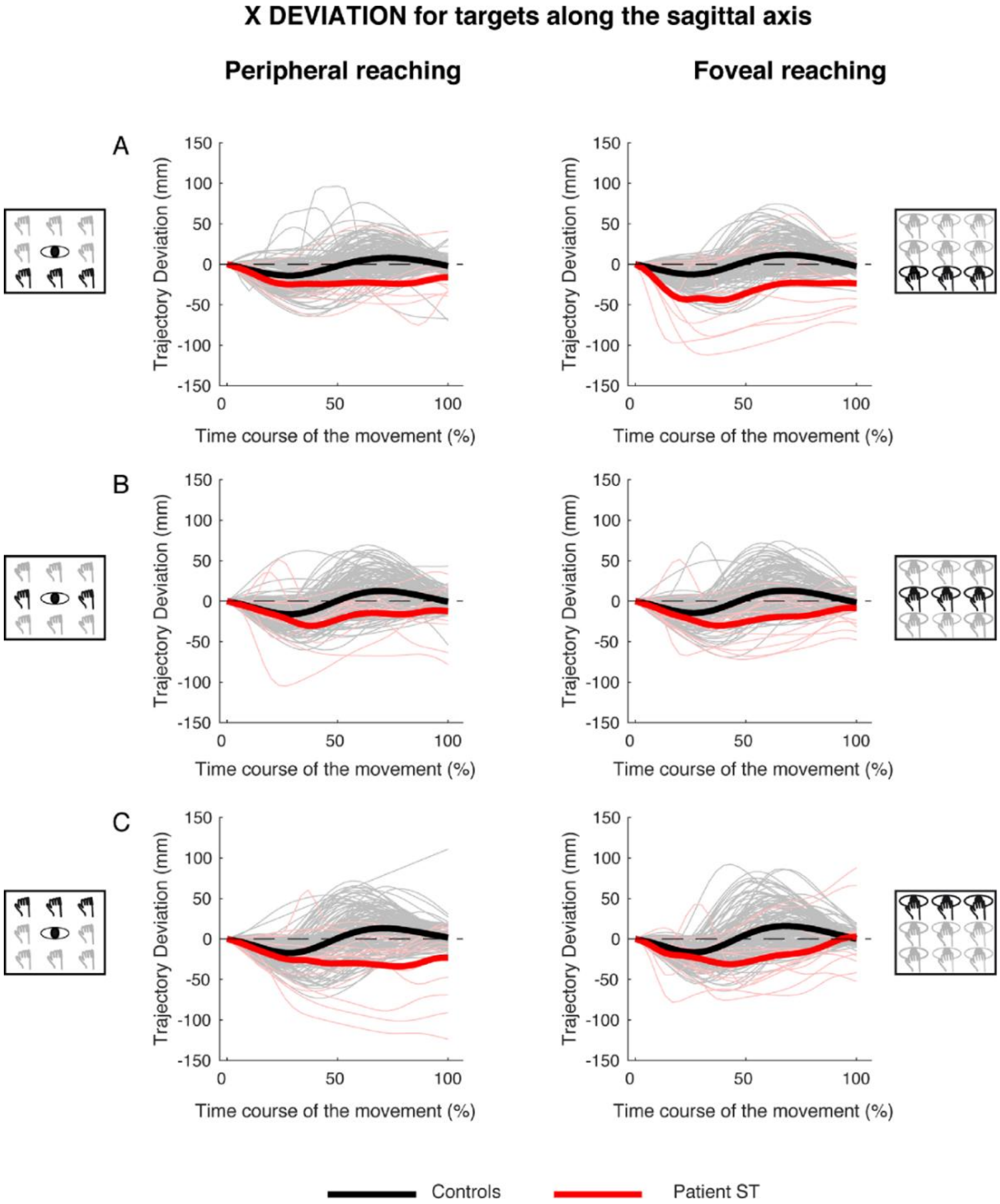

Figure 16. X deviations of reaching trajectory toward targets along the sagittal axis. (A, left) Temporal evolution of the horizontal deviations from the straight trajectory for reaching to near targets in peripheral reaching in patient S.T. (red line) and control participants (black line). (Right) Temporal evolution of the horizontal trajectory deviations for reaching to near targets in foveal reaching. (B, left) Temporal evolution of the horizontal trajectory deviations for reaching to intermediate targets in peripheral reaching. (Right) Temporal evolution of the horizontal

trajectory deviations for reaching to intermediate targets in foveal reaching. (C, left) Temporal evolution of the horizontal trajectory deviations for reaching to far targets in peripheral reaching. (Right) Temporal evolution of the horizontal trajectory deviations for reaching to far targets in foveal reaching.

For the y component of the trajectory, control participants showed deviations that gradually increased from near to far targets (Figures 17A, 17B, and 17C, black lines). At the beginning of movement, the hand showed a small hypometric deviation (negative values), which means that it was behind the corresponding point of the straight trajectory. Then, this trajectory deviation reversed and large hypermetric (positive) values were observed in the remaining 70% of movement (Figure 17, black lines), meaning that the hand was in front of the corresponding point of the straight trajectory. For targets located along the sagittal axis, we calculated the time where maximum deviation toward positive values occurred in patient and controls and then statistically compared them. The patient performed hand movements toward targets at different depths with similar trajectories between the peripheral and foveal reaching (Figure 17, red lines). Patient's trajectories were quite similar to those of control participants in the first 30% of movement, in both peripheral and foveal reaching. However, in the last 70% of movement, trajectories significantly deviated from those of controls, becoming more similar to straight-line trajectories. Notice that, although the control participants showed an increase in deviation for movements toward far targets, the patient showed larger deviations from a straight line trajectory for near targets. No significant differences were found in the time when maximum positive deviation occurred during the movement, both in peripheral (near targets, controls, 0.59 ± 0.1 s; patient S.T., 0.6 ± 0.33 s; $t = 0.097$; $P = 0.925$; center targets, controls, 0.57 ± 0.09 s; patient S.T., 0.63 ± 0.27 s; $t = 0.562$; $P = 0.588$; far targets, controls, 0.6 ± 0.08 s; patient S.T., 0.72 ± 0.33 s; $t = 1.342$; $P = 0.212$) and foveal reaching (near targets: controls, 0.58 ± 0.09 s; patient S.T., 0.59 ± 0.29 s; $t = 0.100$; $P = 0.923$; center targets, controls, 0.59 ± 0.07 s; patient S.T., 0.72 ± 0.30 s; $t = 1.773$; $P = 0.110$; far targets, controls, 0.57 ± 0.08 s; patient S.T., 0.68 ± 0.34 s; $t = 1.316$; $P = 0.221$). However, total movement time was significantly affected only in peripheral reaching for central and far targets (center targets, controls, 0.70 ± 0.09 s; patient S.T., 0.52 ± 0.06 s; $t = -2,051$; $P = 0.035$; far targets: controls, 0.79 ± 0.09 s; patient S.T., 0.58 ± 0.06 s; $t = -2.015$; $P = 0.037$).

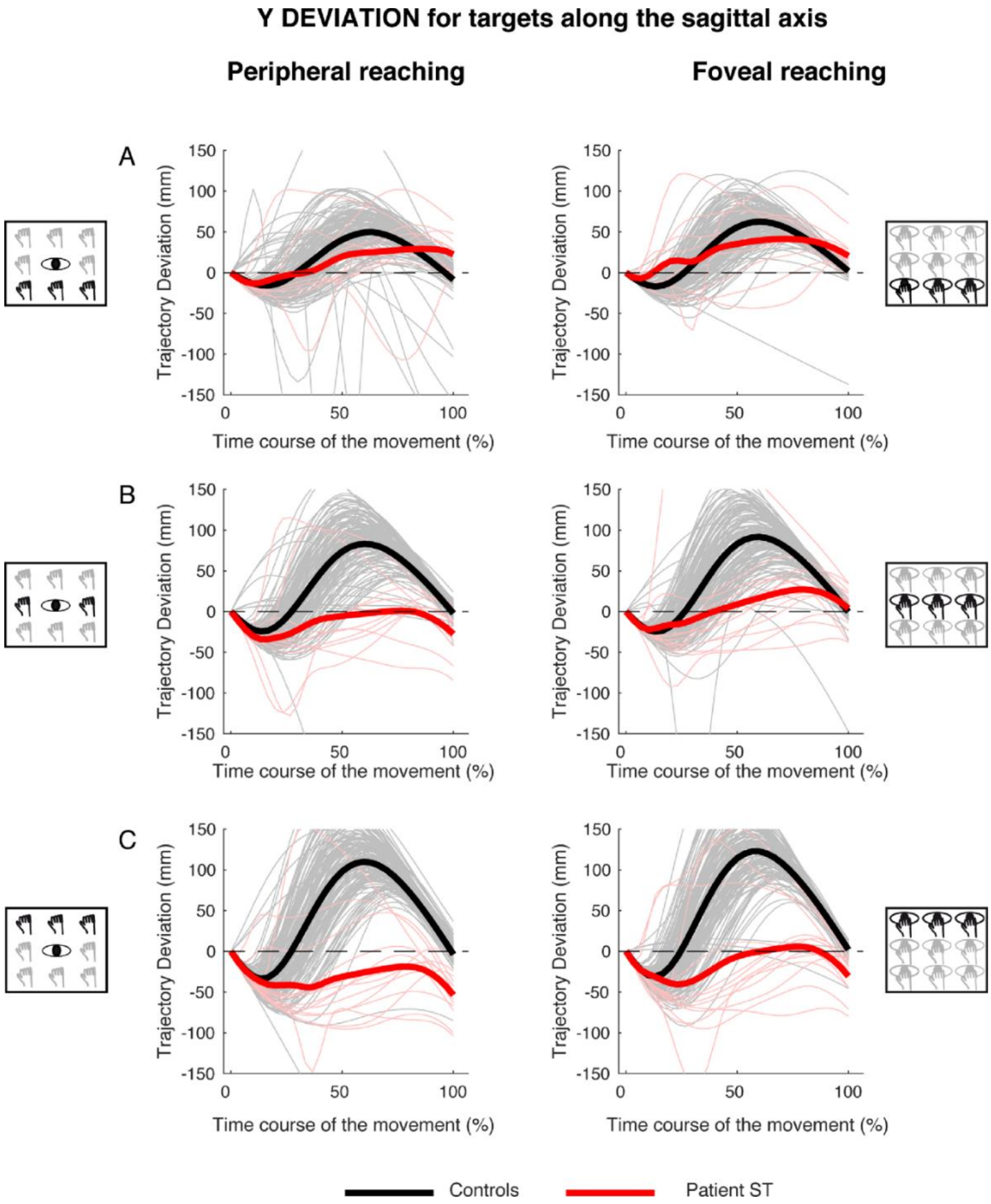

Figure 17. Y deviations of reaching trajectory toward targets along the sagittal axis. (A, left) Temporal evolution of the horizontal deviations from the straight trajectory for reaching to near targets in peripheral reaching in patient S.T. (red line) and control participants (black line). (Right) Temporal evolution of the horizontal trajectory deviations for reaching to near targets in foveal reaching. (B, left) Temporal evolution of the horizontal trajectory deviations for reaching to intermediate targets in peripheral reaching. (Right) Temporal evolution of the horizontal trajectory deviations for reaching to intermediate targets in foveal reaching. (C, left) Temporal evolution of the horizontal trajectory deviations for reaching to far targets in peripheral reaching. (Right) Temporal evolution of the horizontal trajectory deviations for reaching to far targets in foveal reaching.

Figure 18 shows the temporal evolution of the trajectory deviations for the z component for reaching targets distributed along the sagittal axis in peripheral and foveal conditions (Figure 18, left, and Figure 18, right). In the peripheral condition, similarly at the direction dimension, control participants showed a single positive peak at the 50% of the movement execution and the averaged deviation was 31.05 ± 19.54 mm. Also in this case, patient S.T. presented a positive peak more tardive with respect to control participants at the 70% of the movement execution, with a larger average deviation (116.2 ± 18.14 mm, see Figure 18, left). In foveal condition, the results show similar temporal profiles of positive peaks of deviation in control participants and patient (50% and 70%, respectively). The average maximum deviation was 32.32 ± 17.82 mm in control participants and 121.46 ± 13.55 mm in the patient (see Figure 18, right).

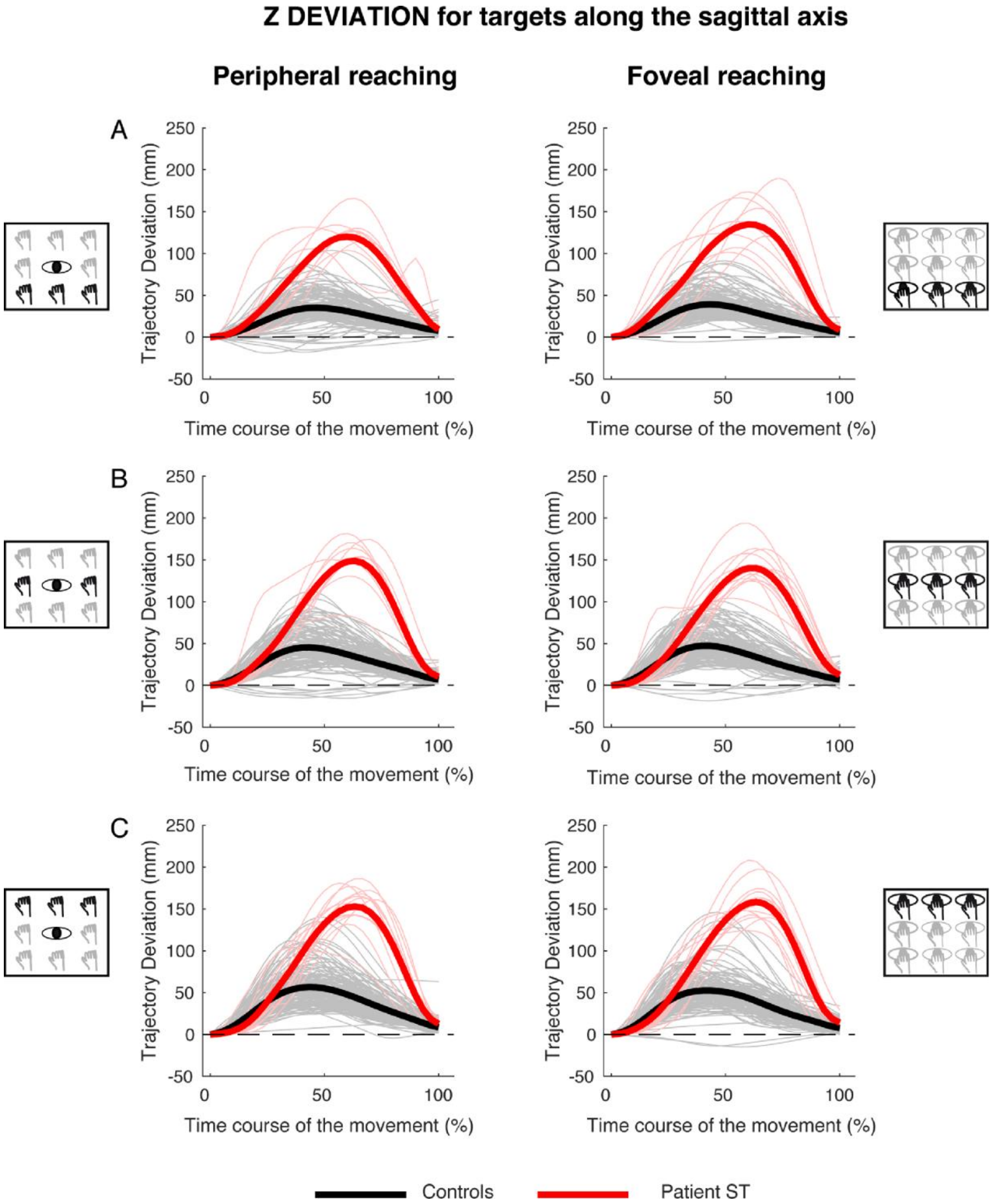

Figure 18. Z deviations of reaching trajectory toward targets along the sagittal axis. (A, left) Temporal evolution of the horizontal deviations from the straight trajectory for reaching to near targets in peripheral reaching in patient S.T. (red line) and control participants (black line).

(Right) Temporal evolution of the horizontal trajectory deviations for reaching to near targets in foveal reaching. (B, left) Temporal evolution of the horizontal trajectory deviations for reaching to intermediate targets in peripheral reaching. (Right) Temporal evolution of the horizontal trajectory deviations for reaching to intermediate targets in foveal reaching. (C, left) Temporal evolution of the horizontal trajectory deviations for reaching to far targets in peripheral reaching. (Right) Temporal evolution of the horizontal trajectory deviations for reaching to far targets in foveal reaching.

4.3.5 Classifier performance

To evaluate whether the performance of the LDA classification analysis, we applied a binary classification analysis that evaluated whether the classifier was more able to discriminate the patient's performance from that of control participants or among controls. Figures 19 and 20 show the average classification accuracy for trajectory deviations across the movement execution for targets located at different directions and depths and in both peripheral and foveal conditions, respectively. We calculated the accuracies through leave-one-out cross-validation and the error bars by 95% bootstrapped confidence intervals. The results show that the classification accuracy was higher in recognizing the patient's performance from that of control participants when they reached targets in all the positions tested (see the red plots above the black ones in Figures 19 and 20). Furthermore, the ability in the classifier recognition was visible from the 20% of the movement execution, suggesting that, in principle, the method can be generalized as it recognizes better the pathological behavior with respect to the neurotypical one in each condition tested and already at the early stage of the action.

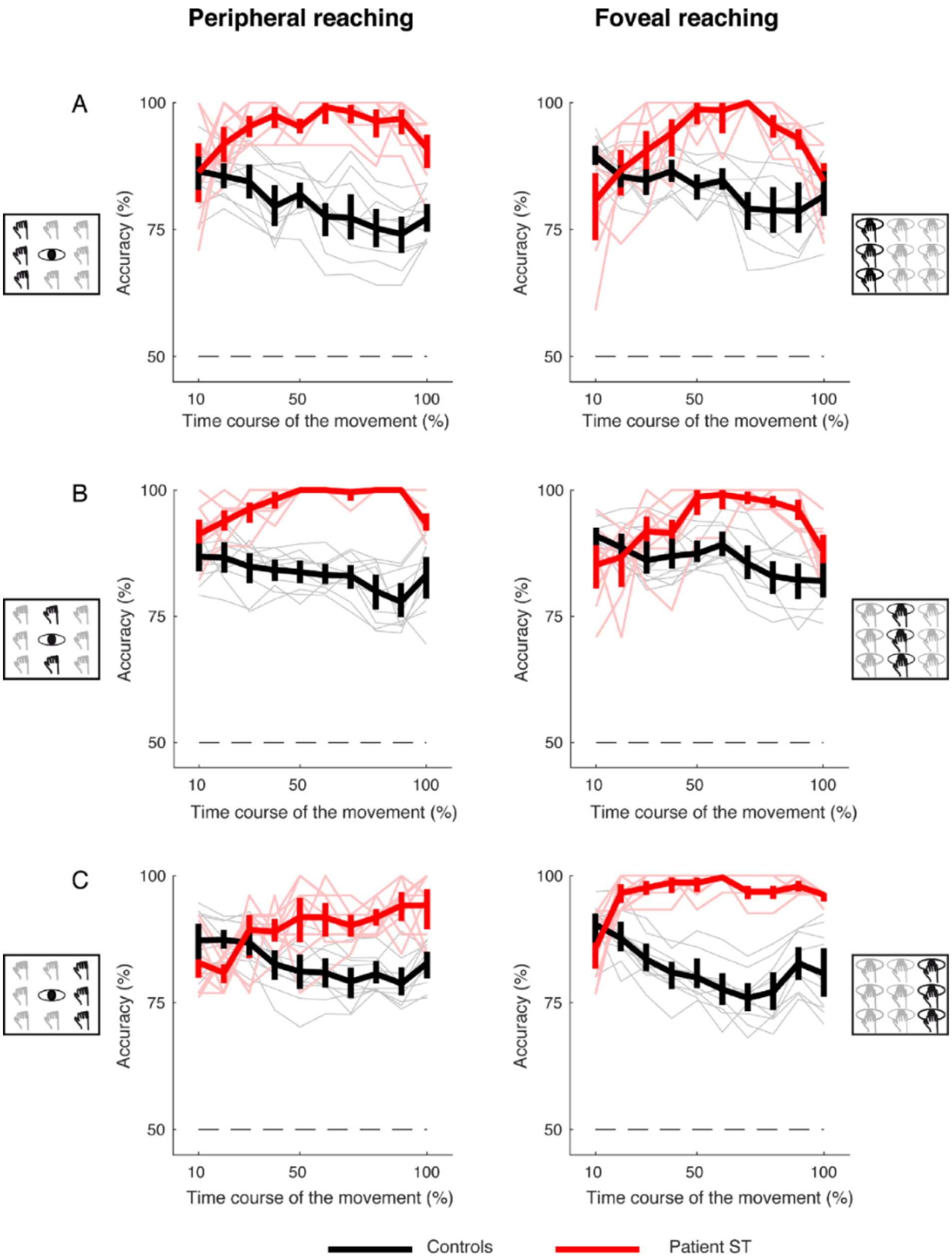

Figure 19. Binary classification analysis comparing the classifier's ability to distinguish patient performance from controls, or to differentiate among controls, along the horizontal axis. (A) Average recognition rate of classification accuracy for left targets between patient and controls (red plots) and between controls (black plots). (B) Averaged recognition rate of classification accuracy for middle targets. (C) Averaged recognition rate of classification accuracy for right targets. The thin lines represent individual accuracies. The straight dotted line represents the chance level (50%).

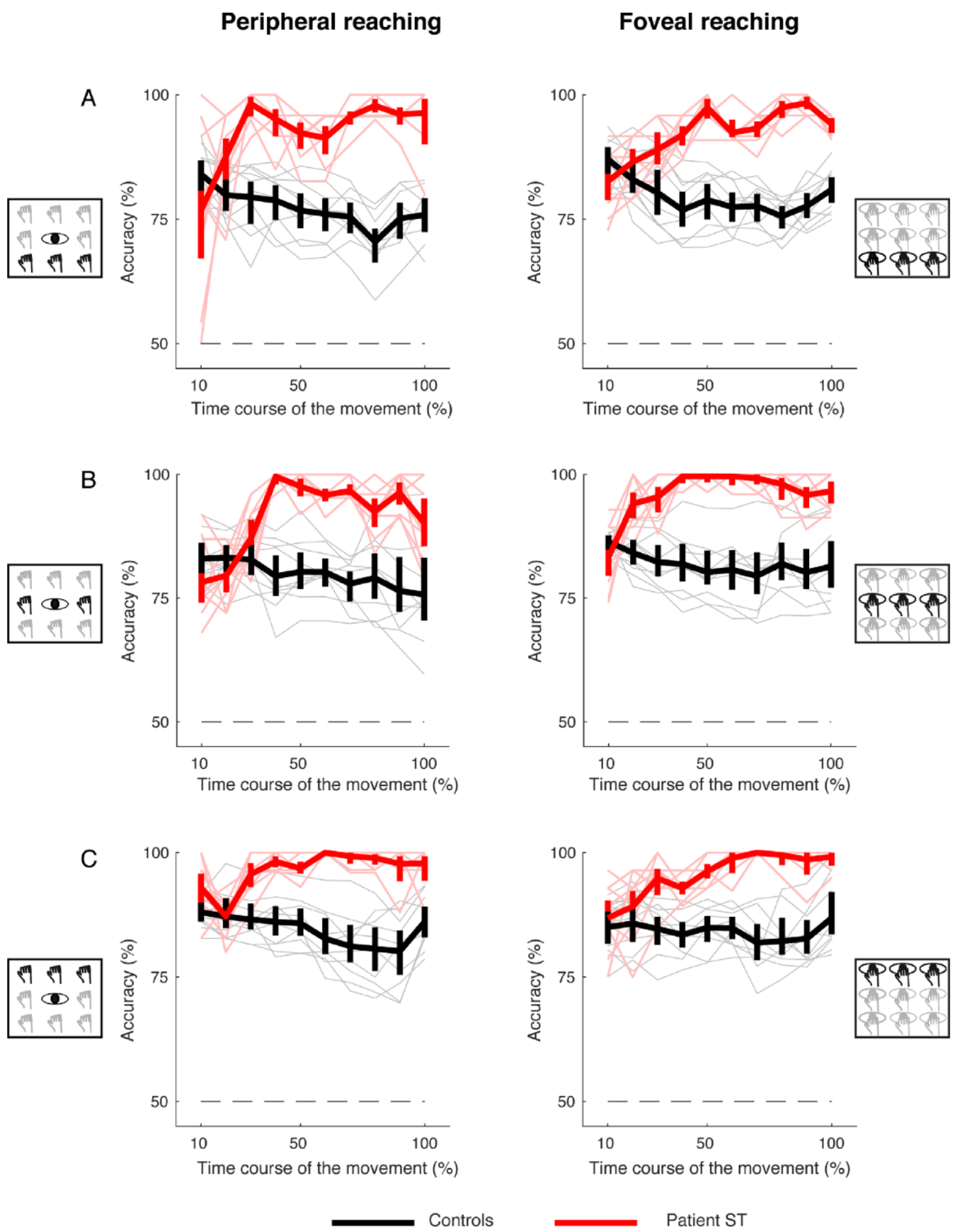

Figure 20. Binary classification analysis comparing the classifier's ability to distinguish patient performance from controls, or to differentiate among controls, along the sagittal axis. (A) Average recognition rate of classification accuracy for near targets between patient and controls (red plots) and between controls (black plots). (B) Averaged recognition rate of classification accuracy for intermediate targets. (C) Averaged recognition rate of classification accuracy for far targets. The thin lines represent individual accuracies. The straight dotted line represents the chance level (50%).

4.4 DISCUSSION

The focus of this study was to characterize the kinematics of reaching movements performed toward targets located at different directions and depths in a patient with a bilateral occipitoparietal damage that included parts of SPL, IPS, and precuneus. To do this, we performed a quantification of trajectories by the adoption of a decoding approach to discriminate, at the individual level, whether reaching movements were performed by the patient or by healthy participants. To our knowledge, this decoding approach has never been applied in studies investigating kinematics in patients with OA. Because it is well-known that PPC damage can differentially affect movements performed under different viewing conditions (Balint, 1909; McIntosh, Mulroue, & Brockmole, 2010; Rossetti, Pisella, & Vighetto, 2003), we tested here both peripheral and foveal reaching. Although several previous studies have investigated reaching behavior in patients with PPC lesions, and the present findings are in line with these, two aspects of the present study qualitatively deviated from the current literature: the first is the combination of movement trajectory analysis with decoding methods that have not been performed so far, and the second is the joint analysis of reaching errors and trajectories performed toward targets located in the 3D space.

Overall, patient S.T. showed abnormal deviations from the virtual straight line used for the trajectory analysis, both in depth and direction, during movements in both foveal and non-foveal conditions. These deviations are not just the result of mechanical limitations but could reflect altered brain processes related to spatial representation of the reaching targets typically observed in patients with OA visuomotor deficit.

Along the horizontal axis, patient S.T. demonstrated anomalous movement trajectories, significantly more deviated toward the left with respect to control participants for targets located on the right, with peculiar, more delayed negative trajectory deviation. This spatiotemporal impairment, visible both in peripheral and in foveal viewing conditions in the x component of the trajectory, was more evident in the second half of the movement. For targets located on the middle of the reaching space, we also found an anomalous left deviation of the patient S.T. with respect the control participants that was more evident in the peripheral condition after the half of the movement. The abnormal deviations increased from left to middle and then to right targets suggesting a worsening of the reaching performance for the targets included in the most affected visual field of the patient, the right visual field. In line with these findings, during the early stage of the movement, the LDA classifier was able to discriminate the patient's motor performance from that of control participants.

The fact that the patient's abnormal performance is mainly expressed in the second half of the movement, hints at a deficit in the movement correction system that becomes more important in the late stages of movement (Desmurget et al., 1999). This view is in line with the evidence that PPC is responsible for the online correction mechanism of the arm movement (Andersen, Andersen, Hwang, & Hauschild, 2014; Archambault, Ferrari-Toniolo, Caminiti, & Battaglia-Mayer, 2015; Desmurget et al., 1999; Gréa et al., 2002; Pisella et al., 2000; Rossetti et al., 2003). Online correction mechanism is constantly required for the performance of accurate visually guided reaching movements (Goodale, Pelisson, & Prablanc, 1986; Pélisson, Prablanc, Goodale, & Jeannerod, 1986) and requires a fast comparison of target and hand location. This mechanism was demonstrated to be active in reaching movements when rapid changes of target location occurred (Blangero et al., 2008; Pisella et al., 2000). In this situation, patients with OA showed a lack of movement correction. However, the performance of patients with OA improved when the vision of the target and the hand was removed (Jackson, Newport, Mort, & Husain, 2005; Milner, Dijkerman, McIntosh, Rossetti, & Pisella, 2003) because, in these conditions, participants relied on previous knowledge of target location and proprioceptive feedback (Lingnau et al., 2012). All these observations support the view that PPC is involved in online visuomotor control (Desmurget et al., 1999; Gréa et al., 2002; Rossetti et al., 2003). Moreover, movements toward stationary objects (i.e., similar to the movements performed in the present study) have been demonstrated to require slight online modifications in normotypical individuals (Jakobson & Goodale, 1989; Prablanc & Martin, 1992). Given that these modifications produce an increased deceleration time during the second part of the movement, it is reasonable to suppose that the differences found in patient S.T. arm trajectory in the second half of movement execution are correlated with an impairment of such control mechanisms.

Along the sagittal axis, patient S.T. displayed different patterns of trajectory deviations across the target distances tested. The maximum spatiotemporal differences between patient and controls were found for movements performed toward the most distant targets. Moving from near to far space, patient S.T. decreased the trajectory deviation with respect to controls, becoming progressively slower. Specifically, for reaching toward far space, patient's trajectories became more stereotyped compared with those of the controls suggesting a difficulty in relying on the online correction system ascribed to this part of the cortex (Desmurget et al., 1999; Pisella et al., 2000). An additional explanation can be found considering that movements executed along the sagittal plane are more difficult to be executed as they mainly rely on proprioceptive information (van Beers, Sittig, & Denier van der Gon, 1998). In fact, in depth, proprioception is more reliable than vision (Flanders, Tillery, &

Soechting, 1992; Monaco et al., 2010; Sainburg, Lateiner, Latash, & Bagesteiro, 2003; van Beers et al., 1998) and the reaching of targets using proprioceptive information is typically more accurate for targets closer to the shoulder (van Beers et al., 1998).

The analysis of trajectory deviations in depth demonstrated differences between peripheral and foveal reaching for near and intermediate targets for the y component of the trajectory. In peripheral reaching and for all target positions, the patient was not able to compensate the trajectory deviation reducing the distance between the deviations of patient S.T. and control participants at the end of movement whereas, in foveal reaching, the patient was able to reduce this distance that became similar to those of controls (see Figures 9A and 9B, left and right diagrams for comparison). These results reflect the limited impairment of patients with OA in foveal vision (Buxbaum & Coslett, 1997; Jeannerod, Decety, & Michel, 1994; Perenin & Vighetto, 1988) and support strong evidence that described OA as a visuomotor deficit characterized by evident misreaches toward peripherally presented targets.

The majority of case studies on patients with PPC lesions focused on quantifying reaching errors. These studies have demonstrated that patients with PPC lesions, and in particular those presenting the OA deficit, show strong inaccuracies in reaching movements toward targets presented in the contralesional visual field (field effect) and/or using the contralesional hand (hand effect) (Blangero et al., 2008; Khan et al., 2007; Rice et al., 2008; Striemer et al., 2009). Danckert, Goldberg, and Broderick (2009) showed that the damage of SPL including regions of the IPS and parieto-occipital junction led to impaired movements more in the sagittal plane than the horizontal one. Other case studies demonstrated a poor representation of the depth dimension and its perception in patients with bilateral lesions of PPC (Baylis & Baylis, 2001; Holmes & Horrax, 1919; Schaadt, Brandt, Kraft, & Kerkhoff, 2015). The present study confirms that lesions of PPC lead to reaching impairments along both horizontal and sagittal dimensions. Despite different behavioral variables analyzed and the different tasks used to test patients with OA, two studies allow a quantitative comparison with the present study, as they investigated movements executed along horizontal and sagittal dimension (Cavina-Pratesi, Ietswaart, Humphreys, Lestou, & Milner, 2010; Danckert et al., 2009). In these studies, the highest differences between the patients and the control participants were found along the depth dimension, similarly to what we found in the present study (Cavina-Pratesi et al., 2010; Danckert et al., 2009) and in particular for the farthest-contralesional target (Cavina-Pratesi et al., 2010). However, Cavina-Pratesi et al. (2010) found differences only in peripheral viewing conditions, whereas Danckert et al. (2009) found strong impairments in free viewing conditions (foveal conditions), similar to the present results.

There is evidence from monkey studies suggesting the existence of common representation of reaching in depth and direction in single neurons of the SPL (Hadjidimitrakis, Bertozzi, Breveglieri, Bosco, et al., 2014; Hadjidimitrakis, Dal Bo', Breveglieri, Galletti, & Fattori, 2015). These findings from monkeys were in contrast with the general view that depth and direction of reaching targets are processed independently (Crawford, Henriques, & Medendorp, 2011; Flanders, Tillery, & Soechting, 1992). The view of separate pathways for depth and direction is based on several behavioral studies (Bagesteiro, Sarlegna, & Sainburg, 2006; Flanders & Soechting, 1990; Gordon, Ghilardi, Cooper, & Ghez, 1994; Sainburg, Lateiner, Latash, & Bagesteiro, 2003; Van Pelt & Medendorp, 2008; Vindras, Desmurget, & Viviani, 2005), although a neurophysiological support to it is relatively weak (De Vitis et al., 2019; Lacquaniti, Guigon, Bianchi, Ferraina, & Caminiti, 1995). The present work allowed a combined study of direction and depth dimensions, similar to what was done in the monkey (Filippini, Breveglieri, Hadjidimitrakis, Bosco, & Fattori, 2018; Hadjidimitrakis, Bertozzi, Breveglieri, Bosco, et al., 2014; Hadjidimitrakis, Bertozzi, Breveglieri, Galletti, & Fattori, 2017) and, in line with evidence in monkeys, an impairment of reaching in both depth and direction was found. This finding suggests that SPL, in addition to inferior parietal lobule, could contribute to reaching trajectory and movement accuracy performed in 3D space.

This study highlights the possibility to discriminate the performance of a given patient by observing kinematic components of arm movement well in advance with respect to the conclusion of the action. However, without assuming that all patients with OA show a pattern similar to S.T., we predict that the results of the classification analysis can be generalized to other patients on the basis of the extent and location of the lesion that causes the OA and whether the reaching trajectories of the patient display abnormalities with respect to their normal execution that typically presents appropriate curvatures and deviations. Specifically, we would expect a primary deficit in reaching executed toward the 3D space when the OA is associated with lesions that include the SPL, that is known to play a role in the encoding of reaching toward targets located in direction and depth (Bosco, Breveglieri, Hadjidimitrakis, Galletti, & Fattori, 2016; Hadjidimitrakis, Bertozzi, Breveglieri, Bosco, et al., 2014; Hadjidimitrakis, Bertozzi, Breveglieri, Fattori, & Galletti, 2014; Hadjidimitrakis et al., 2017, 2015). In general, and taking into account these considerations, the decoding of patient's reaching behavior by the classifier of the present study could represent a suitable model to examine at which stage of the trajectory, movement inaccuracies develop and this information may be used in clinical applications to evaluate the degree of impairment.

4.5 CONCLUSIONS

Taken together, these findings suggest that the occipitoparietal lesion results in the impairment of movements toward targets in the 3D space and that these deficits can be decoded well before the movement end. In particular, these impairments affect both movements directed toward targets located along the horizontal axis and movements toward targets located along the sagittal axis in peripheral and foveal reaching conditions. This shows that the PPC is involved in the encoding of 3D reaching movements as monkey studies demonstrated in the recent literature (Bosco, Breveglieri, Hadjidimitrakis, Galletti, & Fattori, 2016; Hadjidimitrakis, Bertozzi, Breveglieri, Bosco, et al., 2014; Hadjidimitrakis, Bertozzi, Breveglieri, Fattori, & Galletti, 2014; Piserchia et al., 2017). Importantly, the decoding approach applied here to kinematic measures opens a novel perspective in the diagnosis and rehabilitation of visuomotor deficits by analysis of kinematic features of the movement from initial action stages, rather than using the pattern of errors of already accomplished movements.

5. SECOND STUDY

"Different effects of multiple interactions on size perception in virtual reality"

5.1 INTRODUCTION

Distances in virtual environments (VEs) are typically underperceived (Waller & Richardson 2008), whereas real-world distances are often perceived accurately, at least when measured through action-based tasks (Loomis & Knapp 2003; Durgin & Li 2011). One common approach to improve distance perception in virtual reality (VR) allows participants to interact with the VE while receiving visual feedback of their movements (Kelly et al. 2013; Kelly et al. 2014; Mohler et al. 2006; Richardson & Waller 2005, 2007; Waller & Richardson 2008). A study of Waller & Richardson (2008) showed that distance judgments in a VE were unaffected by interactions in which participants viewed only a simulation of visual walking (i.e., optic flow only). Thereby, physical walking was found to be necessary to elicit an increase in post-interaction distance judgments and simulated visual walking without concomitant physical walking was found to be insufficient. Moreover, Kelly et al. (2013) found that distance judgments increased after a walking interaction in the VE, while interacting with the VE by reaching did not influence subsequent distance judgments. This suggests that not all body-based interactions are sufficient to cause an increase in distance judgments.

As a matter of fact, research on action modulation effects in real-world environments has shown that the type of action to be planned biases visual search toward important action-related features, facilitating their perception to execute a more accurate subsequent movement (Wykowska et al. 2009). In the studies by Wykowska et al. (2009, 2011), the preparation of a grasping movement towards two-dimensional (2D) targets presented on a frontal screen facilitated the detection of a size-related parameters, and the preparation of a pointing movement facilitated the detection of a location-related parameters. In fact, size-related parameters are fundamental to prepare the grip aperture for a grasping movement (Wykowska et al. 2009) and location-related parameters, as luminance, are fundamental to prepare a pointing movement (Anderson & Yamagishi 2000; Graves 1996). Likewise, Gutteling et al. (2011) found that preparing for a grasping action increases the detection of object orientation change, relative to the preparation of a pointing action for which orientation is an irrelevant parameter. From these studies, it seems that the perception of object's features, such as size, can be facilitated only when the planned action requires the elaboration of those properties.

Similarly, preparing and performing different actions leads to distinct patterns of fixations on the object. For instance, when preparing a reaching action, the eyes perform a saccade toward an area of interest and then fixate it constantly until it is reached by the hand (Johansson et al. 2001). During a grasping movement, fixations first focus on the contact point for the index finger and then move to the object's center of mass. In contrast, during a viewing task, fixations simply fall on the object's center of gravity (Brouwer et al. 2009).

A significant number of studies on the action modulation effect in the real world focused on the preparation phase of the movement (Deubel & Schneider 1996; Gutteling et al. 2011; Hoffman & Subramaniam 1995; Neggers et al. 2007), while Bosco et al. (2017) found that also after the execution of a grasping movement the perception of 2D object size was modulated, revealing a tendency for the perceived sizes of objects to be scaled by the type of action. Moreover, Bosco et al. (2017) found that grasping affected perceived size more than reaching, again supporting the idea that not all body-based movements can elicit modifications on the perceived size of an object in space. Furthermore, Sanz Diez et al. (2022) confirmed that the execution of a grasping movement affects the perception of the size of a digitally displayed object.

Finally, because of the size-distance variance hypothesis (Sedgwick 1986), which postulates that perceived size and perceived distance are tightly coupled, walking-interaction and some hand movements like grasping could be the most beneficial body-actions to perform to enhance object size perception in VEs. However, no studies were performed to systematically evaluate the influence of multiple actions on the possible facilitation of object size perception in the virtual space.

Building on these findings, the current study aims to address this gap of knowledge by conducting two experiments (Experiment 1 and 2) in which participants estimated the size of an object in a VE before and after interacting with it. We manipulated the interaction conditions and registered participants' size judgments, while also tracking their eye movements, to investigate the effect of different actions, such as grasping and reaching, on object size perception. Additionally, we manipulated the way to arrive at the target location by making participants approach the target via teleportation (Experiment 1) and via walking simulation

(Experiment 2) to assess the influence of different ways to reach target location in VR. First, we hypothesized that after close interaction with the target, the accuracy of size estimations would improve in both experiments across all conditions. Second, we hypothesized that interacting with the object through a grasping movement would result in smaller size estimation errors compared to the conditions where the object's size was irrelevant to the task (reaching and no action). Additionally, we expected to observe different patterns of eye movements on the target depending on the interaction condition. Finally, as an exploratory question, we compared size estimation errors made after the interaction phase between participants who were teleported (Experiment 1) and participants who attended the walking simulation (Experiment 2).

5.2 METHODS

Experiment 1 & 2

5.2.1 Participants

Sixteen participants were recruited to participate in Experiment 1. One participant withdrew from the experiment after experiencing simulator sickness. The final sample comprised fifteen participants (Males=5, range=20-30 years; mean age=24.07 years). Data from one participant were removed from all analyses due to significant deviations from the observed trends in the sample, ensuring the dataset's integrity and consistency. Eleven participants had no experience with VR, and five reported limited experience (once only). Twenty participants were recruited to participate in Experiment 2. Three participants withdrew from the experiment after experiencing simulator sickness during the training phase. Seventeen participants were tested (Males=3, range=22-34 years; mean age=28.35 years), two participants were excluded from the analysis because one reported to be influenced by motion sickness, one reported not having understood the task at the end of the recording session. Five participants had no experience with VR, seven reported experiences limited to one occasion only, and three reported a lot of experience with VEs.

All participants were students or PhD students, were right-handed, had normal or corrected-to-normal vision, normal colour vision and reported no neurological diseases. All participants gave informed consent and were naïve to the purpose of the experiment. Participants that took part in Experiment 2 were compensated with 40$ AUD. The study procedures were approved by the Bioethics Committee of the University of Bologna (Exp. 1) and by the local Ethics Committee of the Faculty of Psychology at Western Sydney University (Exp. 2) and were in accordance with the Ethical standards of the 2013 Declaration of Helsinki.

5.2.2 Materials

In Experiment 1, the HTC Vive Pro headset was used to display the VE with a resolution of 1440 x 1600 pixels per eye, a refresh rate of 90 Hz and 110 degrees field of view. The Pupil Labs eye tracker add-on (Pupil Labs GmbH, Berlin, using Pupil Capture v. 1.11-4) was used to record eye movements at 90 Hz. In Experiment 2, the HTC Vive Pro Eye was used.

In both experiments, one of the HTC Vive controllers was held by participants with the left hand and used to adjust the size of the comparison object during the size estimation phases. Two HTC Vive Base Stations were used to track the location of the headset and the controller during the experimental recordings. The VE was rendered with Unity game engine (Unity Technologies, version 2020.3.23fl) using SteamVR (Valve corporation).

Participants were able to visualize a copy of their real right hand via the Vive Hand Tracking software development kit (see Fig. 1). This kit provides first-person view hand recognition, based on deep learning algorithms that detect twenty-one key points per hand. These points are then rendered as spherical points in the VE, creating a virtual skeletal representation of the detected hand that mimics the movements of the real one. (Figure 21).

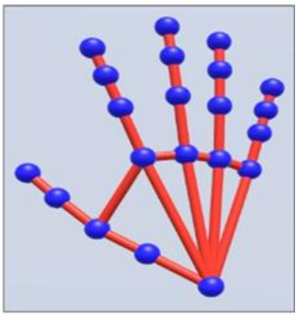

Figure 21. Rendered virtual hand. 21 sphere points (blue spheres) represent the 21 key points of the detected real hand.

5.2.2 Procedure

At the beginning of each experimental session, participants were asked to verbally report their age and their experience with VR technology, then the experimenter gave instructions on the use of the controller and of the experimental task procedure. Participants were requested to perform the interaction and estimation phases promptly and accurately, and to maintain a standing position throughout the experiment, with the possibility of stretching with minor body movements when needed. Before staring the experimental recording, they performed a training block (half of an experimental block) to become familiar with the VE and to learn the task. At the end of the recording session, each participant was asked to verbally report the strategy used to estimate the size of the target by the questions detailed in Table 1. This was done to gain insight into the cognitive processes underlying their task performance and to further analyse the effectiveness of the experimental conditions in eliciting specific action-perception interactions.

We used a within-subject design, where all participants performed all the experimental conditions in four experimental blocks of forty-five trials each. Between each block, participants had a break and could have a seat until the start of the next experimental block. The entire experimental session including breaks and training phase lasted two hours.

Table 3. Questions of the informal interview administered directly after the experiment.

1) Which strategy did you use to give the estimation of target size? (Also: What were you thinking when giving the estimation of the target size?)
2) Did you find any of the interaction conditions more difficult than the others when giving the estimation of the target size? a) If so: can you put the interaction conditions in order of difficulty?

System calibrations

At the start of each block, we ran two system calibrations: the first calibration served to match the height of the virtual targets and comparison objects with the participant's eye's height, the second calibration was run by the Pupil Labs add-on eye tracker to correlate the eye position with the gaze position in VR.

In Experiment 2, we also had to perform a third calibration to correct the distance of the virtual hand from the participant's body. Specifically, we noticed that the distance between the virtual hand and the headset was wrongfully rendered, i.e., the more the hand was extended in space, the more the distance representation was disproportionate. We therefore had to apply a correction to the virtual hand-to-headset distance to match it with the correctly tracked controller-to-headset distance, by performing a linear regression to estimate the best correction factor (r-squared ≥ 0.8). We suspect that the reason for this deviation is a lack of adjustment of the hand tracking algorithm to the camera lenses of the Vive Pro Eye.

5.2.3 Stimuli and task sequence

The experimental VE consisted of a corridor measuring 20 m (length) x 3 m (width) x 3 m (height). Linear perspective cues were added through wall decorations and floor textures. The experiment was structured in three phases: a size judgment task before the interaction with the target (First Size Judgment), the interaction with the target (Interaction) and a size judgment task after the interaction with the target (Second Size Judgment) (see Fig. 2). The target object was a grey sphere with five possible diameters: (1) 65 mm, (2) 70 mm, (3) 75 mm, (4) 80 mm, (5) 85 mm.

The interaction with the object consisted of three different experimental conditions: No Action, Reaching and Grasping, as depicted in Figure 22 (middle panel). Specifically, in the No Action condition, participants were instructed to not perform any movement and wait in front of the target (3 seconds); in the Reaching condition, they were instructed to touch the centre of the target with their right index finger and in the Grasping condition, they were instructed to grasp the target by touching the upper and lower part of the object with their right index and thumb, respectively. Auditory feedback was played any time the target was touched, and no haptic feedback was provided.

In the size judgment phases (right and left panels of Fig. 2), participants adjusted the size of a comparison object using a VR controller to match the target size by increasing, decreasing, or confirming the presented size. The comparison object was also a grey sphere, with sizes set at (a) 80%, (b) 100% or (c) 120% of the target size. Each combination of target size, comparison object size and interaction condition was randomly presented once in each block. The target and comparison objects were positioned on a virtual shelf at 0.5 m from the participant's eyes during the interaction and size judgment phases, respectively.

At the beginning of each trial, participants received text instructions describing the current experimental condition. This information was presented on a blank screen. Subsequently, the corridor was displayed together with a fixation point that appeared in front of the participant's eyes. Following the fixation point, the First Size Judgment phase started, and the target object appeared on a shelf located 3 meters away. After the target presentation, the blank screen reappeared, and the comparison object was then displayed on a shelf - identical to the target's shelf - in front of the participant for the first size judgment. Following this phase, participants of Experiment 1 were automatically teleported in front of the target, i.e. they would automatically jump at target location, while participants of Experiment 2 attended a linear self-motion simulation, which transported them to the target location at a velocity of 1.2 m/sec - which is considered a normal walking speed (Mohamed, O. & Appling, H. 2020). At that stage, participants from both experimental groups interacted with the object based on the trial condition, guided by a text reminder. Upon successful interaction, the Second Size Judgment started, and participants were automatically transported back at the beginning of the corridor where they saw the target from far again, before expressing the second size estimation (same procedure as the first one).

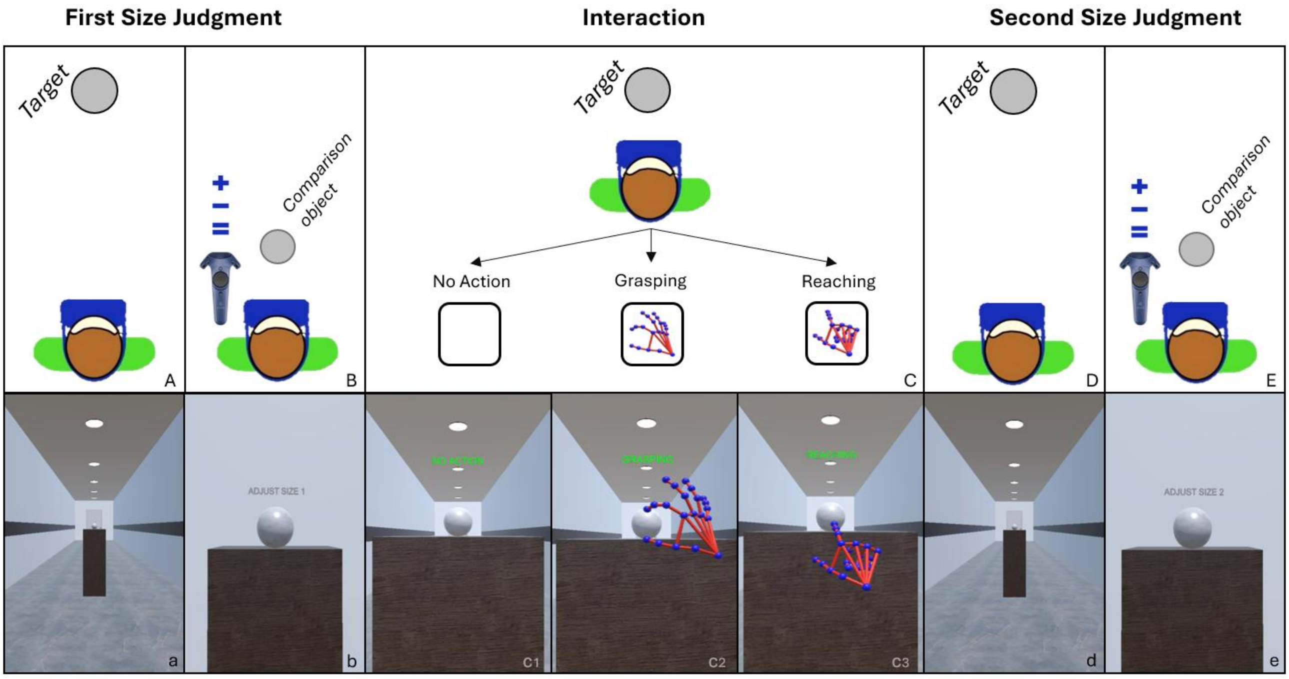

Figure 22. Schematic (first row) and corresponding first-person view (second row) of task sequence of Experiment 1 and 2. A) First Size Judgment phase. Target appears at 3 m distance from the participant. B) First Size Judgment phase. Target disappears and comparison object appears at 0.5 m distance from participant; the controller is used with the left hand to modify the size of the comparison object to match it with the target one. C) Interaction phase. Participant is teleported (Exp. 1) or passively moved (Exp. 2) to stand in front of the target and performs one of the three experimental conditions. D) and E) Same procedure as A) and B) for second size estimation. a) to e) represent corresponding first-person views of these phases. The figure does not include the representation of the approach to the target.

5.2.4 Data analysis

Size Judgments

We calculated the estimated target size in the two size judgment tasks by subtracting the actual target size from the estimated target size. We then evaluated the overall difference between size judgments before and after the Interaction phase and tested the effect of the different interaction conditions on the size estimation error using linear mixed model (LMM) analyses to account for both fixed and random effects. All the analyses were run using R (The R Project for Statistical Computing, version 4.2.1) using the lmer function of the lmerTest package which uses and implementation of Satterthwaite's degrees of freedom method to obtain p-values (Version 3.1-1; Kuznetsova et al., 2017). All models were fitted using the restricted maximum likelihood (REML) method.

We excluded trials in which participants were too slow in response times during the estimation phases. This was achieved by computing the mean duration of both the first and second size judgments separately and then adding three standard deviations to establish the threshold for acceptable response times. Subsequently, we excluded trials where participants pressed the button to confirm the presented size of the comparison object by mistake, i.e. when the number of frames of that trial was below 1. We also excluded trials in which participants were too slow when performing the Interaction phase. This was achieved by computing the mean duration of the Interaction phase and then adding two standard deviations to establish the threshold for acceptable interaction times. Following these criteria, a total amount of 53 trials were excluded.

To test our first hypothesis (H1), we built a LMM with Size Judgment Phase as categorical independent variable to test the overall effect of the two size estimation phases on the Estimation Error, including Participant and Experimental Block as random effects to account for variability. The reference level of Size Judgment Phase variable was set to First Size Judgment. The initial model was formulated as follows:

$$Estimation\ Error \sim Size\ Judgment\ Phase\ +\ (1|Participant)\ +\ (1|Experimental\ Block)$$

Subsequently, we incorporated to this model the variable Target Size, representing the diameter of the target, and the variable Scale Factor, the percentage applied to the target size to obtain the size of the comparison object, as fixed effects. We then performed an ANOVA test to compare the initial model with the new incorporated one (Model 1, see equation below). The AIC (Akaike Information Criterion) and BIC (Bayesian Information Criterion) values for Model 1 were lower than those of the initial model, indicating that the new model has a better fit to the data. The chi-square test comparing the two models was highly significant ($p<0.001$), suggesting that the additional parameters significantly improve the model fit. The final model (Model 1) was:

$$Model\ 1: Estimation\ Error \sim Size\ Judgment\ Phase\ +\ Target\ Size\ +\ Scale\ Factor\ +\ (1|Participant)\ +\ (1|Experimental\ Block)$$

To test our second hypothesis (H2), we built a similar LMM where we added Condition, representing the interaction condition variables, as a categorical predictor with three levels: Grasping, Reaching, and No Action. The reference level of the Condition variable was set to Grasping while the reference level for Size Judgment Phase was set to the Second Size Judgment. This model (Model 2) was formulated as follows:

$$Model\ 2: Estimation\ Error \sim Condition\ *\ Size\ Judgment\ Phase\ +\ Target\ Size\ +\ Scale\ Factor\ +\ (1|Participant)\ +\ (1|Experimental\ Block)$$

Results of all models are reported as estimated value, standard error, t-value, and p-value, where statistical significance is indicated by $p < 0.05$.

After visually checking both Model 1 and 2 assumptions, outlier values were observed in the residuals' plots. Therefore, we calculated the mean and standard deviation of the absolute error in the First and Second Size Judgments phases separately and the outliers were defined as the values above the mean plus two standard deviations of the error values of each task phase. These identified values were then excluded from the analysis to ensure that the residuals' plots of both models conformed to a normal distribution and display constant variance.

To further investigate the effects of the interaction conditions on the Second Size Judgment phase (H2), we computed the magnitude of the size estimation error by taking its absolute value. Due to the non-normal distribution of the absolute error values, we applied the non-parametric Wilcoxon signed-rank test for paired samples to assess for differences across conditions. Specifically, we compared all absolute error values between each pair of conditions and applied the Bonferroni correction to address the multiple comparisons, resulting in a significance threshold of $p < 0.0167$. Results of this analysis are reported as mean, standard deviation, median and p-value. We computed the same analysis to compare the overall magnitude of the size estimation error in the First and Second Size Judgment phases (H1). Due to the presence of ties in the data, the employed Wilcoxon tests applied a continuity correction. Therefore, the reported p-values are an approximation. Statistical significance is indicated by $p < 0.05$.

Reaction times

To explore in more detail the impact of different interaction conditions on the estimation phases, we examined the reaction times associated with reporting the target's size during the First and Second Size Judgment phases in Experiment 1. Specifically, we measured the time between the moment the comparison object was presented and the instant when either the button to adjust the size or the button to confirm the presented size was pressed. Outlier trials where participants were too slow during the Interaction phase or during the estimation phases, were excluded from this analysis. This exclusion was based on the computation outlined in the Size Judgments analysis section. After examining the distribution of reaction times during the size judgment phases, we opted to utilize the non-parametric Friedman rank sum test which handles the unbalanced number of observations per condition resulting from the exclusion of outlier values. To apply the test, we calculated the mean values of the reaction time per participant and per condition. To compare the overall reaction times between the First and Second Size Judgments phases we ran a Wilcoxon signed rank test with continuity correction. Results of this analysis are reported as mean, standard deviation, median and p-value.

Eye data

To determine if different patterns of eye movements were elicited depending on the interaction condition, we analysed eye positions during the interaction phase of Experiment 1.

We extracted eye data registered with the Pupil Labs add-on for VR at 90Hz and merged them with the Unity task data. We detected fixations by using a velocity-based algorithm (Salvucci & Goldberg 2000; velocity-threshold identification [I-VT]), setting a gaze velocity threshold of 80° per second and a minimum fixation duration of 100 ms (like in Gao et al. 2022), excluding frames where the quality of the assessment for the eye image from the eye tracker was below the recommended value (0.60) in the Pupil Labs documentation. Outlier trials where participants were too slow during the Interaction phase or during the Size Judgment phases, were excluded from this analysis. This exclusion was based on the computation outlined in the Size Judgments analysis section.

We analysed the position of the detected fixations on the target during the Interaction phase by computing their centroid position. Subsequently, we computed the following parameters: the distance of the centroid of the initial fixation from the centre of the target and the distance between the centroids of the first and second fixations on the target. Since all variables studied were not normally distributed and since the number of observations per conditions was unbalanced - because of the different number of fixations detected per trial - we applied the Friedman test to compare the effects of the different interaction conditions on the fixation locations on the target. To apply the test, we calculated the mean values of the variables for each participant and for each condition.

Additionally, we aimed to investigate whether different interaction conditions would also influence participants' gaze behaviour when evaluating the target's size. Therefore, we performed the same analysis - as for the Interaction phase - for all fixation positions on the comparison object during the estimation phases. Results of these analyses are reported as mean, standard deviation, median and p-value.

5.3 RESULTS

Experiment 1

5.2.5 Size Judgments

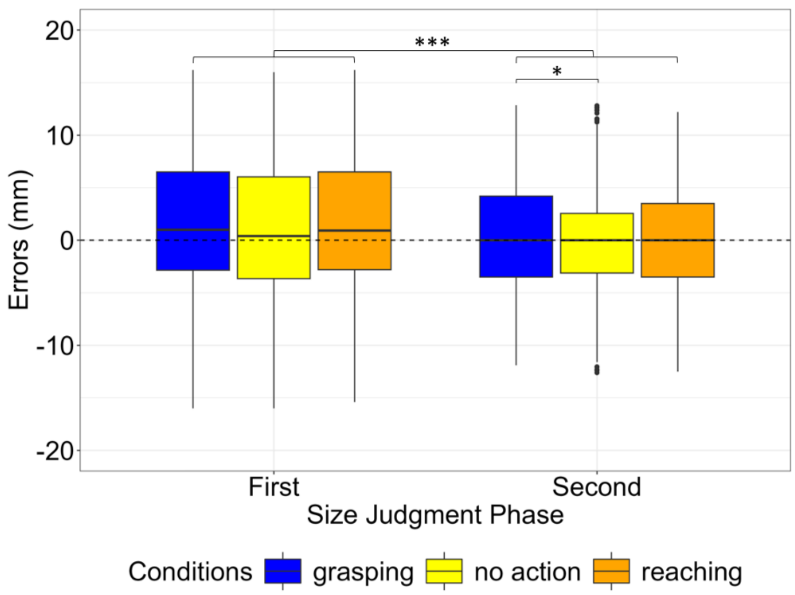

Figure 23. Distributions of the size estimation errors. Boxplots represent the distributions of the errors made in the First (left boxplots) and Second (right boxplots) Size Judgment phases of Experiment 1. Different colours represent the different interaction conditions performed by participants. Positive values (above zero line) indicate overestimation of the target size; negative values (below zero line) indicate underestimation of target size. Asterisks represent significant differences (***p<0.001, *p<0.05).

In this study, the estimated target size was calculated for each participant that performed the experiment. The overall estimation error in the Second Size Judgment phase was significantly smaller than in the First Size Judgment phase (β = -1.498 mm, SE = 0.1321, t = -11.337, p <

0.001, see left and right box plots of Fig. 3), meaning that participants made smaller errors during the Second Size Judgment phase. In the Second Judgment phase, the size estimation error was significantly smaller after the No Action interaction phase compared to the size estimation error after the Grasping interaction phase (β= -0.5232 mm, SE= 0.2293, t= -2.282, p = 0.02254), whereas we found no significant differences between the size estimation error after the Grasping and Reaching interaction phases (p = 0.15123), as it is shown in Figure 3 (right box plots).

Additionally, the overall difference in the magnitude of the error between the First and the Second Size Judgment phases was found to be significant ($p < 0.001$) with the First phase showing a larger error (Mean = 5.4, Std = 4.1, Median = 5) compared to the Second one (Mean = 3.8, Std = 3.2, Median = 3.5) suggesting that after the Interaction phase, participants were more accurate in the size estimation. The difference in the magnitude of the error between the interaction conditions in the Second Size Judgment phase was also found to be significant. After applying the Bonferroni correction, we found a significant difference ($p < 0.0167$) between Grasping (Mean = 4.1, Std = 3.2, Median = 3.8) and No action (Mean = 3.4, Std = 3.1, Median = 3) and a significant difference ($p < 0.0167$) between Reaching (Mean = 3.9, Std = 3.1, Median = 3.5) and No action. No significant difference was found between Grasping and Reaching ($p > 0.0167$).

5.2.6 Reaction times

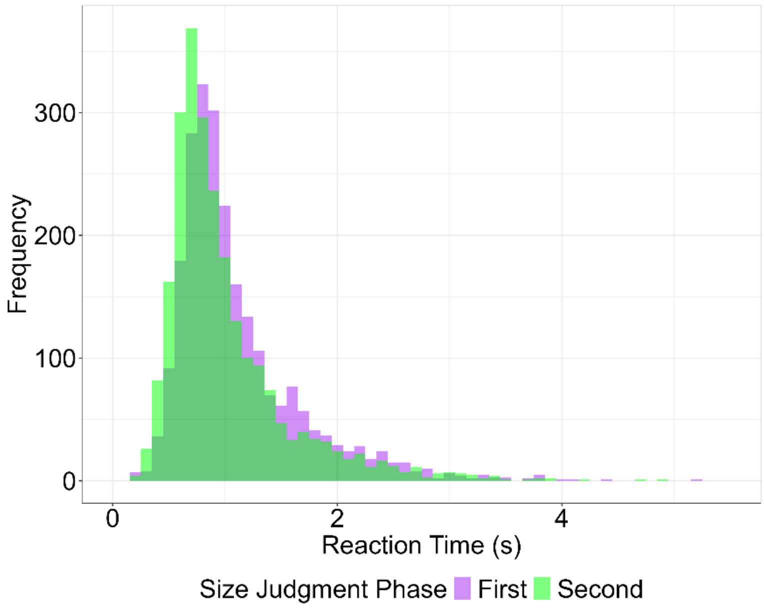

Figure 24. Overlapping histograms of the reaction times of the First (purple histogram) and Second (green histogram) Size Judgment Phases. The figure shows that participants were significantly faster when reporting the size estimation in the Second Size Judgment phase.

We observed overall significantly ($p < 0.001$) faster reaction times in the Second Size Judgment phase (Mean = 1.00 sec, Std = 0.55, Median = 0.83), compared to the First one (Mean = 1.11 sec, Std = 0.56, Median = 0.94), suggesting that participants were faster in their response after the Interaction phase across all conditions. However, we did not find any significant difference between conditions not in the First nor in the Second Size Judgment phases ($p > 0.05$).

5.2.7 Fixation locations

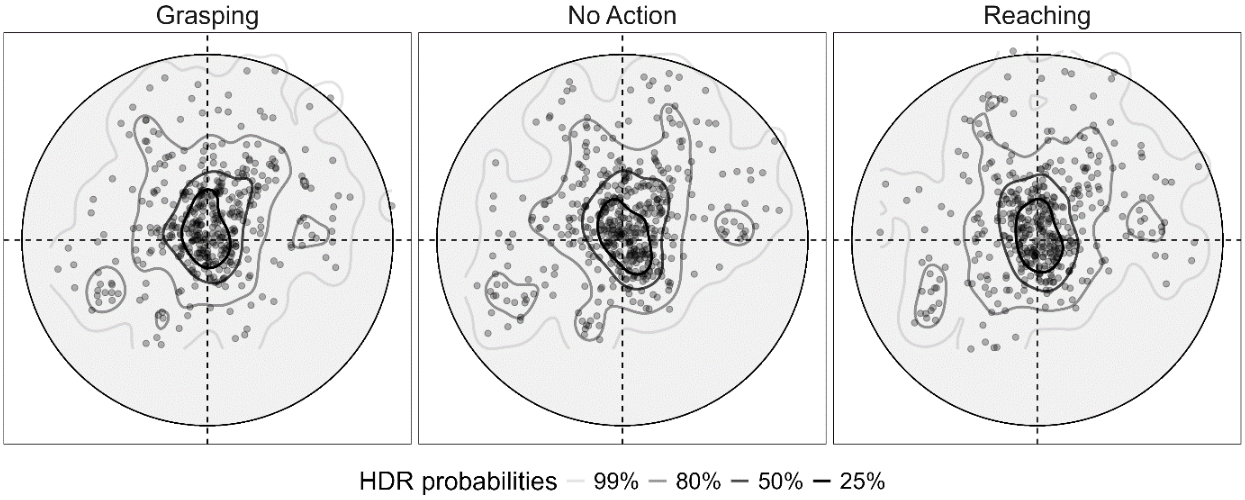

Figure 25. HDRs of the first fixation made on target for each interaction condition. Each circle represents the 2D view of the sphere-target. The represented diameter of the circles is the average of all five possible diameter values (75 mm) so that the points outside the circles represent fixations on the larger sizes (80 mm and 85 mm). Lines outline different regions which represent different percentages (HDR probabilities) of the total probability distribution of the first fixations made on the target.

The pattern of the initial fixation centroid positions during the Interaction phase is depicted in Figure 25, revealing a consistent pattern within the central 50% of fixations across all conditions.

The analysis of fixations patterns on the target during the Interaction phase did not show significant differences between conditions. Specifically, the distance of the first fixation centroids from the centre of the target did not show significant differences ($p > 0.05$), as well as the distance between the first and the second fixations centroids.

The analysis of the eye positions on the comparison object during the estimation phases revealed an overall significant difference between the First and Second Size Judgment phases ($p < 0.05$), with the latter showing a shorter distance of the fixations from the centre of the object (Mean = 0.007, Std = 0.006, Median = 0.006), compared to the former one (Mean = 0.008, Std = 0.006, Median = 0.006). The Friedman test used to assess differences between interaction conditions in eye pattern on the object during the First Size Judgment phase, did not find a significant difference ($p > 0.05$), while the same test applied to the Second Size Judgment found a significant difference between conditions ($p < 0.05$). To further analyse this result, we performed the Wilcoxon signed-rank test for paired samples on the means calculated per participant and per condition. However, no significant pairwise differences were observed ($p > 0.05$), possibly due to the lower statistical power inherent in analysing the calculated means.

5.2.7 Informal debriefing interview

The results of the informal interview administered immediately after the experiment (see Table 1) are summarized in Table 2 and 3 (below). The most frequent strategy reported by participants was trying to recollect the target's image when adjusting the size of the comparison object during the Second Size Judgment phase (Table 2).
Interestingly, when participants were asked to rate the difficulty of the interaction conditions (Table 3) some participants did not report any noticeable distinctions between conditions, while the majority reported Reaching as the most difficult condition. Conversely, No Action was identified as the easiest condition.

Table 4. Reported strategies for estimating target size. The table represents the number and the percentage of participants per reported strategy. Most participants recollected the target's image, while others combined recollecting the target's image with using the environment spatial relationships, and one used other object in the environment as reference.

Strategy Used	Number of participants	Percentage
Target's image recollection	9	60%
Combing target's image recollection and spatial relationships	5	33.33%
Using only other objects as reference	1	6.67%
Total	15	100%

Table 5. Summary of participants' ratings of interaction conditions. The table details the number of participants for each rating. Most participants reported that the Reaching condition was the most difficult to perform, while the No Action condition was the easiest.

Interaction Condition	Most Difficult	Easiest
Reaching	4	2
No Action	3	6
Grasping	3	2
No noticeable distinctions	5	5
Total	15	15

Experiment 2

5.2.8 Size Judgments

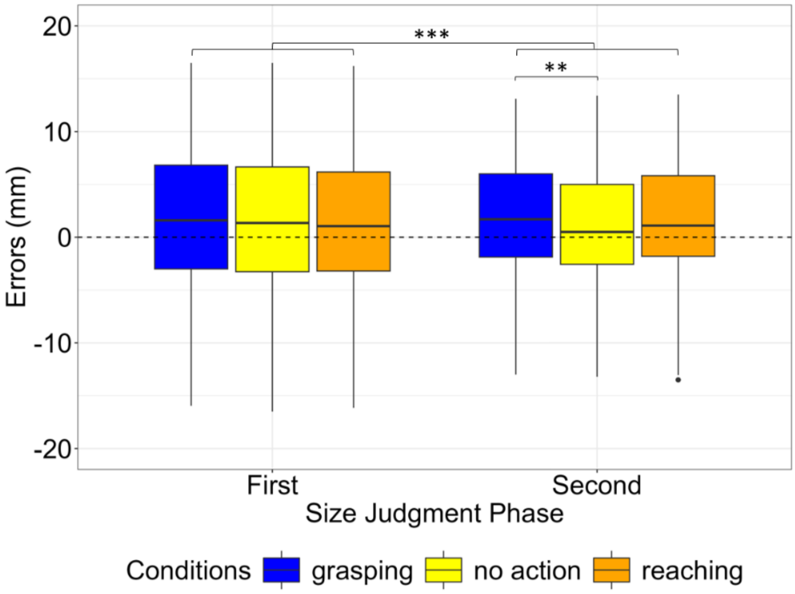

Figure 26. Distributions of the size estimation errors. Boxplots represent the distributions of the errors made in the First (left boxplots) and Second (right boxplots) Size Judgment phases of Experiment 2. Different colours represent the different interaction conditions performed by participants. Positive values (above zero line) indicate overestimation of the target size; negative values (below zero line) indicate underestimation of target size. Asterisks represent significant differences (***$p<0.001$, **$p<0.01$).

Similarly to Experiment 1, the overall difference in the magnitude of the error between the First and the Second Size Judgment phases was found to be significant ($p < 0.001$) with the First phase showing larger errors (Mean = 6.3, Std = 5.1, Median = 5.5) compared to the Second one (Mean = 5.1, Std = 4.3, Median = 4.5), suggesting improved accuracy in the estimation of the target size after the Interaction phase. On the contrary, the difference in the raw value of the estimation error during the judgment phases did not reach significance ($p = 0.0911$).

In the Second Judgment phase, the raw estimation error was significantly smaller after the No Action interaction phase compared to the size estimation error after the Grasping interaction phase (β= -0.71753 mm, SE= 0.25721, t= -2.790, $p = 0.0053$), whereas we found no significant differences between the size estimation error after the Grasping and Reaching interaction phases ($p = 0.4606$), as it is shown in Figure 6 (right box plots).

On the contrary, the difference in the magnitude of the error between the interaction conditions in the Second Size Judgment phase was found to be significant ($p < 0.05$) between Grasping

(Mean = 4.5, Std = 3.2, Median = 4.5) and No Action (Mean = 4.2, Std = 3.3, Median = 3.9), but the observed difference did not remain significant after the Bonferroni correction.

5.2.9 Informal debriefing interview

The results of the informal interview administered immediately after the experiment (see Table 1) are summarized in Table 4 and 5 (below). Most of participants reported relying on recollecting the target image while adjusting the size of the comparison object during the Second Size Judgment phase. When participants were asked to rate the difficulty of the interaction condition, the majority reported No Action as the most difficult condition. Conversely, Grasping was identified as the easiest condition.

Table 4. Reported strategies for estimating target size**.** The table represents the number and the percentage of participants per reported strategy. Most participants recollected the target's image, while others combined recollecting the target's image with using the environment spatial relationships, two relied on the virtual fingers grip aperture during grasping, and one used other objects in the environment as reference.

Strategy Used	Number of participants	Percentage
Target's image recollection	9	60%
Combing target's image recollection and spatial relationships	3	20%
Using virtual fingers grip aperture	2	13.33%
Using only other objects as reference	1	6.67%
Total	15	100%

Table 5. Summary of participants' ratings of interaction conditions. The table details the number of participants for each rating. Most participants reported that the No Action condition was the most difficult to perform, while the Grasping condition was the easiest.

Interaction Condition	Most Difficult	Easiest
Reaching	4	7
No Action	7	6
Grasping	2	0
No noticeable distinctions	2	2

Experiment 1 and Experiment 2

5.2.8 Comparison between Size Judgments

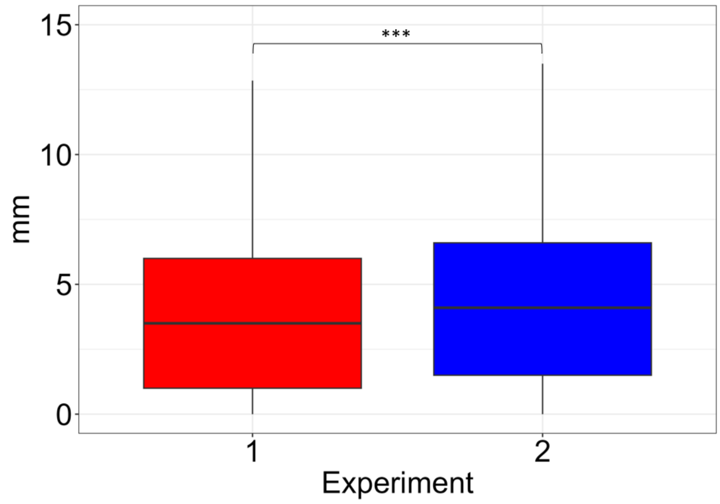

Figure 27. Distributions of the absolute size estimation errors of the two experiments. Boxplots represent the distributions of the errors made during in the Second Size Judgment phase in Experiment 1 (left boxplot) and Experiment 2 (right boxplot). Asterisks represent significant difference (***p<0.001).

We performed a comparison analysis between the two experiments to assess the difference in estimation errors, resulting from different means to arrive at the target location. In Experiment 1, participants arrived at target location via teleportation, while in Experiment 2, participants attended a walking simulation.

Therefore, we applied a Welch Two Sample t-test to compare the overall raw errors of the Second Size Judgment phase of the two experiments. We found an overall significant lower error value ($p < 0.001$) for Experiment 1 (Mean = 0.03, Std = 4.96) compared to Experiment 2 (Mean = 1.41, Std = 5.31), as well as between each interaction condition of the two experiments.

Subsequently, we performed the Mann Whitney U test to compare the absolute errors of the Second Size Judgment phase and we found a significant difference ($p < 0.001$), with Experiment 1 showing a significant smaller error (Mean = 3.81 mm, Std = 3.17) compared to Experiment 2 (Mean = 4.40, Std = 3.29), as well as between each interaction condition across the two experiments. The distributions of the magnitude of the errors in both experiments are represented in Figure 27.

Finally, we compared the absolute errors of the First Size Judgment phase of the two experiments. This analysis aimed to assess the possible effect of the different approaches to arrive at the target location on the overall task difficulty. Therefore, we again applied the Mann Whitney U test and found no significant difference ($p = 0.3376$) between the two groups in the magnitude of the error in the First Size Judgment phase, suggesting that the different means to arrive at the target location did not affect differently the overall difficulty of the task.

5.4 DISCUSSION

In the current study, we found that different types of interactions can lead to different effects on the perception of the size of an object in VR. This was observed using a size judgment task where participants estimated the size of a target before and after interacting with it, alongside with approaching the target via teleportation (Experiment 1) or via walking simulation (Experiment 2).

Overall, size estimations after the Interaction phase showed significantly more accurate and faster responses compared to the estimations given before the interaction with the target, conform to our first hypothesis (H1) in both experiments. This improvement can be attributed to the interaction with the target, where participants viewed the object up close, potentially allowing them to adjust their first response in the Second Size Judgment phase. This way, our manipulation may have introduced a perceptual bias, leading participants to systematically recalibrate their first response after the Interaction phase. As a result, the observed overall improvement may be due to a general test-retest effect rather than an actual enhancement in perceptual accuracy.

However, contrary to our second hypothesis (H2), it is not Grasping that leads to significantly smaller errors compared to the other two interaction conditions in the Second Size Judgment phase. Participants were significantly more accurate in reporting the target size after the No Action condition compared to the Grasping one. This suggest that participants made significantly better estimations when they did not have to perform any hand movement on the target in both experiments.

These results are not consistent with real world studies where the preparation of a grasping movement can facilitate the perception of the size of an object (Wykowska et al. 2009), improve the detection of deviations in object size (Fagioli et al. 2007), or scale size perception by using hands' grasping abilities as perceptual rulers (Linkenauger et al. 2011). Here, it seems that participants were not relying on the hand's presence at all; as a matter of fact, only two participants explicitly reported to have used the virtual hand grip aperture during the grasping movement as a reference when giving the size estimation in Experiment 1. Additionally, the analysis of the fixation patterns on the target during the Interaction phase of Experiment 1 revealed different results compared to real-world studies. It is known that the pattern of fixation locations on a 2D object varies between viewing and grasping tasks. During grasping movements, there is a tendency for gaze to shift towards the index finger contact point on the object, following a fixation on the centre of gravity. In contrast, during viewings tasks, all fixations tend to fall closer to the object's centre of gravity (Brouwer et al. 2009). Our findings indicate no significant differences in the distance between the first and second fixations, nor in the distance between first fixation and the centre of the target across all conditions. This suggests that, during Grasping, there was likely no gaze shift towards the upper part of the object, which participants aimed with their index finger. Furthermore, we did not find significantly different effects between the interaction conditions on the fixation locations on the comparison object in both estimation phases (First and Second), indicating that neither the preparation nor the execution of different interactions influenced the way participants looked at the comparison object. Nevertheless, participants looked significantly closer to the centre of the comparison object after interacting with it (Second Size Judgment phase). Therefore, it seems participants were not looking at the target any differently than they were looking at the comparison object. One possible explanation is that the VR environment may not evoke the same depth cues and tactile feedback present in real-world interactions, which are critical for the perceptual-motor coordination seen in natural grasping tasks. In VR, the absence of haptic feedback and the reliance on visual cues alone may cause participants to rely on a more generalized viewing strategy, focusing on the object's center rather than specific contact points. This could indicate that, in VR, participants' fixations are less influenced by their interaction intentions (such as grasping or reaching), leading them to treat the target and comparison objects similarly in terms of gaze distribution. This reliance on centralized fixation might also reflect a compensatory strategy to enhance size perception in the absence of detailed tactile and proprioceptive information, highlighting a perceptual adjustment unique to virtual environments.

The fact that participants were not looking at the target any differently than they were looking at the comparison object can also be partially explained by the informal verbal debriefing conducted at the end of the experiment. Participants were asked to explicitly report the strategy used to judge the size of the target during the estimation phases. The most frequently reported strategy by both groups of participants was the recollection of the target image. This implies that, participants tried to memorize the visual representation of the target during the Interaction phase. Therefore, the presence of the hand during Grasping, might have functioned, not as facilitator, but rather as an element of interference during the memorization process, thus leading to a less accurate estimation of the target size. This aspect could be connected to the observation that most of participants tended to eventually close their index and thumb fingers more than the real dimension of the target when grasping it, as also observed in a study of Chessa and colleagues (2019), where participants grasped objects with a virtual hand. Hence, the smaller improvement in estimating the size of the target after the Grasping interaction could be ascribed to the absence of tactile feedback, as also pointed out in Bosco and colleagues (2017), where it was found that grasping 2D objects modulated the perception of their size, but not resulting in increased accuracy.

Remarkably, when participants were also asked to rate the difficulty of the conditions, the majority reported No Action as the most difficult, and Grasping as the easiest only in Experiment 2. When participants were further prompted to explain why Grasping was perceived as the easiest condition, they reported that the presence of the hand was helpful during the Interaction phase, even if they did not initially mention it, in response to the first structured question asked. This result may indicate that participants recognized that the grip aperture of the hand during the grasping action could have been informative on the target size, only when explicitly prompted to logically think about their answers. This finding is in line with the importance of the demand characteristics of the task and the influence of the context of it, as illustrated in the study of Collier et al. (2017). In fact, the authors demonstrated how the scaling effect found in a study of Linkenauger and colleagues (2011), where participants estimated objects as smaller depending on the intended hand to use for grasping them (predominant vs. non-predominant), likely occurred because an explicit connection between judging the graspability of the object and judging its size was provided. Therefore, since in our experiment no explicit information about the connection between grasping and the facilitation of the object's size perception was given prior the experiment execution, participants may not have relied on the additional information that the use of the virtual hand during grasping could have potentially provided during the Interaction phase. On the other hand, most participants that took part in Experiment 1 did not report differences in the interaction conditions difficulty, but the No Action phase was reported as the most helpful one to perform when evaluating the target's size.

Finally, the comparison between the two experiments of this study indicates that the different means to arrive at the target location to interact with it, influenced the accuracy of the estimation of the target size. As a matter of fact, participants that were teleported in Experiment 1 were significantly more accurate in reporting the target's size after the Interaction phase than participants that attended the self-motion simulation in Experiments 2. This observation suggests that approaching the target via walking simulation led participants to be significantly less accurate after the Interaction phase. This finding is consistent with existing literature on the impact of optic flow stimulation on distance perception within VEs. Notably, prior research has demonstrated that the improvement in distance perception only comes from a real walking action, rather than a simulated one (Waller & Richardson 2008). Furthermore, our study reveals that optic flow stimulation had a negative effect on participants' perception of target size compared to teleportation (without optic flow stimulation). This result could potentially be attributed to the presence of unreported subtle motion sickness symptoms during the self-motion simulation. In VR, the lack of congruent sensory information between optic flow and the vestibular and proprioceptive feedback can lead to disorientation, which may interfere with spatial accuracy. In fact, the optic flow simulation used in Experiment 2 resembles joystick navigation in VR—a method known to potentially compromise the VR experience compared to the more traditional teleportation technique (Coomer et al., 2018). By contrast, teleportation by eliminating continuous optic flow and minimizing these sensory conflicts, potentially allowed participants to focus on the size estimation task without interference from virtual self-motion.

5.5 CONCLUSIONS

Our findings indicate that overall approaching and interacting with a target in VR, leads to faster responses and better estimations of its size. But more interestingly, we found that performing a grasping movement towards the object does not lead to significantly more improvement compared to a reaching action or a condition where no hand movement is required. Moreover, we observed a deviation from the typical fixation patterns associated with grasping movements in real-world studies, suggesting that, at least in this context when relying only on visual inputs, the grasping action elicited different perceptual processes compared to real-world scenarios.

Notably, different kinematic aspects of reach-to-grasp movements, such as longer movement times and larger maximum grip aperture, have already been found in VR (Itaguchi et al. 2021). Therefore, it would be worth exploring how grasping movement characteristics could also influence the perception of objects in our VR experiment. Finally, we observed how approaching the target via walking simulation led to significantly larger errors in the estimation of the target size, compared to teleportation, which is the most used way to navigate in VR. Considering this, it would be interesting to investigate whether approaching the target via a real walking action would improve the estimation of size more than teleportation.

These investigations hold the potential to deepen our understanding of the intricate relationship between action dynamics and perceptual outcomes in VEs. For instance, VR could be used to design new rehabilitation techniques that support individuals with visuomotor impairments by simulating different types of interactions and movements that enhance perceptual accuracy and motor skills. As a matter of fact, the use of VR technology potentially enhances the degree of the patient engagement in therapy to limit boredom, fatigue, lack of enthusiasm, and lack of cooperation, which may negatively affect motor recovery (Tinson et al. 1989). Understanding the specific factors that influence perception and action in VR will be crucial for creating effective therapeutic interventions and improving the overall efficacy of VR-based rehabilitation programs.

6. GENERAL DISCUSSION

The studies conducted in this thesis aimed to contribute to a deeper understanding of sensorimotor integration in both real and virtual environments.

In particular, the first study focused on characterizing the kinematics of reaching movements in a patient with a bilateral occipitoparietal damage. To this aim, a decoding approach was used to distinguish between the patient's movements and those of a group of healthy participants. The study found that the posterior parietal cortex plays a crucial role in encoding reaching movements within three-dimensional space. Specifically, damage to this area affected the ability of the patient to accurately perform movements along both the horizontal and sagittal axes, especially when the target displayed during the task was positioned at the periphery of the field of view (i.e. in the non-foveated condition), consistent with the literature on optic ataxia (Perenin & Vighetto, 1988).

These findings underscore the critical role of the posterior parietal cortex in sensorimotor integration and highlight the potential of novel decoding methods to identify and characterize visuomotor impairments based on the analysis of motor trajectories. In fact, in the specific case of optic ataxia, literature on its rehabilitation is sparse, probably because it is a rare and thus less adequately studied deficit (Jacob et al., 2002).

In contrast, the rehabilitation of reaching movements has been more extensively studied in patients with hemiparesis. In these cases, examining spontaneous compensatory strategies has resulted in effective therapies. For instance, therapies may involve restraining trunk movements if the patient uses them to compensate for upper limb deficits (Thielman et al., 2008). Moreover, motor and sensory deficits can be attenuated by experience-dependent plasticity in the central nervous system, which can be induced through repetitive motor training (Michaelsen et al., 2006; Teasell et al., 2006).

However, the effect of mere movement repetition, as well as the evolution of spontaneous compensation strategies, has been scarcely studied in the field of optic ataxia. Interestingly, a single case study of Baumard et al. (2019) described a patient suffering from optic ataxia who benefited from a single training session consisting of repetitive reaching movements (see Figure 27). This finding may encourage therapists to propose intensive training sessions instead of short treatment sessions several days apart. In terms of strategies, restoring automatic object-hand automatization through repetitive training may be a relevant therapeutic goal in the treatment of optic ataxia.

These insights emphasize the importance of further research into the neural mechanisms and kinematic characteristics underlying these impairments, providing a foundation for restoring and support sensorimotor abilities with different techniques.

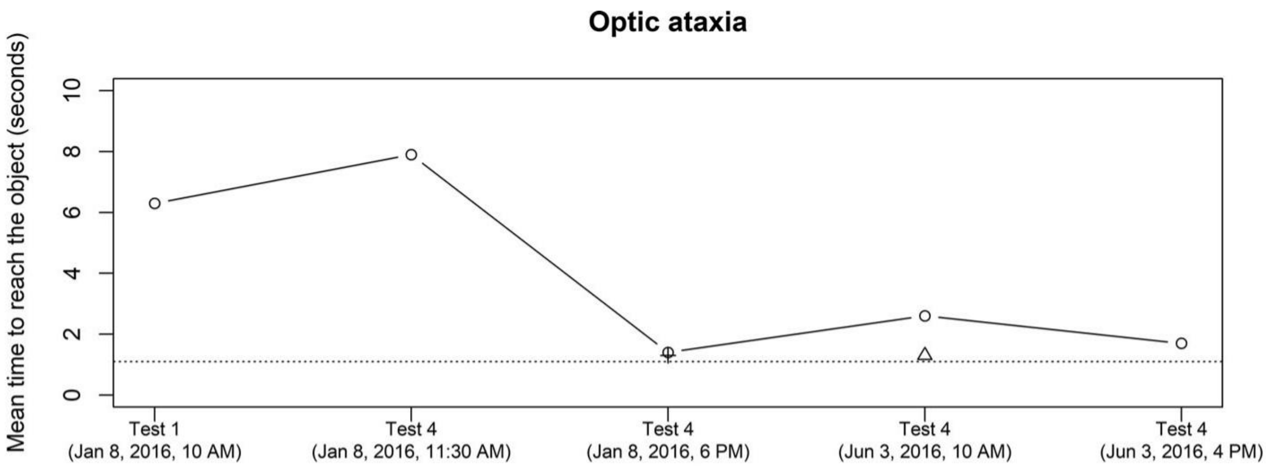

Figure 27. Effect of repetitive training on a patient with optic ataxia. Different testing sessions performed with the affected right hand in the central visual field. Test 1 consisted in reaching a cube under visual control. Test 4 consisted in reaching different objects under visual control. "+": mean reaching time with four alternative objects. Test 4 was proposed again on June 3rd to verify whether improvement was sustainable. "Δ": mean reaching time in Test 4, using the left hand as a point of comparison. The horizontal dotted line corresponds to the mean reaching time of one healthy 70-year-old man in Test 4. (modified from Baumard et al., 2019)

To support the possibility to use new contexts to rehabilitate visuomotor disorders, the second study of this thesis aimed to investigate sensorimotor integration from a different perspective by exploring the effects of various interactions on object perception in virtual reality.

Given that previous research indicates perception in virtual environments is often less accurate than in physical environments, this study aimed to systematically evaluate how different types of interactions, such as simulated walking, reaching, and grasping, can improve the perception of objects in virtual spaces. This approach not only broadens the scope of sensorimotor integration research but also addresses a gap in knowledge concerning the effects of multiple interactions on perception in virtual environments.

Contrary to our hypothesis, we found that the most beneficial interaction condition for improving the perception of an object's size in virtual reality was observation. Moreover, we found that approaching the object via teleportation induced more beneficial effects on perception compared to approaching the target via self-motion simulation. These findings suggest that, at least in the proposed virtual reality context where participants relied solely on visual inputs, action and perception interact differently to what is expected in the real world. This is particularly relevant in the context of studying sensorimotor integration in virtual reality and possibly using this technology to rehabilitate and support patients with visuomotor impairments. For instance, reach-to-grasp movements are a standard of virtual environments based upper-extremity neurorehabilitation (Merians et al., 2019). However, since tactile feedback cannot be provided due to the cost and limitations of wearable haptic devices, it is still unclear to what extent movements produced in virtual reality resemble those produced in the physical space (Furmanek et al., 2019). Nevertheless, virtual reality provides the opportunity for adaptive and progressive motor learning through perceptual modifications such as activity and workplace scaling, and error augmentation, resulting in greater dosage, intensity and engagement in training (Adamovich et al., 2009; Pallesen et al., 2018). By enhancing the degree of interaction between the patient and the therapy virtual reality can limit boredom, fatigue, lack of enthusiasm, and lack of cooperation, which may negatively affect motor recovery (Tinson et al., 1989).

As previously mentioned, the repetition of motor actions has been already used to rehabilitate visuomotor deficits, such as in the optic ataxia case described by Baumard et al. (2020). This type of training can be easily incorporated into virtual reality environments to make rehabilitation more engaging. The advantage of this approach is that training tasks can be individualized to the motor abilities and preferences of the learner, as well as to the therapeutic goal (Knaut et al., 2009).

The integration of findings from the studies presented in this thesis provides further understanding of sensorimotor integration. By examining the effects of neurological impairments on movement trajectories and the influence of different actions on perception in virtual reality, this thesis offers valuable insights into the mechanisms of sensorimotor processing and their implications for clinical rehabilitation and virtual reality use.

8. BIBLIOGRAPHY

Adamovich, S. V., Fluet, G. G., Tunik, E., & Merians, A. S. (2009). Sensorimotor training in virtual reality: a review. NeuroRehabilitation, 25(1), 29–44. doi: 10.3233/NRE-2009-0497

Aflalo, T., Kellis, S., Klaes, C., Lee, B., Shi, Y., Pejsa, K., ... Heck, C. (2015). Decoding motor imagery from the posterior parietal cortex of a tetraplegic human. Science, 348(6237), 906–910

Andersen, R. A., Andersen, K. N., Hwang, E. J., & Hauschild, M. (2014). Optic ataxia: From Balint’s syndrome to the parietal reach region. Neuron, 81(5), 967–983, https: //doi.org/10.1016/j.neuron.2014.02.025

Anderson, S. J., & Yamagishi, N. (2000). Spatial localization of colour and luminance stimuli in human peripheral vision. Vision Research, 40, 759– 771. https://doi.org/10.1016/S0042-6989(99)00240-0

Archambault, P. S., Ferrari-Toniolo, S., Caminiti, R., & Battaglia-Mayer, A. (2015). Visually-guided correction of hand reaching movements: The neurophysiological bases in the cerebral cortex. Vision Research, 110, 244–256, https://doi.org/10.1016/j.visres.2014.09.009

Bagesteiro, L. B., Sarlegna, F. R., & Sainburg, R. L. (2006). Differential influence of vision and proprioception on control of movement distance. Experimental Brain Research, 171(3), 358–370, https://doi.org/10.1007/s00221-005-0272-y

Balint, R. (1909). Seelenlahmung des "schauens" optische Ataxie, raumliche Storung der Aufmerksamkeit. Monatsschr Psychiatr Neurol, 25, 51–81. Retrieved from http://ci.nii.ac.jp/naid/10005280654/en/

Battaglia-Mayer, A., Ferraina, S., Genovesio, A., Marconi, B., Squatrito, S., Molinari, M., ... Caminiti, R. (2001). Eye-hand coordination during reaching. II. An analysis of the relationships between visuomanual signals in parietal cortex and parieto-frontal association projections. Cerebral Cortex (New York, N.Y. : 1991), 11(6), 528–44

Battaglini, P.P., Muzur, A., Galletti, C. et al. Effects of lesions to area V6A in monkeys. Exp Brain Res 144, 419–422 (2002). https://doi.org/10.1007/s00221-002-1099-4

Baumard, J., Etcharry-Bouyx, F., Chauviré, V., Boussard, D., Lesourd, M., Remigereau, C., ... Le Gall, D. (2019). Effect of object substitution, spontaneous compensation and repetitive training on reaching movements in a patient with optic ataxia. Neuropsychological Rehabilitation, 30(9), 1786–1813. doi: 10.1080/09602011.2019.1607397

Baylis, G., & Baylis, L. (2001). Visually misguided reaching in Balint’s syndrome. Neuropsychologia, 39(8), 865–875

Blangero, A., Gaveau, V., Luauté, J., Rode, G., Salemme, R., Guinard, M., ... Pisella, L. (2008). A hand and a field effect in on-line motor control in unilateral optic ataxia. Cortex, 44(5), 560–568, https://doi.org/10.1016/j.cortex.2007.09.004

Blangero A, Ota H, Delporte L, Revol P, Vindras P, Rode G, Boisson D, Vighetto A, Rossetti Y, Pisella L. Optic ataxia is not only 'optic': impaired spatial integration of proprioceptive information. Neuroimage. 2007;36 Suppl 2:T61-8. doi: 10.1016/j.neuroimage.2007.03.039

Blangero, A., Ota, H., Rossetti, Y., Fujii, T., Ohtake, H., Tabuchi, M., ... Pisella, L. (2010). Systematic retinotopic reaching error vectors in unilateral optic ataxia. Cortex, 46(1), 77–93, https://doi.org/10.1016/j.cortex.2009.02.015

Bosco, A., Breveglieri, R., Chinellato, E., Galletti, C., & Fattori, P. (2010). Reaching activity in the medial posterior parietal cortex of monkeys is modulated by visual feedback. Journal of Neuroscience, 30(44), 14773–14785, https: //doi.org/10.1523/JNEUROSCI.2313-10.2010

Bosco, A., Breveglieri, R., Hadjidimitrakis, K., Galletti, C., & Fattori, P. (2016). Reference frames for reaching when decoupling eye and target position in depth and direction. Scientific Reports, 6(February), 21646, https://doi.org/10.1038/srep21646

Bosco, A., Breveglieri, R., Reser, D., Galletti, C., & Fattori, P. (2015). Multiple representation of reaching space in the medial posterior parietal area V6A. Cerebral Cortex, 25(6), 1654

Bosco, A., Piserchia, V., & Fattori, P. (2017). Multiple coordinate systems and motor strategies for reaching movements when eye and hand are dissociated in depth and direction. Frontiers in Human Neuroscience, 11, 323, https://doi.org/10.3389/fnhum.2017.00323

Bosco, A., Sanz Diez, P., Filippini, M., & Fattori, P. (2023). The influence of action on perception spans different effectors. Frontiers in systems neuroscience, 17, 1145643. doi: 10.3389/fnsys.2023.1145643.

Brain, W. R. (1941). Visual disorientation with spatial reference to lesions of the right cerebral hemisphere. Brain, 64(4), 244–272, https://doi.org/10.1093/brain/64.4.244

Brainard, D. H. (1997). The psychophysics toolbox. Spatial Vision, 10, 433–436, https: //doi.org/10.1163/156856897X00357.

Brouwer, A., Franz, V. H., & Gegenfurtner, K. R. (2009). Differences in fixations between grasping and viewing objects. Journal of Vision, 9(1):18, 1–24, http://journalofvision.org/9/1/18/, doi:10.1167/9.1.18

Buiatti, T., Skrap, M., & Shallice, T. (2013). Reaching a moveable visual target: Dissociations in brain tumour patients. Brain and Cognition, 82(1), 6–17, https://doi.org/10.1016/j.bandc.2013.02.004

Buxbaum, L. J., & Coslett, H. B. (1997). Subtypes of optic ataxia: Reframing the disconnection account. Neurocase, 3(3), 159–166. https://doi.org/10.1080/13554799708404050

Caffarra, P., Vezzadini, G., Dieci, F., Zonato, F., & Veneri, A. (2002). Rey-Osterrieth complex figure: normative values in an Italian population sample. Neurological Sciences, 22(6), 443–447, https://doi.org/10.1007/s100720200003.

Carey, D. P., Hargreaves, E. L., & Goodale, M. A. (1996). Reaching to ipsilateral or contralateral targets: Within-hemisphere visuomotor processing cannot explain hemispatial differences in motor control. Experimental Brain Research. Experimentelle Hirnforschung. Experimentation Cerebrale, 112(3), 496–504, https://doi.org/10.1007/ BF00227955.

Carey DP, Coleman RJ, Della Sala S. Magnetic misreaching. Cortex. 1997 Dec;33(4):639-52. doi: 10.1016/s0010-9452(08)70722-6

Castiello, U. The neuroscience of grasping. Nat Rev Neurosci 6, 726–736 (2005). https://doi.org/10.1038/nrn1744

Cavina-Pratesi, C., Ietswaart, M., Humphreys, G. W., Lestou, V., & Milner, A. D. (2010). Impaired grasping in a patient with optic ataxia: Primary visuomotor deficit or secondary consequence of misreaching? Neuropsychologia, 48(1), 226–234, https://doi.org/10.1016/j.neuropsychologia.2009.09. 008

Cavina-Pratesi, C., Connolly, J. D., & Milner, A. D. (2013). Optic ataxia as a model to investigate the role of the posterior parietal cortex in visually guided action: evidence from studies of patient M.H. Frontiers in human neuroscience, 7, 336. doi: 10.3389/fnhum.2013.00336

Chessa M., Maiello G., Klein L. K., Paulun V. C., and Solari F., "Grasping objects in immersive Virtual Reality," 2019 IEEE Conference on Virtual Reality and 3D User Interfaces (VR), Osaka, Japan, 2019, pp. 1749-1754, https://doi.org/10.1109/VR.2019.8798155

Collier, E.S., Lawson, R. Does grasping capacity influence object size estimates? It depends on the context. Atten Percept Psychophysics 79, 2117–2131 (2017). https://doi.org/10.3758/s13414-017-1344-3

Coomer, N., Bullard, S., Clinton W., & Williams-Sanders, B. (2018). Evaluating the effects of four VR locomotion methods: joystick, arm-cycling, point-tugging, and teleporting. In Proceedings of the 15th ACM Symposium on Applied Perception (SAP '18). Association for Computing Machinery, New York, NY, USA, Article 7, 1–8. https://doi.org/10.1145/3225153.3225175

Crawford, J. D., Henriques, D. Y. P., & Medendorp, W. P. (2011). Three-dimensional transformations for goal-directed action. Annual Review of Neuroscience, 34(1), 309–31, https://doi.org/10. 1146/annurev-neuro-061010-113749

Crawford, J. R., & Garthwaite, P. H. (2002). Investigation of the single case in neuropsychology: Confidence limits on the abnormality of test scores and test score differences. Neuropsychologia, 40(8), 1196–1208, https://doi.org/10.1016/S0028-3932(01) 00224-X

Crawford, J. R., & Howell, D. C. (1998). Comparing an individual's test score against norms derived from small samples. Clinical Neuropsychologist, 12(4), 482–486, https://doi.org/10.1076/clin.12.4.482.7241

Culbertson, W., & Zillmer, E. (2000). Tower of London - DX. Danckert, J., Goldberg, L., & Broderick, C. (2009). Damage to superior parietal cortex impairs pointing in the sagittal plane. Experimental Brain Research, 195(2), 183–191, https: //doi.org/10.1007/s00221-009-1766-9

De Vitis, M., Breveglieri, R., Hadjidimitrakis, K., Vanduffel, W., Galletti, C., & Fattori, P. (2019). The neglected medial part of macaque area PE: Segregated processing of reach depth and direction. Brain Structure and Function, 224(7), 2537–2557, https://doi.org/10.1007/s00429-019-01923-8

Desanghere, L., Marotta, J.J. "Graspability" of objects affects gaze patterns during perception and action tasks. Exp Brain Res 212, 177–187 (2011). https://doi.org/10.1007/s00221-011-2716-x

Desmurget, M., Epstein, C. M., Turner, R. S., Prablanc, C., Alexander, G. E., & Grafton, S. T. (1999). Role of the posterior parietal cortex in updating reaching movements to a visual target. Nature Neuroscience, 2(6), 563–567, https://doi.org/10.1038/9219

Deubel H, Schneider WX. Saccade target selection and object recognition: evidence for a common attentional mechanism. Vision Res. 1996 Jun;36(12):1827-37. doi: 10.1016/0042-6989(95)00294-4

Dijkerman, H. C., McIntosh, R. D., Anema, H. A., de Haan, E. H. F., Kappelle, L. J., & Milner, A. D. (2006). Reaching errors in optic ataxia are linked to eye position rather than head or body position. Neuropsychologia, 44(13), 2766–2773, https: //doi.org/10.1016/j.neuropsychologia.2005.10.018

Durgin, F. H., & Li, Z. (2011). Perceptual scale expansion: An efficient angular coding strategy for locomotor space. Attention, Perception, & Psychophysics, 73, 1856–1870. doi:10.3758/s13414-011-0143-5

Fagioli, S., Hommel, B. & Schubotz, R.I. Intentional control of attention: action planning primes action-related stimulus dimensions. Psychological Research 71, 22–29 (2007). https://doi.org/10.1007/s00426-005-0033-3

Fattori, P., Gamberini, M., Kutz, D. F., & Galletti, C. (2001). “Arm-reaching” neurons in the parietal area V6A of the macaque monkey. European Journal of Neuroscience, 13(12), 2309–2313, https://doi.org/10.1046/j.0953-816x.2001.01618.x

Fattori, P., Kutz, D. F., Breveglieri, R., Marzocchi, N., & Galletti, C. (2005). Spatial tuning of reaching activity in the medial parieto-occipital cortex (area V6A) of macaque monkey. European Journal of Neuroscience, 22(4), 956–972, https://doi.org/10.1111/j.1460-9568.2005.04288.x

Faugier-Grimaud, S., Frenois, C. & Peronnet, F. Effects of posterior parietal lesions on visually guided movements in monkeys. Exp Brain Res 59, 125–138 (1985). https://doi.org/10.1007/BF00237673

Ferraina, S., Garasto, M. R., Battaglia-Mayer, A., Ferraresi, P., Johnson, P. B., Lacquaniti, F., Caminiti, R. (1997). Visual control of hand reaching movement: activity in parietal area 7m. European Journal of Neuroscience, 9(5), 1090–1095, https://doi.org/10.1111/j.1460-9568.1997.tb01460.x

Ferrari-Toniolo, S., Papazachariadis, O., Visco Comandini, F., Salvati, M., D’Elia, A., Di Berardino, F., Battaglia-Mayer, A. (2014). A visuomotor disorder in the absence of movement: Does optic ataxia generalize to learned isometric hand action? Neuropsychologia, 63, 59–71, https: //doi.org/10.1016/j.neuropsychologia.2014.07.029

Filippini, M., Breveglieri, R., Hadjidimitrakis, K., Bosco, A., & Fattori, P. (2018). Prediction of reach goals in depth and direction from the parietal cortex. Cell Reports, 23(3), 725–732, https://doi.org/10.1016/j.celrep.2018.03.090

Flanders, M., & Soechting, J. F. (1990). Parcellation of sensorimotor transformations for arm movements. Journal of Neuroscience, 10(7), 2420LP–2427LP, https://doi.org/10.1523/JNEUROSCI.10-07-02420.1990

Flanders, M., Tillery, S. I. H., & Soechting, J. F. (1992). Early stages in a sensorimotor transformation. Behavioral and Brain Sciences, 15, 309–320, https://doi.org/10.1017/S0140525X00068813

Frassinetti, F., Bonifazi, S., & Làdavas, E. (2007). The influence of spatial coordinates in a case of an optic ataxia-like syndrome following cerebellar and thalamic lesion. Cognitive Neuropsychology, 24(3), 324–337, https://doi.org/10.1080/02643290701275857

Furmanek, M.P., Schettino, L.F., Yarossi, M. et al. Coordination of reach-to-grasp in physical and haptic-free virtual environments. J NeuroEngineering Rehabil 16, 78 (2019). doi: 10.1186/s12984-019-0525-9

Gao H., Frommelt L. and Kasneci E., "The Evaluation of Gait-Free Locomotion Methods with Eye Movement in Virtual Reality," 2022 IEEE International Symposium on Mixed and Augmented Reality Adjunct (ISMAR-Adjunct), Singapore, Singapore, 2022, pp. 530-535, doi: 10.1109/ISMAR-Adjunct57072.2022.00112

Gaveau V, Pélisson D, Blangero A, Urquizar C, Prablanc C, Vighetto A, Pisella L (2008). Saccade control and eye-hand coordination in optic ataxia. Neuropsychologia. Jan 31;46(2):475-86. doi: 10.1016/j.neuropsychologia.2007.08.028

Goodale, M. A., Pelisson, D., & Prablanc, C. (1986). Large adjustments in visually guided reaching do not depend on vision of the hand or perception of target displacement. Nature, 320(6064), 748–750, https://doi.org/10.1038/320748a0

Goodale M. A., Milner A. D. Separate visual pathways for perception and action. Trends Neurosci. 1992 Jan;15(1):20-5. doi: 10.1016/0166-2236(92)90344-8

Goodale, M. A., Meenan, J. P., Bülthoff, H. H., Nicolle, D. A., Murphy, K. J., & Racicot, C. I. (1994). Separate neural pathways for the visual analysis of object shape in perception and prehension. Current Biology, 4(7), 604–610, https://doi.org/10.1016/S0960-9822(00)00132-9

Gordon, J., Ghilardi, M. F., Cooper, S. E., & Ghez, C. (1994). Accuracy of planar reaching movements - II. Systematic extent errors resulting from inertial anisotropy. Experimental Brain Research, 99(1), 112–130, https://doi.org/10.1007/BF00241416

Grafton, S. T. (2010). The cognitive neuroscience of prehension: recent developments. Experimental Brain Research. Experimentelle Hirnforschung. Experimentation Cerebrale, 204(4), 475–491, https://doi.org/10.1007/s00221-010-2315-2

Graves R. E. (1996). Luminance and color effects on localization of briefly flashed visual stimuli. Visual neuroscience, 13(3), 567–573. https://doi.org/10.1017/s0952523800008245

Gréa, H., Pisella, L., Rossetti, Y., Desmurget, M., Tilikete, C., Grafton, S., & Vighetto, A. (2002). A lesion of the posterior parietal cortex disrupts on-line adjustments during aiming movements. Neuropsychologia, 40(13), 2471–2480, https://doi.org/10.1016/S0028-3932(02)00009-X.

Gutteling, T. P., Kenemans, J. L., & Neggers, S. F. (2011). Grasping preparation enhances orientation change detection. PloS one, 6(3), e17675. doi: 10.1371/journal.pone.0017675.

Hadjidimitrakis, K., Bertozzi, F., Breveglieri, R., Bosco, A., Galletti, C., & Fattori, P. (2014). Common neural substrate for processing depth and direction signals for reaching in the monkey medial posterior parietal cortex. Cerebral Cortex, 24(6), 1645–1657, https://doi.org/10.1093/cercor/bht021

Hadjidimitrakis, K., Bertozzi, F., Breveglieri, R., Fattori, P., & Galletti, C. (2014). Body-centered, mixed, but not hand-centered coding of visual targets in the medial posterior parietal cortex during reaches in 3D space. Cerebral Cortex, 24(12), 3209–3220, https://doi.org/10.1093/cercor/bht181

Hadjidimitrakis, K., Bertozzi, F., Breveglieri, R., Galletti, C., & Fattori, P. (2017). Temporal stability of reference frames in monkey area V6A during a reaching task in 3D space. Brain Structure and Function, 222(4), 1959–1970, https://doi.org/10.1007/s00429-016-1319-5

Hadjidimitrakis, K., Dal Bo', G., Breveglieri, R., Galletti, C., & Fattori, P. (2015). Overlapping representations for reach depth and direction in caudal superior parietal lobule of macaques. Journal of Neurophysiology, 114(4), 2340–52, https://doi.org/10.1152/jn.00486.2015

Hoffman, J.E., Subramaniam, B. The role of visual attention in saccadic eye movements. Perception & Psychophysics 57, 787–795 (1995). https://doi.org/10.3758/BF03206794

Holmes, G., & Horrax, G. (1919). Disturbance of spatial orientation and visual attention, with loss of stereoscopic vision. Archives of Neurology & Psychiatry, 1(4), 385–407, https://doi.org/10.1001/archneurpsyc.1919.02180040002001

Hwang, E. J., Hauschild, M., Wilke, M., & Andersen, R. A. (2012). Inactivation of the parietal reach region causes optic ataxia, impairing reaches but not saccades. Neuron, 76(5), 1021–1029, https://doi.org/10.1016/j.neuron.2012.10.030

Hwang, E. J., Hauschild, M., Wilke, M., & Andersen, R. A. (2014). Spatial and temporal eye–hand coordination relies on the parietal reach region. Journal of Neuroscience, 34(38), 12884–12892, https://doi.org/10.1523/JNEUROSCI.3719-13.2014

Itaguchi, Y. (2021). Size Perception Bias and Reach-to-Grasp Kinematics: An Exploratory Study on the Virtual Hand With a Consumer Immersive Virtual-Reality Device. Frontiers in Virtual Reality, 2, Article 712378. https://doi.org/10.3389/frvir.2021.712378

Jackson, S. R., Newport, R., Mort, D., & Husain, M. (2005). Where the eye looks, the hand follows: Limb-dependent magnetic misreaching in optic ataxia. Current Biology, 15(1), 42–46, https://doi.org/10.1016/j.cub.2004.12.063

Jackson S.R., Newport R, Husain M, Fowlie JE, O'Donoghue M, Bajaj N. (2009) There may be more to reaching than meets the eye: re-thinking optic ataxia. Neuropsychologia. May;47(6):1397-408. https://doi.org/10.1016/j.neuropsychologia.2009.01.035.

Jacob, S. S., Jacob, S., Albornoz, A. M., & Biswas, D. (2002). Balint's syndrome—Missed or mistaken? The American Journal of Medicine, 112(6), 509–510. doi: 10.1016/S0002-9343(01)01133-0

Jakobson, L., & Goodale, M. (1989). Trajectories of reaches to prismatically-displaced targets: evidence for "automatic" visuomotor recalibration. Exp Brain Res, 78(3), 575–87

Jakobson LS, Archibald YM, Carey DP, Goodale MA. (1991) A kinematic analysis of reaching and grasping movements in a patient recovering from optic ataxia. Neuropsychologia.;29(8):803-9. doi: 10.1016/0028-3932(91)90073-h.ja

Jeannerod M. (1986) The formation of finger grip during prehension. A cortically mediated visuomotor pattern. Behav Brain Res. Feb;19(2):99-116. doi: 10.1016/0166-4328(86)90008-2

Jeannerod, M., Decety, J., & Michel, F. (1994). Impairment of grasping movements following a bilateral posterior parietal lesion. Neuropsychologia, 32(4), 369–380, https://doi.org/10.1016/0028-3932(94)90084-1

Jeannerod M, Arbib MA, Rizzolatti G, Sakata H. Grasping objects: the cortical mechanisms of visuomotor transformation. Trends Neurosci. 1995 Jul;18(7):314-20. https://doi.org/10.1016/0166-2236(95)93921-J

Johansson, R. S., Westling, G., Bäckström, A., and Flanagan, J. R. (2001). Eye–hand coordination in object manipulation. J. Neurosci. 21, 6917–6932. doi: 10.1523/JNEUROSCI.21-17-06917.2001

Karnath, H.-O., & Perenin, M.-T. (2005). Cortical control of visually guided reaching: evidence from patients with optic ataxia. Cerebral Cortex, 15(10), 1561–1569, https://doi.org/10.1093/cercor/bhi034

Kasuga, S., Telgen, S., Ushiba, J., Nozaki, D., & Diedrichsen, J. (2015). Learning feedback and feedforward control in a mirror-reversed visual environment. Journal of Neurophysiology, 114(4), 2187–2193, https://doi.org/10.1152/jn.00096.2015

Kelly, J. W., Donaldson, L. S., Sjolund, L. A., & Freiberg, J. B. (2013). More than just perception–action recalibration: Walking through a virtual environment causes rescaling of perceived space. Attention, Perception, & Psychophysics, 75(7), 1473–1485. doi: 10.3758/s13414-013-0503-4

Kelly, J. W., Hammel, W. W., Siegel, Z. D., & Sjolund, L. A. (2014). Recalibration of perceived distance in virtual environments occurs rapidly and transfers asymmetrically across scale. IEEE transactions on visualization and computer graphics, 20(4), 588–595. https://doi.org/10.1109/TVCG.2014.36

Kelly, J. W., Cherep, L. A., Klesel, B., Siegel, Z. D., & George, S. (2018). Comparison of two methods for improving distance perception in virtual reality. ACM Transactions on Applied Perception, 15(2), 1–11. https://doi.org/10.1145/3165285

Khan, A. Z., Crawford, J. D., Blohm, G., Urquizar, C., Rossetti, Y., & Pisella, L. (2007). Influence of initial hand and target position on reach errors in optic ataxic and normal subjects. Journal of Vision, 7(5), 8, https://doi.org/10.1167/7.5.8

Khan, A. Z., Pisella, L., Vighetto, A., Cotton, F., Luauté, J., Boisson, D., & Rossetti, Y. (2005). Optic ataxia errors depend on remapped, not viewed, target location. Nature Neuroscience, 8(4), 418–420, https://doi.org/10.1038/nn1425

Knaut, L. A., Subramanian, S. K., McFadyen, B. J., Bourbonnais, D., & Levin, M. F. (2009). Kinematics of pointing movements made in a virtual versus a physical 3-dimensional environment in healthy and stroke subjects. Archives of physical medicine and rehabilitation, 90(5), 793–802. doi: 10.1016/j.apmr.2008.10.030

Kuznetsova, A., Brockhoff, P. B., & Christensen, R. H. B. (2017). lmerTest Package: Tests in Linear Mixed Effects Models. Journal of Statistical Software, 82(13), 1–26. https://doi.org/10.18637/jss.v082.i13

Lacquaniti, F., Guigon, E., Bianchi, L., Ferraina, S., & Caminiti, R. (1995). Representing spatial information for limb movement: Role of area 5 in the monkey. Cerebral Cortex, 5(5), 391–409. Retrieved from http://www.ncbi.nlm.nih.gov/pubmed/8547787

Lamotte RH, Acuña C. Defects in accuracy of reaching after removal of posterior parietal cortex in monkeys. Brain Res. 1978 Jan 13;139(2):309-26. doi: 10.1016/0006-8993(78)90931-9

Lingnau, A., Strnad, L., He, C., Fabbri, S., Han, Z., Bi, Y., & Caramazza, A. (2012). Cross-modal plasticity preserves functional specialization in posterior parietal cortex. Cerebral Cortex, 24(2), 541–549, https://doi.org/10.1093/cercor/bhs340

Linkenauger, S. A., Witt, J. K., & Proffitt, D. R. (2011). Taking a hands-on approach: Apparent grasping ability scales the perception of object size. Journal of Experimental Psychology: Human Perception and Performance, 37(5), 1432–1441. https://doi.org/10.1037/a0024248

Loomis, J., & Knapp, J. (2003). Visual perception of egocentric distance in real and virtual environments. In L. J. Hettinger & M. W. Haas (Eds.), Virtual and adaptive environments: Applications, implications, and human performance issues (pp. 21–46). Lawrence Erlbaum Associates Publishers. https://doi.org/10.1201/9781410608888.pt1

Marcia, K. V., Kent, J. T., & Bibbia, J. N. (1995). Multivariate analysis. In Birnbaum, Z. W., Lukacs, E. (Eds.). San Diego, CA: Academin press

Martin, J. A., Karnath, H.-O., & Himmelbach, M. (2015). Revisiting the cortical system for peripheral reaching at the parieto-occipital junction. Cortex, 64, 363–379, https://doi.org/10.1016/j.cortex.2014.11.012

Maselli, A., Dhawan, A., Cesqui, B., Russo, M., Lacquaniti, F., & d'Avella, A. (2017). Where are you throwing the ball? I better watch your body, not just your arm!. Frontiers in Human Neuroscience, 11, 505. Retrieved from https://www.frontiersin.org/article/10.3389/fnhum.2017.00505

McGuire, L. M., & Sabes, P. N. (2011). Heterogeneous representations in the superior parietal lobule are common across reaches to visual and proprioceptive targets. Journal of Neuroscience, 31(18), 6661–6673, https://doi.org/10.1523/JNEUROSCI.2921-10.2011

McIntosh, R. D., Mulroue, A., & Brockmole, J. R. (2010). How automatic is the hand's automatic pilot? Experimental Brain Research, 206(3), 257–269, https://doi.org/10.1007/s00221-010-2404-2

Merians AS, Tunik E, Adamovich SV. Virtual reality to maximize function for hand and arm rehabilitation: exploration of neural mechanisms. Stud Health Technol Inform. 2009;145:109–25. doi: 10.3233/978-1-60750-018-6-109

Michaelsen, S. M., Dannenbaum, R., & Levin, M. F. (2006). Task-specific training with trunk restraint on arm recovery in stroke: randomized control trial. Stroke, 37(1), 186–192. doi: 10.1161/01.STR.0000196940.20446.c9

Milner A. D., Dijkerman HC, Pisella L, McIntosh RD, Tilikete C, Vighetto A, Rossetti Y. (2001) Grasping the past. delay can improve visuomotor performance. Curr Biol. Nov 27;11(23):1896-901. doi: 10.1016/s0960-9822(01)00591-7

Milner, A. D., Dijkerman, H. C., McIntosh, R. D., Rossetti, Y., & Pisella, L. (2003). Delayed reaching and grasping in patients with optic ataxia. Progress in Brain Research, 142, 225–42, https://doi.org/10.1016/S0079-6123(03)42016-5

Milner, A.D., & Goodale, M.A. (2008). Two visual systems re-viewed. Neuropsychologia, 46, 774-785. doi:10.1016/j.neuropsychologia.2007.10.005

Mishkin M, Ungerleider LG. Contribution of striate inputs to the visuospatial functions of parieto-preoccipital cortex in monkeys. Behav Brain Res. 1982 Sep;6(1):57-77. doi: 10.1016/0166-4328(82)90081-x

Mohamed, O. & Appling, H., (2020). Clinical Assessment of Gait. Orthotics and Prosthetics in Rehabilitation, pp 102–143

Mohler, B. J., Creem-Regehr, S. H., & Thompson, W. B. (2006). The influence of feedback on egocentric distance judgments in real and virtual environments. In ACM SIGGRAPH Symposium on Applied Perception in Graphics and Visualization (pp. 9–14). Washington, DC: ACM. https://doi.org/10.1145/1140491.1140493

Monaco, S., Kroliczak, G., Quinlan, D. J., Fattori, P., Galletti, C., Goodale, M. A., & Culham, J. C. (2010). Contribution of visual and proprioceptive information to the precision of reaching movements. Experimental Brain Research, 202(1), 15–32, https://doi.org/10.1007/s00221-009-2106-9

Neggers SF, Huijbers W, Vrijlandt CM, Vlaskamp BN, Schutter DJ, Kenemans JL. (2007) TMS pulses on the frontal eye fields break coupling between visuospatial attention and eye movements. J Neurophysiol. Nov;98(5):2765-78. doi: 10.1152/jn.00357.2007

Novelli, G., Papagno, C., Capitani, E., Laiacona, M., Cappa, S., & Vallar, G. (1986). Three clinical tests for the assessment of verbal long-term memory function. Norms from 320 normal subjects. Archive of Psychology, Neurology and Psychiatry, 47, 278–296

Orsini, A., Grossi, D., Capitani, E., Laiacona, M., Papagno, C., & Vallar, G. (1987). Verbal and spatial immediate memory span: normative data from 1355 adults and 1112 children, 8(6), 539–548

Osterrieth, P. A. (1944). Le test de copie d'une figure complexe; contribution à l'étude de la perception et de la mémoire. [Test of copying a complex figure; contribution to the study of perception and memory.]. Archives de Psychologie, 30, 206–356

Pallesen, H., Andersen, M. B., Hansen, G. M., Lundquist, C. B., & Brunner, I. (2018). Patients' and Health Professionals' Experiences of Using Virtual Reality Technology for Upper Limb Training after Stroke: A Qualitative Substudy. Rehabilitation research and practice, 2018, 4318678. doi: 10.1155/2018/4318678

Pélisson, D., Prablanc, C., Goodale, M. A., & Jeannerod, M. (1986). Visual control of reaching movements without vision of the limb. Experimental Brain Research, 62(2), 303–311, https://doi.org/10.1007/BF00238849

Perenin, M. T., & Vighetto, A. (1988). Optic ataxia: a specific disruption in visuomotor mechanisms. I. Different aspects of the deficit in reaching for objects. Brain : A Journal of Neurology, 111(3), 643–674

Pisella, L., Gréa, H., Tilikete, C., Vighetto, A., Desmurget, M., Rode, G., & Rossetti, Y. (2000). An “automatic pilot” for the hand in human posterior parietal cortex: Toward reinterpreting optic ataxia. Nature Neuroscience, 3(7), 729–736, https://doi.org/10.1038/76694

Pisella, L., Michel, C., Gréa, H., Tilikete, C., Vighetto, A., & Rossetti, Y. (2004). Preserved prism adaptation in bilateral optic ataxia: Strategic versus adaptive reaction to prisms. Experimental Brain Research, 156(4), 399–408, https://doi.org/10.1007/s00221-003-1746-4

Piserchia, V., Breveglieri, R., Hadjidimitrakis, K., Bertozzi, F., Galletti, C., & Fattori, P. (2017). Mixed body/hand reference frame for reaching in 3D space in macaque parietal area PEc. Cerebral Cortex (New York, N.Y. : 1991), 27, 1976–1990, https://doi.org/10.1093/cercor/bhw039

Prablanc, C., & Martin, O. (1992). Automatic control during hand reaching at undetected two-dimensional target displacements. Journal of Neurophysiology, 67(2), 455–469, https://doi.org/10.1152/jn.1992.67.2.455

Prado J, Clavagnier S, Otzenberger H, Scheiber C, Kennedy H, Perenin MT. Two cortical systems for reaching in central and peripheral vision. Neuron. 2005 Dec 8;48(5):849-58 https://doi.org/10.1016/j.neuron.2005.10.010

Proffitt, D. R. (2006). Distance Perception. Current Directions in Psychological Science, 15(3), 131-135. https://doi.org/10.1111/j.0963-7214.2006.00422.x

R Core Team. R: A Language and Environment for Statistical Computing; R Foundation for Statistical Computing: Vienna, Austria, 2018

Rice, N. J., Edwards, M. G., Schindler, I., Punt, T. D., McIntosh, R. D., Humphreys, G. W., & Milner, A. D. (2008). Delay abolishes the obstacle avoidance deficit in unilateral optic ataxia. Neuropsychologia, 46(5), 1549–1557, https://doi.org/10.1016/j.neuropsychologia.2008.01.012

Richardson, A. R., & Waller, D. (2005). The effect of feedback training on distance estimation in virtual environments. Applied Cognitive Psychology, 19, 1089–1108. https://doi.org/10.1002/acp.1140

Richardson, A. R., & Waller, D. (2007). Interaction with an immersive virtual environment corrects users' distance estimates. Human Factors, 49, 507–517. https://doi.org/10.1518/001872007X200139

Rondot P, de Recondo J, Dumas JL. Visuomotor ataxia. Brain. 1977 Jun;100(2):355-76. doi: 10.1093/brain/100.2.355

Rorden, C., & Brett, M. (2000). Stereotaxic display of brain lesions. Behavioural Neurology, 12, 421719, https://doi.org/10.1155/2000/421719

Rossetti, Y., Pisella, L., & Vighetto, A. (2003). Optic ataxia revisited. Experimental Brain Research, 153(2), 171–179, https://doi.org/10.1007/s00221-003-1590-6

Rzepka AM, Hussey KJ, Maltz MV, Babin K, Wilcox LM, Culham JC. Familiar size affects perception differently in virtual reality and the real world. Philos Trans R Soc Lond B Biol Sci. 2023 Jan 30;378(1869):20210464. doi: 10.1098/rstb.2021.046

Sainburg, R. L., Lateiner, J. E., Latash, M. L., & Bagesteiro, L. B. (2003). Effects of altering initial position on movement direction and extent. Journal of Neurophysiology, 89(1), 401–415, https://doi.org/10.1152/jn.00243.2002

Salvucci Dario D. and Goldberg Joseph H. 2000. Identifying fixations and saccades in eye-tracking protocols. In Proceedings of the 2000 symposium on Eye tracking research & applications (ETRA '00). Association for Computing Machinery, New York, NY, USA, 71–78. https://doi.org/10.1145/355017.355028

Sanz Diez, P., Bosco, A., Fattori, P., & Wahl, S. (2022). Horizontal target size perturbations during grasping movements are described by subsequent size perception and saccade amplitude. PloS one, 17(3), e0264560. doi: 10.1371/journal.pone.0264560

Schaadt, A., Brandt, S., Kraft, A., & Kerkhoff, G. (2015). Holmes and Horrax (1919) revisited: Impaired binocular fusion as a cause of "flat vision" after right parietal brain damage - A case study. Neuropsychologia, 69, 31–38

Schindler, I., Rice, N. J., McIntosh, R. D., Rossetti, Y., Vighetto, A., & Milner, A. D. (2004). Automatic avoidance of obstacles is a dorsal stream function: evidence from optic ataxia. Nature Neuroscience, 7(7), 779–784, https://doi.org/10.1038/nn1273

Schultheis MT, Himelstein J, Rizzo AA: Virtual reality and neuropsychology: upgrading the current tools. J Head Trauma Rehabil 2002, 17:378-394. doi: 10.1097/00001199-200210000-00002

Sedgwick, H. A. (1986). Space perception. In K. R. Boff, L. Kaufman, & J. P. Thomas (Eds.), Handbook of perception and human performance: Vol I. Sensory processes and perception (pp. 21.1–21.57). New York, NY: Wiley

Snyder, L., Batista, A., & Andersen, R. (1997). Coding of intention in the posterior parietal cortex. Nature, 386, 167–170

Spinnler, H., & Tognoni, G. (1987). Standardizzazione e taratura italiana di test neuropsicologici. Masson Italia periodici, Milano e 1987

Stefanucci, J. K., Creem-Regehr, S. H., Thompson, W. B., Lessard, D. A., & Geuss, M. N. (2015). Evaluating the accuracy of size perception on screen-based displays: Displayed objects appear smaller than real objects. Journal of Experimental Psychology: Applied, 21(3), 215–223. https://doi.org/10.1037/xap0000051

Striemer, C., Locklin, J., Blangero, A., Rossetti, Y., Pisella, L., & Danckert, J. (2009). Attention for action? Examining the link between attention and visuomotor control deficits in a patient with optic ataxia. Neuropsychologia, 47(6), 1491–1499, https://doi.org/10.1016/j.neuropsychologia.2008.12.021

Subramanian, S.K., Levin, M.F. Viewing medium affects arm motor performance in 3D virtual environments. J NeuroEngineering Rehabil 8, 36 (2011). https://doi.org/10.1186/1743-0003-8-36

Teasell, R., Bayona, N., Salter, K., Hellings, C., & Bitensky, J. (2006). Progress in clinical neurosciences: stroke recovery and rehabilitation. The Canadian journal of neurological sciences. Le journal canadien des sciences neurologiques, 33(4), 357–364. doi: 10.1017/s0317167100005308

Thielman, G., Kaminski, T., & Gentile, A. M. (2008). Rehabilitation of reaching after stroke: Comparing 2 training protocols utilizing trunk restraint. Neurorehabilitation and Neural Repair, 22(6), 697–705. doi: 10.1177/1545968308315998

Tinson D. J. (1989). How stroke patients spend their days. An observational study of the treatment regime offered to patients in hospital with movement disorders following stroke. International disability studies, 11(1), 45–49. doi: 10.3109/02599148909166380

Ustinova, K. I., Perkins, J., Szostakowski, L., Tamkei, L. S., & Leonard, W. A. (2010). Effect of viewing angle on arm reaching while standing in a virtual environment: potential for virtual rehabilitation. Acta psychologica, 133(2), 180–190. doi: 10.1016/j.actpsy.2009.11.006

van Beers, R. J., Sittig, A. C., & Denier van der Gon, J. J. (1998). The precision of proprioceptive position sense. Experimental Brain Research, 122(4), 367–77. Retrieved from http://www.ncbi.nlm.nih.gov/pubmed/9827856

Van Pelt, S., & Medendorp, W. P. (2008). Updating target distance across eye movements in depth. Journal of Neurophysiology, 99, 2281–2290, https://doi.org/10.1152/jn.01281.2007

Vindras, P., Desmurget, M., & Viviani, P. (2005). Error parsing in visuomotor pointing reveals independent processing of amplitude and direction. Journal of Neurophysiology, 94(2), 1212–1224, https://doi.org/10.1152/jn.01295.2004

Vingerhoets G. (2014). Contribution of the posterior parietal cortex in reaching, grasping, and using objects and tools. Front Psychol. Mar 5;5:151. doi: 10.3389/fpsyg.2014.00151

Waller, D., & Richardson, A. R. (2008). Correcting distance estimates by interacting with immersive virtual environments: Effects of task and available sensory information. Journal of Experimental Psychology. Applied, 14, 61–72. doi: 10.1037/1076-898X.14.1.61

Witt, J. K., Proffitt, D. R., & Epstein, W. (2004). Perceiving distance: A role of effort and intent. Perception, 33(5), 577–590. https://doi.org/10.1068/p5090

Wykowska, A., Schubö, A., & Hommel, B. (2009). How you move is what you see: Action planning biases selection in visual search. Journal of Experimental Psychology. Human Perception and Performance, 35(6), 1755–1769, doi.org/10.1037/ a0016798

Wykowska, A., Hommel, B., & Schubö, A. (2011). Action-induced effects on perception depend neither on element-level nor on set-level similarity between stimulus and response sets. Attention, Perception, & Psychophysics, 73, 1034–1041. https://doi.org/10.3758/s13414-011-0122-x

Zhang, C. Y., Aflalo, T., Revechkis, B., Rosario, E. R., Ouellette, D., Pouratian, N., & Andersen, R. A. (2017). Partially mixed selectivity in human posterior parietal association cortex. Neuron, 95(3), 697–708.e4, https://doi.org/10.1016/j.neuron.2017.06.040

Zimmermann, P., & Fimm, B. (1992). Testbatterie zur Aufmerksamkeitsprufung (TAP). Freiburg: Psytest

Zoccolotti, P., Pizzamiglio, L., Pittau, P., & Galati, G. (1994). Batteria di Test per l'esame dell'Attenzione. PSYTEST, Roma